



PACIFIC EARTHQUAKE ENGINEERING RESEARCH CENTER

PEER Testbed Study on a Laboratory Building: Exercising Seismic Performance Assessment

Mary C. Comerio
Editor

Department of Architecture
University of California, Berkeley

PEER Testbed Study on a Laboratory Building: Exercising Seismic Performance Assessment

**Mary C. Comerio
Editor**

Department of Architecture
University of California, Berkeley

PEER Report 2005/12
Pacific Earthquake Engineering Research Center
College of Engineering
University of California, Berkeley
November 2005

ABSTRACT

From 2002 to 2004 (years five and six of a ten-year funding cycle), the PEER Center organized the majority of its research around six testbeds. Two buildings and two bridges, a campus, and a transportation network were selected as case studies to “exercise” the PEER performance-based earthquake engineering methodology. All projects involved interdisciplinary teams of researchers, each producing data to be used by other colleagues in their research. The testbeds demonstrated that it is possible to create the data necessary to populate the PEER performance-based framing equation, linking the hazard analysis, the structural analysis, the development of damage measures, loss analysis, and decision variables.

This report describes one of the building testbeds—the UC Science Building. The project was chosen to focus attention on the consequences of losses of laboratory contents, particularly downtime. The UC Science testbed evaluated the earthquake hazard and the structural performance of a well-designed recently built reinforced concrete laboratory building using the OpenSees platform. Researchers conducted shake table tests on samples of critical laboratory contents in order to develop fragility curves used to analyze the probability of losses based on equipment failure. The UC Science testbed undertook an extreme case in performance assessment—linking performance of contents to operational failure. The research shows the interdependence of building structure, systems, and contents in performance assessment, and highlights where further research is needed.

The Executive Summary provides a short description of the overall testbed research program, while the main body of the report includes summary chapters from individual researchers. More extensive research reports are cited in the reference section of each chapter.

ACKNOWLEDGMENTS

We would like to thank the many individuals who made this research possible. In particular, we thank the senior administration at the University of California, Berkeley, for their commitment to and support of seismic safety initiatives and research on the campus: former Chancellor Robert Berdahl, Vice Chancellor for Research Mary Beth Burnside, Vice Provost for Academic Planning and Facilities William Webster, and Sarah Nathe, Disaster Resistant University Program Manager. In addition, we would like to thank the faculty researchers and staff who gave us access to their laboratories and answered countless questions. In particular, Barbara Duncan, the building manager, opened doors, answered questions, and helped the research team in countless ways. We could not have completed this research without Barbara's cooperation. Vice Chancellor Ed Denton and his staff in Capital Projects provided drawings and specifications of the original building construction.

We would also like to thank our PEER colleagues who have reviewed and critiqued our work, particularly Research Director Greg Deierlein, and Helmut Krawinkler, team leader for the hotel building testbed. In addition, special thanks are due to our Business and Industry Partners: William T. Holmes of Rutherford and Chekene provided critical input every step of the way and pushed researchers to find the practical engineering applications within the research agenda. Paul Somerville of URS Corporation provided the hazard analysis and answered many questions over the course of the project.

This work was supported primarily by the Earthquake Engineering Research Centers Program of the National Science Foundation, under award number EEC-9701568 through the Pacific Earthquake Engineering Research (PEER) Center.”

RESEARCH TEAM

University of California, Berkeley

Prof. Mary C. Comerio—Team Leader, Department of Architecture

John C Stallmeyer, Ph.D. candidate

Ryan Smith, M. Arch 2003

Prof. Nicos Makris, Department of Civil and Environmental Engineering

Dimitrios Konstantinidis, Ph.D. candidate

Professor Khalid Mosalam, Department of Civil and Environmental Engineering

Tae-Hyung Lee, Ph.D. candidate

California Institute of Technology

Prof. James L. Beck, Department of Applied Mechanics and Engineering

Dr. Keith A. Porter, Senior Research Fellow

Rustem Shaikhutdinov, Ph.D. candidate

University of California, Irvine

Prof. Tara Hutchinson, Department of Civil and Environmental Engineering

Samit Ray Chaudhuri, Ph.D. candidate

University of Washington

Prof. Stephanie E. Chang, Department of Geography

Anthony Falit-Baiamonte, Ph.D. candidate

Business and Industry Partners

William T. Holmes, Rutherford and Chekene

Paul Somerville, URS Corporation

CONTENTS

ABSTRACT	iii
ACKNOWLEDGMENTS	iv
RESEARCH TEAM	v
TABLE OF CONTENTS	vii
LIST OF FIGURES	xi
LIST OF TABLES	xv
EXECUTIVE SUMMARY	xvii
1 INTRODUCTION	1
1.1 Background.....	1
1.2 Objectives and Scope.....	2
1.3 Overview of PEER’s PBEE Methodology	3
1.4 Organization of Report	7
2 FACILITY DEFINITION	9
2.1 Objectives and Scope.....	9
2.2 Case Study Building Characteristics	9
2.3 Contents Inventory	12
2.4 Identification of Critical Factors Affecting Inventory.....	18
2.5 Implications of Using Critical Factors to Estimate Seismic Performance	19
2.6 Costs of Anchoring Laboratory Contents.....	19
2.7 References	20
3 HAZARD ANALYSIS	23
3.1 Hazard Levels and <i>IM</i> Values	23
3.2 Selecting Ground Motion Recordings	24
3.3 References	26
4 STRUCTURAL ANALYSIS	29
4.1 Objective and Scope	29
4.2 Description of Structural System.....	29
4.3 OpenSees Modeling.....	31
4.4 Intensity Measure (<i>IM</i>)	34

4.5	Engineering Demand Parameters (<i>EDPs</i>)	34
4.6	Probability Distribution Estimate of <i>EDP/IM</i>	36
4.7	Deterministic Sensitivity Analysis	36
4.8	Concluding Remarks	41
4.9	References	42
5	PERFORMANCE CHARACTERIZATION OF BENCH- AND SHELF-MOUNTED EQUIPMENT AND CONTENTS	45
5.1	Small Bench- and Shelf-Mounted Equipment Studies	45
5.2	Experimental Studies	46
5.3	Analytical Formulation	51
5.4	Development and Generalization of Fragility Curves	53
5.5	References	59
6	EXPERIMENTAL AND ANALYTICAL STUDIES ON THE SEISMIC RESPONSE OF SLENDER LABORATORY EQUIPMENT	61
6.1	Motivation	61
6.2	Objectives of the Research	61
6.3	Seismic Hazard	62
6.4	Friction Tests	63
6.5	Shake Table Tests	67
6.6	Response Analysis of Freestanding Equipment	69
6.7	Estimation of Sliding Displacement of Freestanding Equipment	70
6.8	Response of Restrained Equipment	76
6.9	Shake Table Tests of Scale Models	77
6.10	Conclusions	78
6.11	References	78
7	DAMAGE ANALYSIS.....	81
7.1	Role of Damage Analysis in PBEE Analysis	81
7.2	Assemblies and Operational Units	81
7.3	Assembly-Level Damage-Analysis Methodology	82
7.4	Application to UC Science Building Testbed	88

7.5	Concluding Remarks	91
7.6	References	91
8	LOSS ANALYSIS.....	95
8.1	Decision Variables and Performance Metrics	95
8.2	Loss Model	97
8.3	Calculating Performance Metrics	101
8.4	Application to the UC Science Building Testbed.....	102
8.5	Risk-Management Decision Making.....	108
8.6	Concluding Remarks	109
8.7	References	110
9	STAKEHOLDERS AND DECISION ISSUES.....	111
9.1	Overview	111
9.2	Nonstructural Retrofit Decision Making for UC Science Testbed.....	113
9.3	Conceptualizations of Performance.....	115
9.4	Implications for Performance-Based Earthquake Engineering	116
9.5	References	116
10	PRACTITIONERS USE OF TESTBED DATA AND METHODS.....	117
10.1	Direct Use of Experimental Results	117
10.2	General Review of Testbed Project.....	119
10.3	Practical Use of Testbed Methodology	121
11	LESSONS AND FUTURE RESEARCH DIRECTIONS	123
11.1	References	126

LIST OF FIGURES

Location of testbed building relative to Hayward fault	xxi
Typical floor plan.....	xxii
Deterministic sensitivity results of different <i>EDPs</i> for transverse frame	xxvi
Bench and shelf system on shake table at UC Irvine.....	xxvii
Heavy equipment on shake table at UC Berkeley	xxviii
Fig. 1.1 Overview of PEER performance assessment methodology	4
Fig. 2.1 Typical floor plan 2 nd through 5 th floors.....	11
Fig. 2.2 Typical laboratory conditions	13
Fig. 2.3 Sample report page describing critical lab contents	17
Fig. 4.1 Structural plan of UC Science Building	30
Fig. 4.2 Structural elevation of (a) transverse frame and (b) longitudinal frame	30
Fig. 4.3 OpenSees 2D models of (a) transverse frame and (b) longitudinal frame	32
Fig. 4.4 Time history plots at midpoint of transverse frame due to high hazard Erzincan (Turkey) earthquake for (a) relative roof displacement, (b) absolute roof displacement, (c) relative roof acceleration, and (d) absolute roof acceleration	35
Fig. 4.5 (a) Peak absolute floor responses and IDR of transverse frame for 10 high hazard earthquakes and (b) mean and mean \pm standard deviation bounds of data shown in (a)	35
Fig. 4.6 Empirical CDF and probability distribution estimate by normal and lognormal distributions of transverse frame for PARA and IDR of 7 th story for (a) low hazard, (b) medium hazard, and (c) high hazard	37
Fig. 4.7 Empirical CDF and probability distribution estimate by normal and lognormal distributions of longitudinal frame (column 8) for PARA and IDR of 7 th story for (a) low hazard, (b) medium hazard, and (c) high hazard	38
Fig. 4.8 Deterministic sensitivity results of different <i>EDPs</i> for (a) transverse frame and (b) longitudinal frame (column 8)	42
Fig. 5.1 Photograph of bench-shelf system-level shake table tests conducted at UC Irvine ...	48
Fig. 5.2 Maximum equipment movement (relative to bench surface) versus peak horizontal <i>bench</i> acceleration (PHBA) for (a) analyzer, (b) small microscope,	

	and (c) large microscope, and maximum equipment movement (relative to bench surface) versus peak horizontal <i>floor</i> acceleration (PHFA) for (d) analyzer, (e) small microscope, and (f) large microscope.....	50
Fig. 5.3	Sample seismic fragility curves for small equipment, considering displacement = 5 cm, a range ϕ values, and: (a) $\mu_s = 0.3$ and (b) $\mu_s = 0.7$	55
Fig. 5.4	Sample generalized lognormal parameters \tilde{m} and cov for $DM =$ maximum relative displacement, bench-mounted equipment category 1 ($\mu_s = 0.35, \mu_k = 0.90$).....	56
Fig. 5.5	Lognormal parameters \tilde{m} and cov for $DM =$ maximum relative displacement, bench-mounted equipment category 2 ($\mu_s = 0.45, \mu_k = 0.90$).....	57
Fig. 5.6	Lognormal parameters \tilde{m} and cov for $DM =$ maximum relative displacement, bench-mounted equipment category 3 ($\mu_s = 0.65, \mu_k = 0.95$).....	57
Fig. 5.7	Lognormal parameters \tilde{m} and cov for $DM =$ maximum relative displacement, bench-mounted equipment category 4 ($\mu_s = 0.70, \mu_k = 0.90$).....	58
Fig. 5.8	Lognormal parameters \tilde{m} and cov for $DM =$ maximum relative displacement, bench-mounted equipment category 5 ($\mu_s = 0.85, \mu_k = 0.95$).....	58
Fig. 6.1	Schematic diagram of experimental setup for friction tests	64
Fig. 6.2	Three pieces of equipment of interest.....	64
Fig. 6.3	Recorded load-displacement plots for three pieces of equipment obtained from pull tests; elastoplastic idealization with μ_k from pull tests; and elastic idealization with μ_k from best fit of shake table tests	65
Fig. 6.4	FORMA incubator resting atop shaking table at Richmond Field Station earthquake simulation laboratory. Locations of wire pots are indicated with white lines, and locations of accelerometers indicated with dark arrows	68
Fig. 6.5	Response time history for Kelvinator refrigerator plotted for Aegion earthquake record	72
Fig. 6.6	Response time history for Kelvinator refrigerator plotted for Coyote Lake, Gilroy Array #6 earthquake record	72
Fig. 6.7	Response time history for Kelvinator refrigerator plotted for Coyote Lake, Gilroy Array #6 earthquake record on 6 th floor level.....	73

Fig. 6.8	Difference between experimental and analytically predicted permanent displacements as a function of rotation about vertical axis	73
Fig. 6.9	Peak recorded sliding displacement of equipment as a function of strength of predominant pulse of excitation; and best linear fit of data.....	75
Fig. 6.10	Comparison of recorded peak equipment accelerations of restrained and freestanding equipment.....	77
Fig. 8.1	Lab fragility functions (a) lab S; (b) lab M; (c) lab LO; (d) lab LL	104
Fig. 8.2	Laboratory capacity as a function of number of critical components (a) median; (b) logarithmic standard deviation.....	105
Fig. 8.3	Lab fragility as a function of <i>IM</i> (a) operability, (b) life safety	106
Fig. 8.4	Lab failure hazard (a) operability and (b) life-safety.....	107

LIST OF TABLES

UC Science Building failure probabilities at three hazard levels	xxxi
Mean failure frequencies and failure recurrence periods.....	xxxi
Table 2.1 Common types of furniture and equipment in laboratories.....	14
Table 2.2 Life-safety priority levels assigned to furniture and equipment	15
Table 2.3 Importance measures for equipment and materials in laboratories.....	16
Table 3.1 Site uniform hazard spectra, 5% damping, S_a at 0.45 seconds.....	24
Table 3.2 Time histories representing 50% exceedance probability of S_a in 50 years.....	25
Table 3.3 Time histories representing 10% and 2% exceedance probability of S_a in 50 years	26
Table 4.1 Correlation matrices of <i>EDPs</i> of transverse frame.....	38
Table 4.2 Correlation matrices of <i>EDPs</i> of longitudinal frame (column 8).....	39
Table 4.3 Ground motion profiles selected for best estimate, 10 th and 90 th percentiles, for transverse and longitudinal frames.....	40
Table 5.1 Summary details of equipment tested in this study.....	46
Table 5.2 Earthquake input motions selected for small equipment shake table tests.....	49
Table 5.3 Generalized categories for small equipment	56
Table 6.1 List of selected records.....	63
Table 6.2 Coefficients of friction and yield displacements obtained from slow pull tests and from best fit of shake table test data	67
Table 6.3 Input motions for shake table tests conducted on three laboratory specimens. Peak table accelerations and peak sliding displacements of freestanding equipment.....	71
Table 7.1 Blunt-force trauma hazard.....	92
Table 7.2 Inventory and fragility functions for critical components in laboratory M.....	93
Table 7.3 Quantity of critical equipment in operational units (labs) examined here	94
Table 7.4 Simplified equipment categories and displacement parameters	94
Table 7.5 Failure distance parameters for shelf and countertop equipment.....	94
Table 8.1 Parameters of operational-unit lognormal fragility functions.....	104
Table 8.2 UC Science Building lab failure probabilities at three hazard levels.....	106

Table 8.3	Mean failure frequencies and failure recurrence periods	108
Table 9.1	Stakeholder roles in nonstructural mitigation decision making	113

EXECUTIVE SUMMARY

Introduction

The Pacific Earthquake Engineering Research (PEER) Center is one of three National Science Foundation (NSF) research centers for earthquake engineering research. The PEER Center's research program is focused on developing a methodology for performance-based design assessment—techniques for simulating ground motions, together with the behavior of structures, to better predict the potential losses as well as the societal impacts of an earthquake event. The goal of performance engineering is to clarify trade-offs and benefits from various design decisions and outcomes. The concept of performance-based engineering for seismic design was first introduced in the late 1970s, when the concept of uncertainty was included in seismic design provisions (ATC 1978). More recently, an approach to performance-based seismic design based on post-earthquake operational capacity was outlined by California structural engineers in “Vision 2000” (SEAOC 1995).

The PEER performance-based assessment methodology formalizes the uncertainty in the relationship between critical analytic stages in an overall framing equation linking hazard analysis, structural analysis, damage probabilities, and calculations of loss. The methodology allows for in-depth analysis of a single facility (such as a building or bridge) and it allows for comparison of alternative design options through multiple probabilistic simulations. The methodology can also be applied to the assessment of transportation networks or groups of buildings in a campus setting. The PEER methodology is different from contemporary loss-estimation approaches in that the formulation attempts to account for sources of uncertainty in each analytic stage and avoid reliance on expert opinion.

From 2002 to 2004 (years five and six of a ten-year funding cycle), the PEER Center organized the majority of its research around four testbeds. Two buildings and two bridges were selected to “exercise” the PEER methodology. These projects involved interdisciplinary teams of researchers, each of whom focused on one aspect of the methodology, producing data to be used by other colleagues in their research. The testbeds demonstrated that it is possible to create the data necessary to populate the PEER performance-based framing equation, but the projects also showed where further research and development were needed.

This report describes one of the building testbeds—the UC Science Building. This project was chosen to focus attention on the consequences from losses to laboratory contents, particularly downtime. While the other building testbed studied performance of an older reinforced concrete hotel building damaged in the Northridge earthquake, the UC Science testbed focused on a well-designed, recently built reinforced concrete laboratory building with high-value and sensitive contents. Detailed data on the UC Science Building were available because the building and the campus were studied in a research program, the Disaster Resistant University (DRU) initiative, funded by the Federal Emergency Management Agency (FEMA) and the University of California, Berkeley (Comerio 2000, 2003).

The Disaster Resistant University Initiative provided risk assessment and mitigation and recovery strategies for other academic institutions (FEMA 2003). At the University of California, Berkeley, the research identified economic and operational vulnerabilities within the university that were not addressed by its seismic retrofit programs. The potential loss of research funding and the impacts on teaching and research from building closures resulting from nonstructural and contents damage (particularly in laboratory buildings) suggested that a better understanding of contents losses as well as the development of mitigation strategies were needed. Using the UC Science Building in one of the PEER testbeds provided an opportunity to take advantage of the data collected in the FEMA/UC project and to focus the PEER methodology on contents as a specific subset of nonstructural losses, and downtime—one of the three decision variables.

Overview of the PEER Methodology

The PEER performance-based assessment methodology is expressed by an equation in which the probability of exceeding losses—expressed as decision variables (*DV*) in terms of casualties, dollar losses, and downtime—is conditioned on the hazard analysis, structural analysis, and damage analysis. Each of the analytic components is done in probabilistic terms, so hazard is defined as the frequency with which an intensity measure (*IM*) is exceeded. The structural analysis is done to determine the engineering demand parameters (*EDP*) such as peak interstory drift, peak floor accelerations, and/or peak forces on structural members. The damage analysis quantifies the frequency that certain damage measures (*DMs*) are exceeded. Because each

component of the analysis is done as a probability of exceeding defined limits, the overall equation represents the integration of independently considered conditional probabilities.

$$G[DV] = \int_{DM} \int_{EDP} \int_{IM} (1 - P[DV | DM]) dP[DM | EDP] dP[EDP | IM] | dG[IM]$$

What is unique to the PEER methodology is the capacity to aggregate data across each discrete disciplinary assessment tool by creating commonly used definitions and methods for sharing data. Conceptually, the PEER methodology would allow an engineer to simulate numerous design alternatives, compare the economic and human consequences of each, and discuss trade-offs among the design schemes with the client. Conceptually, the PEER methodology offers a rigorous and probabilistic assessment of structural and nonstructural performance of building components and systems in order to better predict specific levels of damage, repair costs, and other loss consequences. In application, the individual analytic components demand detailed data which are not always fully available. As a result, the judgments and simplifications may not provide the clear trade-offs necessary for design decisions.

The UC Science Testbed

The UC Science Building is located on the University of California, Berkeley campus, where a significant effort has been made to characterize soil conditions and define the ground motions to be used in retrofitting of campus buildings. Paul Somerville adopted the existing campus hazard analysis to the testbed structure by scaling available campus ground motions to the estimated fundamental period of the building. A survey of all building contents and nonstructural systems was completed by Mary Comerio and William Holmes in the FEMA/UC funded study and these data were made available to the testbed researchers. Mary Comerio (UCB) served as the testbed manager and identified the “mission critical” contents in the building. Khalid Mosalam (UCB) conducted the structural analysis of the building in OpenSees. Tara Hutchinson (UCI) conducted shake table testing on sensitive bench-top equipment, and Nicos Makris (UCB) tested tall, heavy equipment, in order to produce fragility curves. Jim Beck, with Keith Porter (Caltech), estimated the damage and potential operational failures caused by content damage. Stephanie Chang (UW) interviewed stakeholders to assess their understanding of downtime and its contribution to

mitigation choices. Professor Chang also studied how the findings from the UC Science Building testbed could be used in estimating downtime for laboratory space on the campus.

Objectives and Scope

In certain building types, such as museums, high-technology fabrication facilities, and research laboratories, the contents are far more valuable than the building, and in some circumstances may represent a potential hazard to the occupants and the general public. This is the situation at the testbed structure and therefore the objectives were to (1) develop engineering demand parameters (e.g., peak floor accelerations, floor displacements, interstory drift ratios) from a structural analysis of the building; (2) define the critical contents in terms of life-safety, value, and research importance; (3) develop fragility data (the probability of sliding more than a specified distance based on peak horizontal floor acceleration) for critical contents subjected to shake-table tests; and (4) estimate operational and life-safety failure resulting from content damage.

The scope of work did not include a full analysis of the performance of the nonstructural systems in the building (mechanical, electrical, plumbing), nor did it include a loss estimate based on the aggregate of structural, nonstructural, and contents losses. As a result, it is hard to compare the testbed findings to other loss-estimation methods. However, the PEER methodology is not simply a loss-estimating tool in need of calibration; it is a sequence of analytic techniques aimed at assessing the performance of a building and providing data for design decisions. To that end, the testbed demonstrates how the assessment can be undertaken, even if it does not succeed in clarifying design trade-offs or performance outcomes.

The Case Study Building

The UC Science Building is located in the southwest quadrant of the campus, within two kilometers of the Hayward fault. It is a modern concrete building completed in 1988 to provide high-tech research laboratory space for the biological sciences. The building is six stories plus a basement, rectangular in plan, with more than 200,000 square feet (122,000 square feet net useable space) serving approximately 40 individual laboratories. The building is designed with a

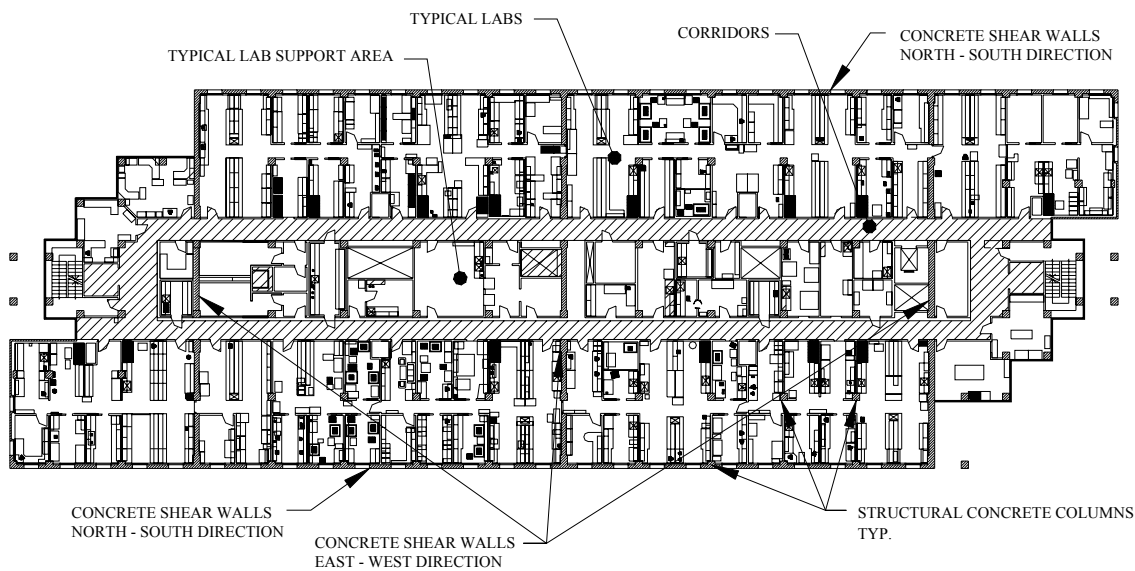
central core of mechanical rooms, circulation, and shared storage and equipment rooms. A loop circulation plan connects the laboratories on the perimeter. Eighty-two percent of the net useable space is in laboratories, with the remainder in offices, conference rooms, stock rooms and other support facilities.



**Location of testbed building
relative to Hayward fault**

The building exterior is simply made of cast-in-place concrete panels. The windows have painted extruded aluminum frames and solar grey glass. The roof is a built-up bituminous roofing system with ceramic tiles used as a mechanical screen. Inside, the building has steel-stud (3-5/8" x 20" gage) and gypsum partition walls, with open ceilings and exposed mechanical piping in the laboratories. Some offices include acoustical drop ceilings, and corridors contain a metal-grid hanging ceiling, concealing mechanical equipment. Floors are either vinyl tile or exposed concrete.

The University of California rated the seismic structural performance of the building to be above average, in the “operational” to “safe” range for moderate (72-year return) to extreme events (2500-year return) (UCB 1997; Comerio 2000). A separate engineering evaluation of the nonstructural systems indicated that anchorage and bracing of systems was more complete than average for this vintage of building. At the same time, the bracing installed for the large pipe systems was judged to be relatively ineffective, leading to a greater chance of water damage from broken pipes (Comerio 2003).



Typical floor plan

Contents

The contents of the UC Science Building was inventoried in the FEMA/UC-funded Disaster Resistant University project focused on seismic protections for laboratory contents (Comerio 2003). In total, there are about 10,500 items in the building—44% is furniture (laboratory benches, wall shelves, desk units), and 56% is equipment (tanks, cylinders, microscopes, computers, refrigerators, freezers, etc.). Shelving is almost half of the furniture, and computer equipment is nearly one quarter of the equipment category. Heavy equipment such as refrigerators and freezers are the next largest group—8% of the equipment.

The contents were documented according to their physical location in the building (in drawings and a database) and they were coded with information specific to each item. Three critical attributes were value, life-safety hazard, and importance to research. Although only 2% of the equipment was considered high-value and 5% was designated by researchers as necessary for continued research, some of these items were highly specialized and difficult to replace, and some were ordinary but contained fragile (and irreplaceable) biological samples. The life-safety hazard category included an assessment of the object as a falling hazard and as a chemical hazard. About one third of all the contents had a high-priority life-safety issue. Any item with

one or more of the three attributes—important, valuable, or a life-safety concern—must be considered when evaluating overall seismic performance.

Based on the inventory of contents in the building, it was clear that small high-value equipment (computers, DNA sequencers, etc.) on bench tops and shelves, hazardous chemicals on shelves, and large heavy equipment (refrigerators and freezers storing samples) were most important in terms of research, value, and life safety. These became the subjects for the shake table tests.

Hazard and Structural Analysis

The first task in evaluating how a building will perform in an earthquake is to estimate accurately the ground motion at the site, and the direction and duration of the shaking. This work is done by seismologists, who base their estimates of ground motion on soil conditions, proximity to the fault, seismic activity estimated for the region, and experience from past earthquakes. Using recorded ground motions from past earthquakes (known as acceleration time history), geotechnical engineers scale the acceleration amplitudes from the records of past earthquakes to match the soil conditions at the site. Because there is so much uncertainty in estimating what could possibly happen at any given site, the determination of adequate intensity measures (*IMs*) is a critical research topic. Although spectral acceleration (S_a) was used in this study, the PEER research program is investigating whether there are better scalar or vector methods to improve ground motion inputs, especially for near-fault motions.

For this testbed, alternative methods of creating intensity measures were not studied. Instead, the ground motions used in the structural analysis were based on the three common earthquake ground motion “scenarios” used by the University of California, Berkeley, for the design of new or retrofitted buildings on the campus. These “scenario earthquakes” represent ground motions defined as a 50% probability of being exceeded in the next 50 years, 10% probability in 50 years, and 2% probability in 50 years, respectively (Somerville 2001). The intensity measure (*IM*) employed in the present study is a 5%-damped elastic spectral acceleration response at an estimated small-amplitude fundamental period of the building model of 0.45 seconds. The research team felt it was important to work on this testbed within the university conventions so that outcomes could be reviewed in comparison to other studies.

Using Somerville's ground motion inputs, Lee and Mosalam (2004) modeled and evaluated the seismic demands on the building using the state-of-the-art OpenSees program, developed by McKenna and Fenves (2001). The modeling includes behavior of the superstructure and the soil-foundation interface in response to seismic input, from near-elastic to near-collapse conditions. The outcomes are expressed in a probability distribution of engineering demand parameters (*EDPs*), such as peak floor acceleration, peak floor displacements, and interstory drift. Lee and Mosalam's research also includes a deterministic sensitivity analysis of the *EDPs* in relation to seismic demand, as these would significantly affect damage to the building contents.

The OpenSees modeling of the building was done at two levels: first, a two-dimensional (2D) analysis of one transverse and one longitudinal frame was completed; and second, a three-dimensional (3D) model of the entire building using multi-directional ground motions was undertaken. Each exercise demonstrated the computational capacity of the OpenSees model for nonlinear elastic analysis. This method essentially takes into account how various components of the structure behave and interact under the motions induced by earthquakes. Although other commercially available structural analysis computer programs (e.g., DRAIN, SAP, etc.) also compute the nonlinear behavior of the structure, OpenSees allows the engineer to see and adjust the assumptions in the code.

Equally important, nonlinear analysis methods are not routine in everyday engineering practice, but they are used by sophisticated practitioners for important projects. Most buildings are designed to meet the minimum standards of the building code using static design methods. This more conventional design process allows engineers to meet legally accepted design standards but does not provide a framework for comparing performance among varying design solutions. By contrast, computer programs created for nonlinear design methods¹, used primarily

¹ For most engineering practitioners, dynamic analysis means modal and elastic analysis, but for structural designers able to spend additional time and conduct more complex analyses, dynamic analysis infers "time history analysis" where the computations follow the behavior of the structure over time.

for complex or important buildings, offer a deeper understanding of building performance and allow the designer to calibrate design outcomes to meet client needs.

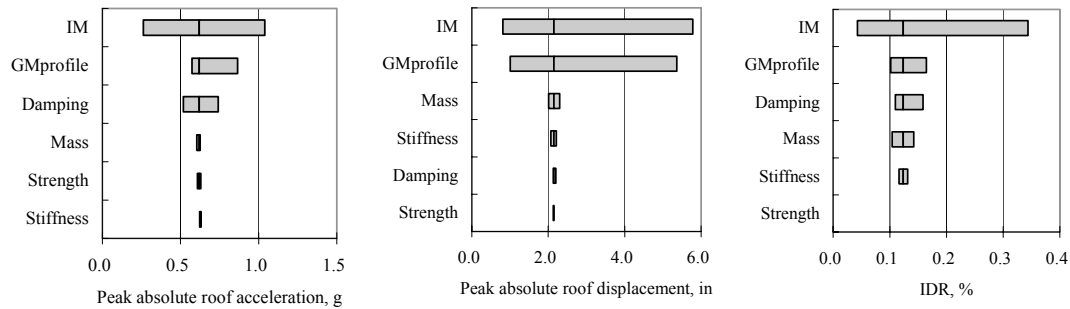
In the UC Science testbed, the outcomes of the structural analysis were used, not for design but to estimate the seismic demand on the structural system and to develop the fragility models of building contents and equipment. These engineering demand parameters (*EDPs*) include the relative and total floor accelerations and displacements², peak absolute floor acceleration and displacement, as well as peak transient interstory drift ratio.

It is important to note that this is one example of the model output for one frame in one earthquake scenario. The 2D and 3D modeling produces significant information on the *EDPs* for each component and for each scenario³. These data are then used in further analysis. In the PEER methodology, the uncertainty in the ground motion causes any *EDP* to be random, and the conditional probability of *EDP*, given *IM*, is estimated based on the sample of mean and standard deviation of the *EDP*. This produces probability distribution curves for each parameter at each story level.

Obviously, changes in other variables affect the outcome of *EDPs* as well. A sensitivity analysis demonstrated that among several variables tested for extreme upper and lower bounds, the intensity measure has the greatest impact on the outcome of *EDP*. Lee and Mosalam checked ground motion intensity and the profile of scaled motions, structural strength and stiffness, building mass, and viscous damping in terms of their impact on peak absolute roof displacement and interstory drift. The figure below demonstrates the influence of the intensity measure on different *EDPs* for both the transverse and longitudinal frame.

² Relative floor acceleration means relative to the ground. Absolute (or total) floor acceleration equals the relative response added to the ground motion, and peak absolute is the maximum total motion expected in a given location.

³ The 3D modeling in OpenSees produced results that were similar but somewhat divergent from the 2D frame analysis. The stiffness of the 2D transverse frame model was underestimated relative to that of the 3D model in the transverse direction, due to the effect of the rigidity of the waffle slab and the longitudinal frames. The actual stiffness of the building in the transverse direction should fall between that of 2D transverse frame model and that of 3D model in the transverse direction. The stiffness estimations in the longitudinal direction by 2D and 3D models match well. Publication of these results are forthcoming.



Deterministic sensitivity results of different *EDPs* for transverse frame

Performance Characteristics of Select Building Contents

Two series of shake table tests were conducted on representative laboratory contents. Samit Ray Chaudhuri and Tara Hutchinson at UC Irvine focused on small equipment positioned on laboratory benches and shelves, and Dimitrios Konstantinidis and Nicos Makris at UC Berkeley tested heavy equipment. In each set of tests, the intent was to understand the behavior of the equipment in various configurations on various floor levels under seismic loading. Both sets of researchers postulated that the seismic excitation would result in sliding-dominated (rather than rocking-dominated) responses based on size and configuration of typical components. For simplification, neither testing program considered vertical motion input. Similarly, each researcher used different earthquake input motions⁴ because the objects and the shake table capacities were different. The horizontal displacement capacity is approximately six inches for the Berkeley table and ten inches for the Irvine table, so tests were done only for ground motions within the limits of the tables. Numerical simulations were necessary to project equipment behavior for larger displacements.

⁴ Because EDPs are expressed in probabilistic terms, the testing cannot represent these estimated motions directly. Instead, the researchers must select a range of ground motions for the shaking table that will cover a broad range of input motions and mathematically simulate the impact at upper floor levels, or at bench-top levels on each floor.

Damage from sliding would result if the equipment fell from a bench or shelf, or if there were impact with a wall or neighboring equipment. The tests characterized how each piece of equipment moved under different loading conditions, and researchers then used analytic methods to estimate the response for loading conditions beyond the shake table's capacity. Each team expressed their findings in the form of a seismic fragility curve, which describes a probability of sliding more than x centimeters, which can then be used to create a seismic fragility function. The fragility function depicts the probability of exceeding a damage measure (DM , such as falling from a countertop or shelf) given an engineering demand parameter (an EDP such as peak horizontal floor acceleration). The damage measures are then used for estimating losses in terms of decision variables (DV) such as operational failure.

The experimental investigation of bench-top equipment included both system- and component-level testing. For the components, the interface between the equipment and the bench or shelf was determined using repeated horizontal and incline pull-tests to determine the coefficients of static and kinetic friction. For the system-level tests four different bench-shelf configurations were built as a mock laboratory. The layout and anchorage details were based on Comerio's documentation of the laboratories.



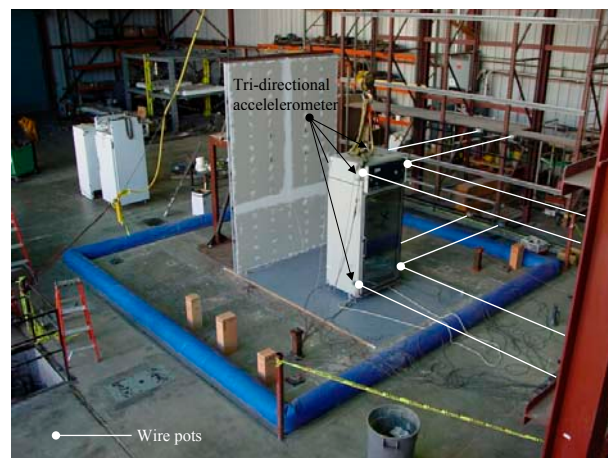
Bench and shelf system on shake table at UC Irvine

The results of the shake table tests show that the maximum displacement (based on an average of multiple positions) relative to the bench surface is less than 10 cm (4 inches) for peak horizontal floor acceleration (PHFA) below 0.8g. It is interesting to note that there is considerable variability in the different bench configurations, illustrating the sensitivity of

response to the different supporting systems. Equally important are the dynamic characteristics (frequency, damping, transmissibility) of the bench-shelf systems. The results from tests on these conditions were combined with analytic data on coefficients of friction and factored into the final results.

Based on the ground motions, using peak horizontal floor acceleration as an *EDP*, the amplifications at the bench tops and the coefficients of friction, the seismic fragility curves were created. An important consideration in this effort is the selection of the damage measure, because the fragility is expressed in terms of a probability of exceeding the damage measure given an *EDP*. Two different measures were examined: sliding displacement and sliding velocity relative to the bench top.

A similar testing procedure was done for the floor-mounted heavy equipment, including pull tests to determine friction between the equipment base and the floor, and full-scale tests of three representative pieces of equipment on a mock-up of the laboratory floor and wall conditions (see following photo). All the tests were one directional and most of the motions of the equipment were along this direction, although the equipment did exhibit some rotations around the vertical axis. The peak sliding distance (PSD) ranges between a low of about 2.5 cm (one inch) to a high of almost 61 cm (24 in.). The researchers attribute the sliding distance to the scale of the main pulse and the restraint from the friction between the base and the floor. They can validate the test results for sliding behavior using mathematical formulations by Newmark (1965) and Makris and Black (2003).



Heavy equipment on shake table at UC Berkeley

The researchers also conducted some tests where the equipment was anchored with chains to a wall, similar to restraint conditions found in the UC Science Building. With the same excitations used in tests on the freestanding equipment, they found that the peak equipment accelerations were significantly higher in all but one test, raising questions about the impact of restraining techniques on the sensitive contents of the equipment. Scale models of the equipment were tested to simulate the behavior of equipment in the stronger earthquake motions causing larger floor displacements. Although the one-quarter scale models exhibited overturning behavior in the experimental tests, it was noted that models had much higher coefficients of friction than those measured for the actual equipment. Numerical simulations with actual values resulted in pure sliding as the mode of response. Finally, this study produced fragility curves for the heavy equipment.

Damage and Loss Analysis

In the PEER methodology, the damage measure (*DM*) is a measure of physical damage to structural and nonstructural building elements, and/or specific contents. The *DM* is quantitative and based on the engineering demand parameters (*EDPs*), as opposed to qualitative measures, such as “light damage.” A fragility function typically expresses the probability of exceeding a specified damage measure for a given *EDP*. Damage is then used to estimate potential losses in one of three areas: repair costs, casualties (or the occurrence of life-threatening damage), or downtime (or the loss of operability). These loss estimate categories represent critical decision variables—categories of information that can inform performance design decisions or trade-offs between one design feature and another.

In this testbed, the research team was interested in the impact from damage to laboratory equipment on downtime. The California Institute of Technology researchers, Beck, Porter, and Shaikhutdinov, defined losses in terms of (1) the overturning of large floor-mounted equipment or (2) damage from falling countertop- or shelf-mounted equipment. To evaluate failure probability in terms of potential operational malfunction or life-safety condition, they focused on the subset of critical equipment in laboratories that was categorized by Comerio as “a life-safety hazard, a chemical hazard, or critically important to research.” In the UC Science Building, there are approximately 40 laboratories run by individual researchers and other shared spaces. In

order to choose a sample of representative operational units, they subdivided the building into 50 operational units (the research labs plus other specialized spaces) and estimated the number of items of critical equipment in each. Four sample operational units were selected:

1. Lab S: a small number of critical components (life-safety and operations)
2. Lab M: a laboratory with a medium quantity of critical components
3. Lab LO: a laboratory with a large quantity of operationally critical components
4. Lab LL: a laboratory with a large quantity of life-safety critical components

The goal was to focus on the performance of critical equipment in representative operational units, measuring the probability that a unit would have to close because of damage to critical equipment. They developed probabilistic edge distances for countertop- and shelf-mounted equipment, and employed the laboratory test sliding-distance data to create equipment fragility functions, which give the probability of an object sliding off its countertop or shelf, as a function of *EDP*. Since tests of the large floor-mounted equipment produced no overturning, they assumed that this equipment would not contribute substantially to failure probabilities, and focused instead on the smaller equipment.

For this study, the researchers evaluate operational failure based on the probability of loss of equipment categorized as “important” and life-safety failure based on probability of loss of equipment listed as “life-safety category D”⁵ or identified by campus personnel as a “chemical hazard.” Shelf- and bench-mounted items are defined as failing in sliding off their shelves or benches (which presumably would cause them to break), and failure of floor-mounted equipment is by overturning (which presumably would cause damage to their contents). For each of the four sample operation units, operational unit fragility functions were developed, and the results were plotted for each lab and as a function of the number of fragile components in each laboratory. This process allows the researchers to estimate potential losses in other laboratories based on the number of critical components.

⁵ Although failure of a single piece of equipment categorized as “important” may well lead to a loss of operations, failures of life-safety category D equipment are unlikely to cause a casualty or injury in every case. An additional casualty rate factor is necessary to relate equipment features to casualties.

The following table shows the failure probability for each sample laboratory type, conditioned on the intensity measure (*IM*) or ground motion. This table also suggests high failure probabilities—that is, high likelihood that equipment damage would limit operations or cause injury. Even at the lowest hazard level, the probability of life-safety failure exceeds 20% for all four labs examined here. Operational failure becomes likely in the 10%/50-yr event or higher. From both perspectives, mitigation is probably called for, but the decision would have to be balanced against cost, and improvements in operability resulting from the mitigation. The second table shows the data described in terms of the mean frequency of failure.

UC Science Building failure probabilities at three hazard levels

Lab	Floor	n_{Op}	n_{LS}	Hazard level					
				$S_a = 0.71g$ 50%/50 yr (0.0139 yr ⁻¹)		$S_a = 1.62g$ 10%/50 yr (0.0021 yr ⁻¹)		$S_a = 2.74g$ 2%/50 yr (0.0004 yr ⁻¹)	
				Operability	Safety	Operability	Safety	Operability	Safety
S	1	1	1	0.2%	20.4%	1.2%	74.2%	7.2%	94.1%
M	3	3	5	7.8%	48.4%	41.6%	93.7%	73.3%	99.5%
LL	4	1	12	4.7%	56.2%	14.2%	95.9%	44.8%	100.0%
LO	4	14	6	11.8%	43.2%	45.0%	95.3%	91.8%	100.0%

Mean failure frequencies and failure recurrence periods

Lab	Operability			Life safety		
	λ, yr^{-1}	T, yr	$P[ruin]$	λ, yr^{-1}	T, yr	$P[ruin]$
S	0.0001	>1000	0.2%	0.0073	140	14%
M	0.0035	290	6.8%	0.0242	41	38%
LO	0.0045	220	8.7%	0.0174	57	29%
LL	0.0018	560	3.5%	0.0414	24	56%

Issues for Decision Makers

While the PEER methodology is focused on the technical assessments of structural and nonstructural system performance, researchers also need to know how owners and users of buildings make decisions about hazard-related building concerns. What kind of information do they need? What kinds of decisions do they make? How do they conceptualize seismic performance? To answer these questions, Falit-Baiamonte and Chang, of the University of Washington, reviewed previous studies of seismic decision making (DeVries et al. 2000; Pannor 2002) and interviewed managers and researchers associated with the UC Science Building. Some of the findings are as follows:

- Faculty researchers were key decision makers.
- Mitigation was largely funded by researchers and implemented by in-house craftsmen.
- Stakeholders conceptualize performance in terms of both life-safety and downtime, but they understand it in binary terms (it is fixed or it is not).
- Downtime is perceived in terms of months to years based on fears of lost data or specialized equipment.

Decisions associated with mitigation of seismic hazards for laboratory contents in the UC Science Building involve a variety of stakeholders, not only the faculty researchers but also the operations staff, the craft professionals, various administrators, and safety managers. These individuals must interact within the framework of existing work processes and schedules. While they would like the labs to be “as safe as possible,” they are unaware of the concept of performance levels or alternative approaches to limit earthquake impacts. The researchers suggested that information on mitigation alternatives needed to be accompanied by estimates of the cost and time required for implementation, the impact of mitigation on lab workflow, and the potential damage states of the equipment in a seismic event after mitigation.

Using the Testbed Experience to Direct Future Research

William T. Holmes, the Business and Industry Partner associated with the UC Science testbed, and co-author of an *Implementation Manual for the Seismic Protection of Laboratory Contents* (Holmes and Comerio 2003), worked with the team throughout the project and pushed researchers to find the practical engineering applications within the research agenda. Because his work focused on the application of the testbed results, he expressed concern that the testbed

research—particularly the shake table testing—did not resolve a number of practical issues for engineering design. These include questions such as:

- Are shelf lips effective to keep contents on shelves? How high should they be?
- Will bench-top and shelf equipment be damaged when packed close together as in the labs?
- Are the outcomes of the testing valid for the much larger floor displacements expected in the building?
- When and how might large equipment overturn, or create life-safety hazards from sliding?
- Will high accelerations for anchored heavy equipment damage equipment contents? What kind of anchorage, if any, should be employed?

These questions are critical to a practicing engineer attempting the design of a mitigation scheme for laboratories, and the testbed did not resolve them. In general, the testbed demonstrated a successful trial of the methodology, but it also demonstrated the high level of complexity required for performance assessment, and the large amount of calibration data needed to predict quantitative damage measures in dollars, casualties, and duration of downtime.

Each component of the PEER methodology—the hazard analysis, the structural analysis, the development of damage measures, loss estimates and decision variables—relies on sophisticated analytic procedures. However, to provide input data from one stage to the next, many simplifications and assumptions were needed to complete the process. For example, the estimate of operational failure of laboratory equipment relied on fragility curves derived from shake table tests of a relatively small number of equipment samples, where the true scale of input motions could not be simulated because of shake table limitations. Further, the estimate of operational and life-safety failure was based primarily on sliding. The results did not take into account the presence of a shelf lip, overturning, and a number of other more subtle damage conditions that were not tested for in our laboratory experiments. Nor did the results consider the likelihood of injury to occupants, given a failure. Unfortunately, an enormous amount of detailed data on how each piece of equipment responds to the shaking at the floor or bench level would be necessary to translate the engineering demand parameters, such as peak floor acceleration, or interstory drift, into accurate measures of damage and its influence on downtime.

The testbed research raises several questions regarding the direction of performance modeling in general, and the development of the PEER methodology specifically. *First, what is the real goal of a performance measure?* The PEER method argues that comparing losses (the probability of exceeding losses such as casualties, repairs costs, or downtime) provides a

rationale for performance design trade-offs. However, researchers who work on loss modeling are typically wary of estimates of losses based on a single building or structure. With the best analytic procedures, it may be possible to accurately represent damage, and estimate construction costs for repairs, but casualties and downtime are difficult to model, as methods and data are scarce. Still, an important outcome from the PEER performance engineering methodology will be to develop a basis for consistent assessment of performance between systems (concrete, steel, wood, etc.). These could be used in the prescriptive code provisions and to allow alternative analysis and design methods that will give equivalent or measurably better performance than the prescriptive code. As a broad goal, this is achievable and PEER's benchmarking studies of existing code buildings will contribute to that goal.

There have been significant breakthroughs in the field of structural engineering in the last decade, in part based on the wealth of measured ground motions and building and infrastructure behavior in recent earthquakes. At the same time, it was the enormity of the financial losses that prompted the engineering community to look for ways to give clients a voice in the "performance expectations." However, the post-event research on losses has demonstrated that costs are largely resulting from damage to nonstructural systems and contents, which leads to the second key question on performance-based design. *How well can structural engineers model the impacts to nonstructural systems and contents?*

There is little fundamental research on the behavior of nonstructural systems, equipment and contents, compared with what has been done for structural systems. Although work is progressing (see ATC 29-2, 2003), it is not clear that we can expect to understand with precision how these building subsystems will be damaged (again, the absence of models and data). As such, the link between coarse estimates of damage and actual losses is tenuous. At first glance, it may appear to be easier to simply estimate whether structural systems will have greater or lesser impacts on damage to nonstructural systems, and focus the performance attention (and the design trade-offs) on the structural system. However, nonstructural performance cannot be predicted solely on structural behavior, as it is dependent on (1) drift, (2) floor accelerations (that trend opposite from drift), and (3) the design of and interaction between the nonstructural systems themselves.

Despite the difficulties in modeling, it is critically important for PEER to continue to include all building components in the performance assessment methodology in order to

represent the relationship between the earthquake hazard, the performance of all systems, and the contents, damage, and consequences associated with specific design decisions or standards. This testbed pushed the limits of performance modeling by attempting to quantify the potential losses to laboratory contents using the PEER methodology. We have shown the difficulty of taking the process down to individual components, or worse, to inter-related groups of components. At the same time, we learned that perhaps we can simplify the procedure by devising fragilities for spatial components—such as an individual laboratory—to make the analysis more manageable.

The third and final question that is raised by the UC Science testbed experience is *Can the methodology be simplified?* This question has a larger philosophical component as well as a more direct pragmatic component. More broadly, it asks whether or not performance design trade-offs are best understood in terms of probable losses (in terms of deaths, dollars, and downtime), given the uncertainties in translating intensity measures into engineering demand parameters, into damage measures, and finally into losses. Today, professionals tend to separate damage estimates (and probable repair costs) from estimates of casualties or downtime. Within the PEER methodology, these are integrated to include a range of alternative and interdependent consequences. At a practical level, however, each of the PEER analytic components (hazard, structure, damage, and loss models) currently employs sophisticated and time-consuming methods. It would be practical to develop simplified approaches to each component so that an engineer could choose which component to explore in detail, or in combination, with shorthand inputs from simplified methods.

In summary, the PEER methodology for performance-based design offers a conceptual approach to quantifying design trade-offs. It lays out the relationships between ground motions, structural behavior, damage, and losses, and suggests that the analytic techniques used by different engineering professionals and decision makers can find common ground through the use of a common language. The PEER testbeds demonstrated applications of this approach in buildings and bridges. The results from that experience have demonstrated the strengths and weaknesses in the methodology and point to a variety of ways to improve and simplify performance-engineering design. Other research is needed to fully investigate how changes in design methods will be adopted into current regulatory systems and decision processes.

References

Applied Technology Council (1978) "Tentative Provisions for the Development of Seismic Regulations in Buildings." Applied Technology Council Publication # ATC-03, (amended as ATC-03-06 in 1982), Redwood City, CA.

Applied Technology Council (2003) Proceedings of Seminar on Seismic Design, Performance, and Retrofit of Nonstructural Components in Critical Facilities, Applied Technology Council Publication # ATC-29-2, Redwood City, CA.

Comerio, M. C., 2003, *Seismic Protection of Laboratory Contents: The U. C. Berkeley Science Building Case Study*, IURD WP #2003-02, University of California, Berkeley, CA. Available at: http://www-iurd.ced.berkeley.edu/pub/abstract_WP200302.htm

Comerio, M. C., and Stallmeyer, J. C., 2003, Laboratory Equipment: Estimating Losses and Mitigating Costs, *Earthquake Spectra*, Vol. 19, No. 4, Nov. 2003.

Comerio, M. C., 2000, *The Economic Benefits of a Disaster Resistant University*, IURD WP #2000-02 University of California, Berkeley, CA. Available at: http://www-iurd.ced.berkeley.edu/pub/abstract_WP200002.htm

Comerio, M. C., and Stallmeyer, J. C., 2001, *Nonstructural Loss Estimation: The UC Berkeley Case Study*, Peer Report # 2002-01, Pacific Earthquake Engineering Research Center, University of California, Berkeley, CA.

Falit-Baiamonte, A. and S. E. Chang. 2003. "Background on non-structural seismic mitigation decision-making at UC Berkeley." PEER Discussion Paper.

Hamburger, R.E., Court, A.B., Soulages, J.R. (1995), "Vision 2000: A Framework for Performance Based Engineering of Buildings," Proceedings of SEAOC Annual Convention. Indian Wells, California.

Holmes, W. T., and Comerio, M. C., 2003. *Implementation Manual for the Seismic Protection of Laboratory Equipment: Format and Case Study Examples*. PEER Report 2003/12, Pacific Earthquake Engineering Research Center, University of California, Berkeley, CA.

Hutchinson, T.C. and Ray Chaudhuri, S. (2003). "Bench and shelf-mounted equipment and contents: shake table experiments." In the Proceedings of the Applied Technology Council Seminar on Seismic Design, Performance, and Retrofit of Nonstructural Components in Critical Facilities. ATC-29-2. Newport Beach, CA. 15 pp.

Konstantinidis, D. and Makris, N. "Experimental and Analytical Results on the Seismic Response of Slender Laboratory Equipment." *Proceedings of the ATC-29-2 Seminar on Seismic Design, Performance, and Retrofit of Nonstructural Components in Critical Facilities*. Newport Beach, California, October 23-24, 2003.

Konstantinidis, D. and Makris, N. (2004), *Experimental and Analytical Seismic Response of Building Contents*, Report No. PEER-2004/xx, Pacific Earthquake Engineering Research Center, University of California, Berkeley, CA.

Lee, T.-H. and Mosalam, K.M. 2003a. Sensitivity of seismic demand of a reinforced concrete shear-wall building. *Proc. Ninth Int. Conf. on Applications of Statistics and Probability in Civil Eng.*, ICASP9, San Francisco, July 6-9, 2003.

Lee, T.-H. and Mosalam, K.M. 2003b. Probabilistic fiber element modeling of reinforced concrete columns. *Proc. Ninth Int. Conf. on Applications of Statistics and Probability in Civil Eng.*, ICASP9, San Francisco, July 6-9, 2003.

Lee, T.-H. and Mosalam, K.M. 2004, Probabilistic modeling of reinforced concrete structural systems subjected to seismic loading. *Pacific Earthquake Engineering Research center*, (PEER Report No. 2004/xx, Pacific Earthquake Engineering Research Center, University of California, Berkeley, CA.

McKenna, F. and Fenves, G.L. 2001. OpenSees Manual. *PEER Center*, <http://opensees.berkeley.edu>.

Ray Chaudhuri, S. and Hutchinson, T.C. (2004). "Fragility of bench-mounted equipment considering uncertain parameters." Submitted to ASCE Journal of Structural Engineering (In Review).

Ray Chaudhuri, S. and Hutchinson, T.C. (2004). "Performance characterization of bench- and shelf-mounted equipment and contents." PEER Report No. 2004/xx. Pacific Earthquake Engineering Research Center, University of California, Berkeley, CA.

Somerville, P.G., 2001, Ground Motion Time Histories for the UC Lab Building, URS Corporation, Pasadena, CA, 15pp.

Structural Engineers Association of California (SEAOC), 1995, "Vision 2000, conceptual framework for performance-based seismic design," *Recommended Lateral Force Requirements and Commentary, 1996, 6th Edition*, Sacramento, CA, 391-416

URS Corporation, 2000, *Probabilistic Ground-Motion Analysis for the Central Campus*, Draft report prepared for the UC Berkeley Seismic Guidelines Project, June 8, 2000.

1 Introduction

Helmut Krawinkler, Stanford University; Keith A. Porter, California Institute of Technology; and Mary C. Comerio, University of California, Berkeley

1.1 BACKGROUND

Since its inception in 1997, PEER has focused on the development of methodologies and tools for performance-based earthquake engineering. Performance-based earthquake engineering (PBEE) implies design, evaluation, and construction of engineered facilities in which performance under common and extreme loads responds to the diverse needs and objectives of owners-users and society. It is based on the premise that performance can be predicted and evaluated by engineers with quantifiable confidence in order to make, together with the client, intelligent and informed trade-offs based on life-cycle considerations rather than construction costs alone. So far, PEER has focused on methods of performance assessment, with due consideration given to the effects of all important uncertainties that enter the performance prediction process, from earthquake occurrence modeling to the assessment of earthquake consequences such as dollar losses or casualties.

If it were not for uncertainties, the performance prediction process would be rather straightforward and would mimic what good engineering companies practice today. Present practice is to describe the earthquake intensity deterministically at discrete hazard levels, develop a deterministic model of the structure, and predict, deterministically, response parameters such as story drifts, which are compared to deterministic limits (e.g., story drift ≤ 0.02) in order to judge the adequacy of a design. It is well established that uncertainties in each part of this process make performance assessment so much more complex, but also so much more realistic. The PEER PBEE methodology tries to face up to these complexities.

Much of the PEER development effort has been directed towards individual parts of the complex process of probabilistic performance assessment. It needs to be found out how the parts of this methodology fit together to make a whole that (1) leads to consistent, understandable, and

repeatable end results, (2) has most of the important parts in place, (3) can be put in perspective with respect to presently employed engineering approaches, (4) can be shown to be implementable by the profession, and (5) can be interpreted by all stakeholders in an understandable manner that helps individuals and organizations to make informed decisions.

1.2 OBJECTIVES AND SCOPE

To address the aforementioned questions, PEER has created a testbed program in which different parts of the PBEE methodology have been applied, tested, and modified as needed, on several testbed structures. In the building domain, two testbed structures have been utilized, one the Van Nuys Hotel Building and the other the UC Science Building. This report is concerned with the latter.

There are many parts and variations to the PBEE methodology being developed in PEER, which is briefly summarized in Section 1.3. The testbeds were selected so that their locations, site conditions, structural configurations, uses, and decision impacts differ to the extent that complementary parts of the PBEE methodology can be tested in the performance assessment process. The UC Science Building was chosen to focus attention on the consequences from losses to high-value contents and downtime. The UC Science Building is a relatively new frame and shear wall structure, located in an area in which near-fault ground motions dominate the long return-period hazard, and its use as a biological laboratory building makes content performance the dominant behavior issue.

On the other hand, for the Van Nuys Hotel Building, the primary performance issues are dollar losses due to structural and nonstructural damage, and the probability of collapse that dominates the life-safety issue. The building is a relatively old, reinforced concrete frame building (built in the 1960s) but is located on firm soil and in an area in which near-fault ground motions are not prevalent.

For the UC Science Building, the emphasis is on estimating life-safety or operational failure, based on contents damage. The seismic hazard and ground motion issues were not investigated in this testbed. Existing ground motion estimates for near-fault conditions on the UC Berkeley campus were used. The research challenges are in the prediction of engineering demand parameters (*EDPs*), which are needed as the basis for shaking table tests of critical contents, in the development of fragility functions for contents, and in the creation of loss

functions that recognize the impact on downtime from damage to research tools, data, and biological samples. These issues will receive much attention in this report.

In addition to testing the research processes developed within PEER, business and industry partners involved in the testbed project have used the data and findings to develop a manual for engineering practitioners outlining an approach to the seismic protection of laboratory contents with case studies of campus buildings. The input from engineering practitioners to the testbed helped guide our research and ensures that the PEER methodology can contribute materially to the value engineering practitioners can offer to users and society.

1.3 OVERVIEW OF PEER'S PBEE METHODOLOGY

The PEER performance assessment methodology has been summarized in various publications; the following ones serve as references for the interested reader: Cornell and Krawinkler 2000; Krawinkler 2002; Deierlein et al. 2003; Krawinkler and Miranda 2004; and Moehle and Deierlein 2004. This summary discussion is concerned with the performance assessment of buildings.

The PEER performance assessment methodology is illustrated in Figure 1.1. As shown, the methodology embodies four stages: hazard analysis (the quantification of the frequency and intensity of earthquakes and of the ground motions that represent the effects of earthquakes at a particular site), structural analysis (the quantification of the response quantities needed for loss, downtime, collapse and casualty evaluation [i.e., collapse analysis, shown separately in Figure 1.1, can be viewed as part of structural analysis], damage analysis (the quantification of damage states and their relation to response parameters), and the evaluation of losses, downtime, and casualties, and their consequences for the owner and society.

The end of the process is a consequence analysis, which necessitates the quantification (in probabilistic terms) of variables that can be employed to judge consequences. These variables are denoted as **decision variables, DVs**. Examples are dollar losses, length of downtime, or number of casualties. The task at hand is to compute these *DVs*, given that all relevant building systems, i.e., the soil/foundation/structure system as well as the nonstructural and content systems, are known and that sufficient information is available to quantify seismic input, structural response, damage, cost of repair, length of business interruptions, operational or life-safety failure, and the probability of collapse, which then needs to be related to the number

of deaths. In the assessment process the key issue is to identify and quantify, with due consideration to all important uncertainties, decision variables of primary interest to the decision makers. The components of the assessment process can be briefly summarized as follows.

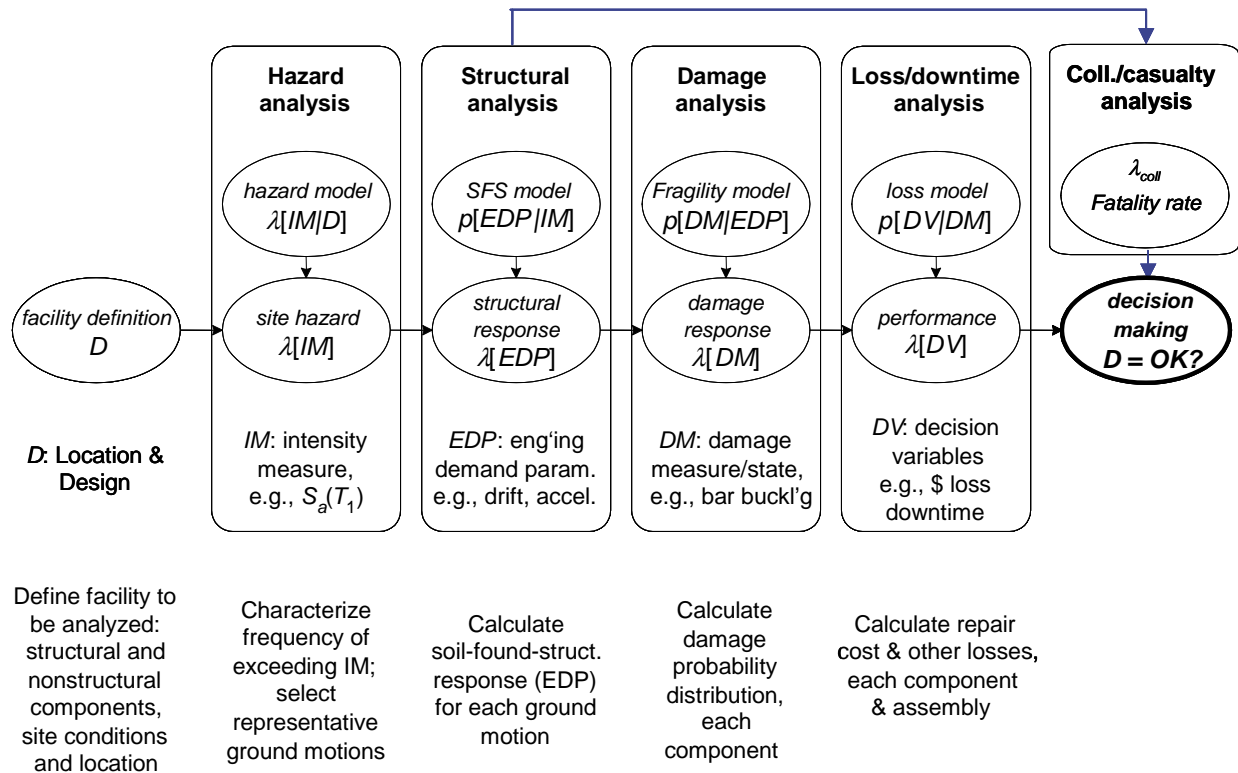


Fig. 1.1 Overview of PEER performance assessment methodology

Hazard analysis. The first step is to calculate the seismic hazard, quantified here as the frequency with which specific values of a relevant scalar or vector **intensity measure (IM)** are exceeded. If a scalar IM is used, such as the 5% damped spectral acceleration at the first mode period, $S_a(T_1)$, the hazard usually is defined in terms of a hazard curve. The outcome of hazard analysis, which forms part of the input to structural analysis, is usually expressed in terms of a mean annual frequency (MAF) of exceedance of $IM(s)$, i.e., $\lambda(IM)$, as shown in the lower half of the first box of Figure 1.1. A challenge that will be discussed in Chapter 3 is the selection of ground motions, which, when scaled to the selected IM , provide an efficient and sufficient means to represent the ground motion effects on the structure associate with the selected IM .

Structural analysis. Given the ground motion hazard, a vector of **engineering demand parameters, EDPs**, (second box in Fig. 1.1) needs to be computed, which defines the response

of the building in terms of parameters that can be related to *DVs*. The *EDP* vector should include all parameters of relevance for damage and losses to the soil/foundation/structure system as well as the nonstructural and content systems. Interstory drift is an example of a relevant *EDP*. Relationships between *EDPs* and *IMs* are typically obtained through inelastic dynamic analyses, which should incorporate, to the extent feasible, the complete structural, geotechnical, SFSI (soil-foundation-structure-interaction), and nonstructural systems. The outcome of this process, which may be referred to as “probabilistic seismic demand analysis,” can be expressed as $p(EDP|IM)$, or more specifically as $P[EDP \geq y | IM = x]$, which is the probability that the *EDP* exceeds a specified value y , given (i.e., conditional) that the *IM* (e.g., $S_a(T_I)$) is equal to a particular value x . When integrated over the appropriate *IM* hazard curve, the MAF of exceedance of *EDP(s)*, i.e., $\lambda(EDP)$, as shown in the lower half of the second box of Figure 1.1 is obtained.

Damage analysis. To close the loop, *EDPs* have to be related to the *DVs* of interest. In most (but not all) cases an intermittent variable, called a “**damage measure,**” ***DM***, has to be inserted between the *EDP* and the *DV*, simply to facilitate the computation of *DVs* from *EDPs*. A *DM* describes the damage and consequences of damage to the structure or to a component of the structural, nonstructural, or content systems, and the term $P(DM|EDP)$ can be viewed as a fragility function for a specific damage (failure) state (probability of being in or exceeding a specific damage state, given a value of *EDP*). The *DMs* in the Van Nuys testbed include, for example, descriptions of necessary repairs to structural or nonstructural components. As used in this testbed, the *DMs* represent significant sliding or overturning that would cause the equipment to fail. The loss of key equipment is equated to lab closures. Specifically, the *DMs* are a result of an equipment fragility function, which gives the probability that the equipment will be damaged in some predefined way, given one or more *EDP* parameters to which it is subjected. If the fragility functions for all relevant damage states of all relevant components are known, the *DVs* of interest can be evaluated either directly or by means of cost or downtime functions that relate the damage states to repair/replacement costs or replacement times.

Loss analysis. The goal of the loss analysis is to estimate the frequency with which various levels of performance are exceeded. Performance can be parameterized via one or more decision variables (*DV*). *DVs* are defined at the system level, such as total repair cost, number of casualties, or repair duration (sometimes called “dollars, deaths, and downtime”). *DVs* can be expressed in terms of expected annual values (most meaningful for cost-benefit analysis),

probability of exceeding certain intolerable levels (relevant to risk-of-ruin analysis and for purchasing insurance), or mean values conditioned on a meaningful scenario event. In this testbed study, the DVs of primary interest are life-safety failure or operational failure, either during a particular planning period or in some large, scenario event.

The framework equation for performance assessment. The aforementioned steps, which form the basis of performance assessment, can be expressed in the following equation for a desired realization of the DV , such as the MAF of the DV , $\lambda(DV)$, in accordance with the total probability theorem:

$$\lambda(DV) = \iiint G\langle DV|DM \rangle dG\langle DM|EDP \rangle dG\langle EDP|IM \rangle d\lambda(IM) \quad (1.1)$$

This equation, which is often referred to as the “framework equation for performance assessment,” suggests a generic structure for coordinating, combining, and assessing the many considerations implicit in performance-based seismic assessment. Inspection of Equation 1.1 reveals that it “de-constructs” the assessment problem into the four basic elements of hazard analysis, structural analysis (demand prediction), damage analysis, and loss analysis, by introduction of the three intermediate variables, IM , EDP , and DM . Then it re-couples the elements via integration over all levels of the selected intermediate variables. This integration implies that in principle one must assess the conditional probabilities $G(EDM|IM)$, $G(DM|EDP)$ and $G(DV|DM)$ parametrically over a suitable range of DM , EDP , and IM levels.

In the form written, the assumption is that appropriate intermittent variables ($EDPs$ and DMs) are chosen such that the conditioning information need not be “carried forward” (e.g., given EDP , the DMs (and DVs) are conditionally independent of IM ; otherwise IM should appear after the EDP in the first factor). So, for example, the $EDPs$ should be selected so that the DMs (and DVs) do not *also* vary with intensity, once the EDP is specified. Similarly one should choose the intensity measures (IM) so that, once it is given, the dynamic response (EDP) is not also further influenced by, say, magnitude or distance (which have already been integrated into the determination of $\lambda(IM)$) (Krawinkler and Miranda 2004).

Role of uncertainties. The performance-assessment process described herein would be routine were it not for the presence of uncertainties. It is the uncertainties and their propagation through the assessment process that pose the challenge in PBEE. A critical aspect is the identification of important uncertainties that have a *significant* effect — not on intermittent

results but on the final result, usually expressed in terms of *DVs*. We identify the major sources of uncertainty in $p[DV]$, quantifying the contribution at each step from *IM*, *EDP*, and *DM* to *DV*, considering propagation and correlation. We identify the sources of uncertainty that are most significant *in this situation*, and those that can be neglected. Of the major contributors, we identify opportunities for reducing uncertainty by additional data-gathering or by changes in modeling. It is understood, however, that the importance of uncertainties is case specific and may vary depending on the type of building, site, and seismic action.

Stakeholders and decision issues. Although decision variables (*DVs*) can be expressed in a variety of formats, it is not always clear which approach would resonate with decision makers. Interviews were conducted at the University of California to assess who the stakeholder groups would be, what kinds of decisions they make, and what information they need. The goals of this review are to understand what drives structural and nonstructural mitigation decisions in this particular case study, and what lessons can be drawn from this experience in presenting loss information in the PEER methodology.

1.4 ORGANIZATION OF REPORT

The present chapter has introduced and provided an overview of the PEER PBEE methodology and explained the purpose of the present study. The following chapters detail the analysis of the study facility. Chapter 2 presents the facility definition. The hazard analysis is provided in Chapter 3. Chapters 4–6 present the structural analysis, and the results of shake table testing. Chapter 7 describes the use of fragility functions developed in tests in the damage analysis, and Chapter 8 discusses the loss analysis. Chapter 9 examines stakeholders and decision issues. A critique of the methodology from the engineering practitioner’s viewpoint is presented in Chapter 10. Chapter 11 draws lessons and discusses future research directions. References are cited at the end of each chapter.

2 Facility Definition

Mary C. Comerio, University of California, Berkeley

2.1 OBJECTIVES AND SCOPE

In certain building types, such as museums, high-technology fabrication facilities, and research laboratories, the contents may be far more valuable than the building, and in some circumstances may represent a potential hazard to the occupants and the general public. At many universities, laboratories are often one-third of the net space on campus. Laboratories represent both a concentration of research (as measured by annual funding) and a concentration of valuable equipment and ideas. For this portion of the study, we inventoried the contents of a modern laboratory building on the University of California, Berkeley campus to develop an understanding of the materials at risk in earthquakes. The inventory allowed the research team to select certain classes of items for shake-table testing and served as the base data for the loss model.

2.2 CASE STUDY BUILDING CHARACTERISTICS

The case study building is a modern concrete building completed in 1988 to provide high-technology research laboratories for organismal biology. It is located in the southwest quadrant of the campus, within 2 km of the Hayward fault. The building is 203,800 square feet overall, with 122,000 assignable (net usable) square feet of research laboratories, animal facilities, offices, and related support spaces. The building is six stories plus a basement, and is rectangular in plan with overall dimensions of approximately 306 feet in the longitudinal (north-south) direction and 105 feet in the transverse (east-west) direction. The basement is contained within the periphery of the building.

This building was built as part of a larger campus plan to upgrade research and teaching facilities in the biological sciences. More than 40 faculty members use its laboratory space. The building is designed with a central core of mechanical rooms, circulation, and shared storage and equipment rooms. A loop circulation plan connects the eight to ten laboratories on the east and west sides of the building. An internal corridor provides a secondary circulation system within the laboratories. Research offices are situated within the laboratories.

The laboratories are designed in a modular format so that a laboratory/office space may expand or contract by adding or removing a module along the corridor. Although the building was planned with all laboratories in a standard configuration, the laboratories undergo regular remodels to accommodate new research techniques and equipment. Two floors—the basement and the sixth floor—include highly specialized laboratory and storage for fragile biological specimens. Eighty-two percent of the net usable area is used for laboratory space and animal facilities. The remainder of the space accommodates offices, administrative space, conference rooms, stockrooms, and other support facilities.

The building's exterior is simple, with cast-in-place concrete panels and a light sandblast finish. The windows have a painted extruded aluminum frame with solar grey glass. The rooftop mechanical penthouse is set back from the walls. Ceramic roof tiles are used as a mechanical screen, but the roof is made of a built-up bituminous roofing system with layers of asphalt and fiberglass felt, covered with black gravel.

Inside, the building has steel-stud (3-5/8" x 20" gage metal) and gypsum partition walls to divide laboratories. Typically ceilings are open in the laboratories, with exposed mechanical piping. Some offices contain acoustical drop-ceilings, and the corridors have a metal-grid hanging ceiling to cover mechanical equipment. Floors are either vinyl tile or exposed concrete. The floors are not impermeable to toxic spills.

The building was selected for this study because the structural system is expected to perform well⁶ in earthquakes and the research focus would be on the performance of building contents and their contribution to losses, particularly downtime. An evaluation of the nonstructural systems indicated a level of anchorage and bracing more complete than average for this vintage of building, confirming the expected low damage levels at least for the occasional shaking. However, in general, the seismic bracing installed for the larger pipe systems was judged relatively ineffective, leading to more expected damage to those systems and a greater chance of water damage from broken pipes.

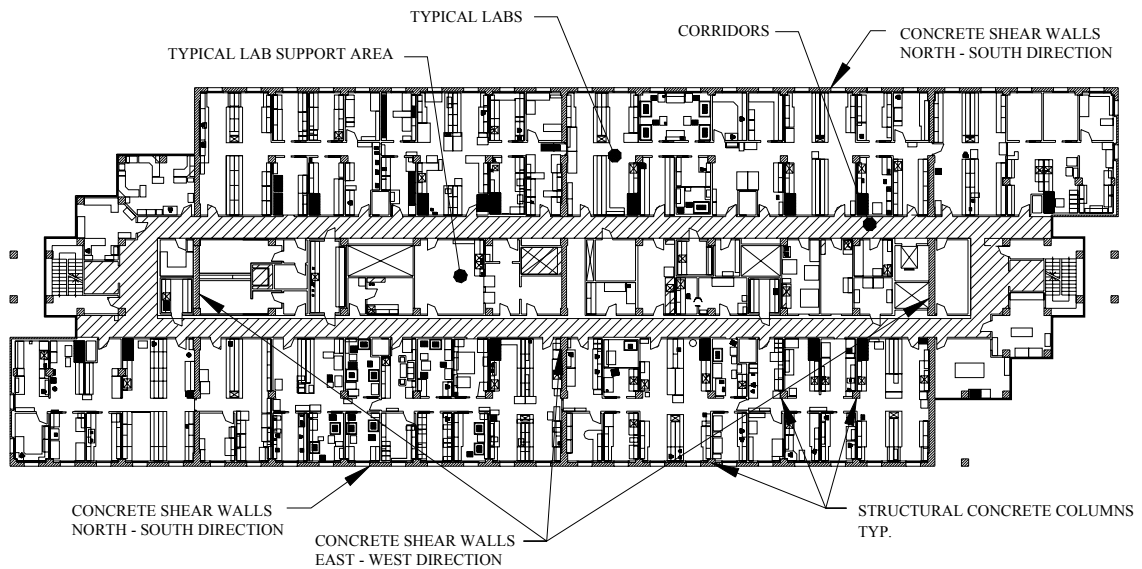


Fig. 2.1 Typical floor plan 2nd through 5th floors

⁶ The seismic performance of the building was evaluated in several campus studies. It is expected to perform above average in the “life-safety” to “operational” levels in a range of moderate to extreme events (UCB, 1997; Comerio, 2000).

2.3 CONTENTS INVENTORY

An inventory of the building contents was completed in a parallel study of retrofit methods for laboratory contents funded by the Federal Emergency Management Agency (FEMA) and UC Berkeley as part of the Disaster Resistant University (DRU) Initiative (Comerio, 2003). The building contents are typical of a wet laboratory: lab benches with storage shelving above, and very densely packed equipment. In total, there are about 10,500 items in the building, of which, 44% is furniture (laboratory benches, wall shelves, desk units, etc.) and 56% is equipment (tanks, cylinders, microscopes, computers, and other bench-top equipment, as well as heavy equipment such as refrigerators, freezers, incubators, and fume hoods).

There are about 15 different types of furniture and 95 different categories of equipment in the building. Shelving dominates among the furniture, and computer equipment (CPUs, monitors, printers, fax machines, and copy machines) all together represents some 1300 items (12% of the total and 22 % of the equipment). Refrigerators and freezers together are the next largest group, with 4.5% of the total and 8% of the equipment, followed by centrifuges and microscopes, each representing about 3% of the total contents and 5% of the equipment. Each laboratory was documented in drawings and in a database. While some labs have changed over time, the research is focused on the aggregate understanding of the types of equipment and typical conditions (see Fig. 2.2 and Table 2.1).

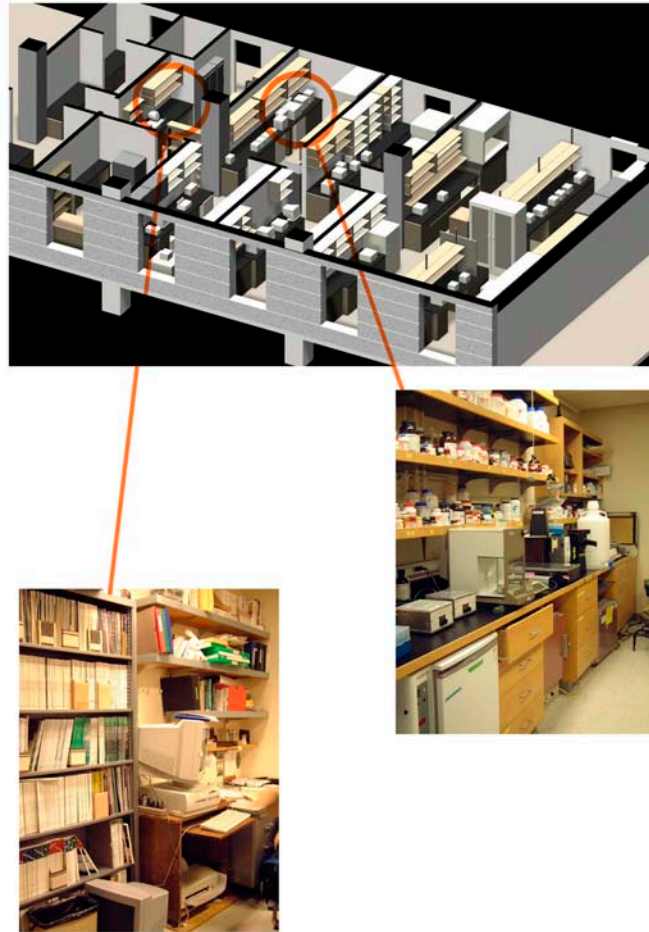


Fig. 2.2 Typical laboratory conditions

Value. The contents in the database were categorized according to their value. The total value of the equipment in the building is estimated at approximately \$23 million (Comerio 2003). Ninety-eight percent of the items are valued between \$1,500 and \$10,000. The majority of these are the bench-top microscopes, stirrers, mixers, and other small equipment. The remaining 2% of the equipment ranges in value from \$10,000 to \$1 million. These include specialized items such as confocal microscopes, valued at \$500,000 each, and laser tables with visualization computers, valued at \$1.2 million each.

Table 2.1 Common types of furniture and equipment in laboratories

<i>Furniture Type</i>	<i>Number of Items</i>
Shelving Unit	2,022
Workbench	674
Cabinet	614
Desk	553
File Cabinet	385
Other	352
Total Furniture	4,600
<i>Equipment Types</i>	<i>Number of Items</i>
Monitor	557
CPU	544
Refrigerator	349
Centrifuge	319
Microscope	279
Equipment Rack	273
Mixer	266
Printer	212
Water Bath	141
Power Supply	139
Incubator	131
Gas Cylinder	122
Freezer	119
Fume Hood	104
Stirrer	102
Other	2,243
Total Equipment	5,900

Life safety. In the FEMA/UC funded study, two assessments were made to evaluate the degree to which each item represented a life-safety hazard. The first evaluated direct life safety, that is, risk of injury from the impact of a moving or falling object. Life safety can be threatened by heavy objects falling or tipping directly onto occupants, or by sliding or tipping into a position to block egress from a work area. The second assessment was on indirect life-safety problems such as the release of hazardous materials, either directly by broken containment or by two or more released materials combining to create a hazardous substance or fire.

In the first assessment, each item in the database was coded as a potential falling hazard. The categories described in Table 2.2 are aimed at prevention of serious injury. A 20-pound object falling from 5 feet or more from the floor clearly could cause a death, but it is more likely

to cause a serious injury. The breakpoint of 20 pounds is somewhat arbitrary but based on the State of California’s code governing hospital construction.

The matrix in Table 2.2 demonstrates how the life-safety priority and the risk will increase from the upper left to the lower right. The table was also used in a separate study to recommend retrofit design strategies for each category—where items classified as B could use commercially available products, items classified as C and D should be designed by professionals. The locations that qualified as low-, medium-, or high-risk were defined for consistent application. For example, a low-risk item might be floor-mounted with a low aspect ratio, while a high-risk item might be directly overhead.

Table 2.2 Life-safety priority levels assigned to furniture and equipment

<i>Weight</i> ¹	<i>Risk of Location</i>		
	Low	Medium	High
< 20 pounds	A ²	B	C
20-400 pounds	B	C	C
> 400 pounds	C	C	D

Notes:

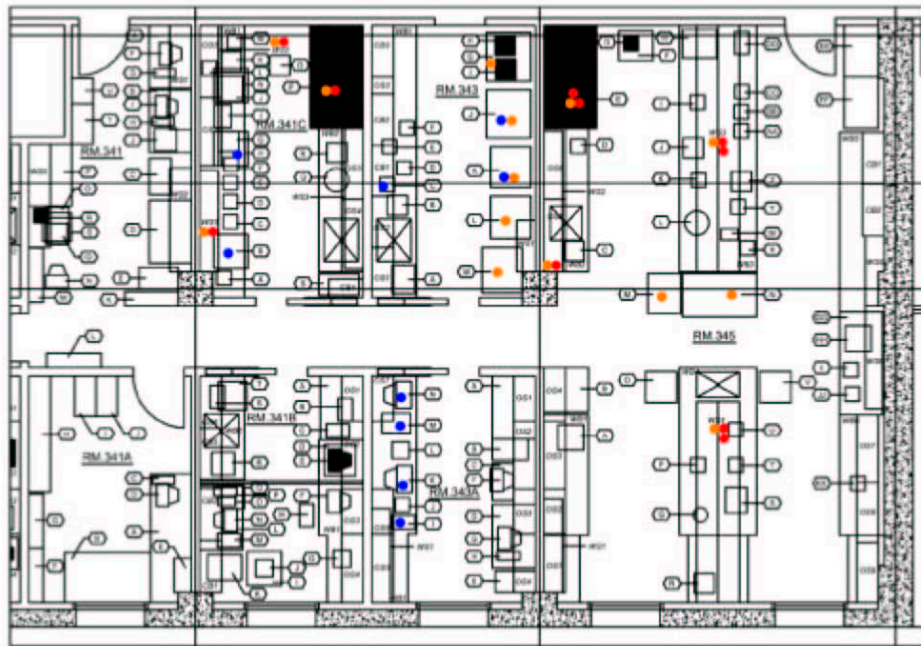
1. The weight cutoffs are set by judgment. Those shown here are weights used for similar priority settings in building codes.
2. Importance levels:
 - A: No specific anchorage requirement; low priority.
 - B: Anchorage using a standard, commercially available product; moderate priority.
 - C: Anchorage designed by professionals; high priority.
 - D: Anchorage designed by professionals; highest priority.

For the assessment of indirect life-safety hazards, a specialist from the campus office of Environment, Health and Safety (EH&S) visited each laboratory and noted potential associated chemical and biological hazards. This review was focused on conditions that could be hazardous in the event of an earthquake, separate from the regular EH&S inspections conducted to enforce basic safety standards. In the review undertaken for this study, associated chemical hazards were noted when hazardous materials could cause contamination, fire, release of poisonous gases, or other life-threatening conditions. Overall there were 333 conditions cited. These were coded as to whether the “fix” was administrative (e.g., moving the substance to a safer location) or whether some retrofit was required.

Importance. As the surveys of the laboratories were being conducted, the study team spoke with researchers in the laboratories to get an understanding of the kinds of work they did. These conversations led to a more formal survey of research faculty and/or their lab managers to ascertain which of the items in their laboratories were critical to their research. The survey provided examples of “importance measures” (see Table 2.3) and asked researchers to list the equipment, data, animals, and storage systems that were critical to their ability to work. Overall, about 500 items were rated as critical to continuing research. Of these, about 30% are genetically designed experimental samples, 20% are refrigerators and freezers containing fragile cell lines, 15% are microscopes, and 15% are CPUs where current data are stored.

Table 2.3 Importance measures for equipment and materials in laboratories

Equipment replacement cost
Equipment replacement time (weeks, months)
Data or material replacement cost
Data or material replacement time (weeks, months)
Irreplaceability
Interruption sensitivity (can tolerate none, or very little)
Loss of research benefits (income, salutary applications)
Related hazards that may occasion long clean-up periods (chemicals, biohazard)



● importance

● value

● chemical

● life safety 'D'

Figure 21: Sample Lab #1, Examples of Critical Items

Fig. 2.3 Sample report page describing critical lab contents

2.4 IDENTIFICATION OF CRITICAL FACTORS AFFECTING INVENTORY

Together, the detailed drawings documenting the equipment in each laboratory and the database provide a mechanism for understanding the number and types of equipment.⁷ Any item designated important by the researcher is essential to continued research—whether it is an animal, a cell line that took years to develop, or customized equipment. Similarly, high-value equipment is essential because it may require a long lead-time for purchase or may require specialized equipment funding not always available to researchers. Life-safety designations C or D imply real hazards to the occupants of the laboratories. Likewise, chemical hazards put the occupants at risk and also may be a risk to the larger community. Equally important, a chemical spill could add months or years to a building being out of service after an earthquake (even if the building has no damage) as a result of the time needed for cleanup.

Only 1,287 items (about 10%) are tagged as Important, Chemical Hazard, or Life Safety Priority D, or some combination of these codes. With Life Safety Category C, the total reaches 3,993 items. The High Value category was found to be a subset of those designated Important. There are only 65 items in the building valued at more than \$20,000. Thus, the combination of Important, Chemical Hazard, Life Safety Priority C and D, and High-Value, puts the number of items that could be considered critical to operations at 40% of the total contents in the building. If this subset of items could be protected from earthquake damage, the overall benefit to limiting losses and downtime would be significant.

⁷ In a separate study, the data were used to plan for the seismic retrofit of laboratory contents at U C Berkeley. This information is contained in W. T. Holmes and M. C. Comerio, *Implementation Manual for the Seismic Protection of Laboratory Contents: Format and Case Studies*, 2003, PEER Report 2003/12, Pacific Earthquake Engineering Research Center, University of California, Berkeley.

2.5 IMPLICATIONS OF USING CRITICAL FACTORS TO ESTIMATE SEISMIC PERFORMANCE

In evaluating the kinds of equipment and furnishings that populate the laboratories of the UC Science Building, the three categories of critical factors—important, valuable, and a life-safety concern (including falling and chemical hazards)—are the obvious first priority for evaluating seismic performance of contents. This applies not only to this case study building but also to any science laboratory with a similar taxonomy of contents.

One response to the threat of damage from earthquakes is to provide restraint for all contents in the laboratory environment. There are three primary reasons why this may not always be necessary or appropriate: (1) the need to understand how the equipment will perform in a seismic event, (2) the potential effects of seismic restraint on the function of the element or the laboratory as a whole, and (3) the cost of anchorage. Given cost and functionality concerns, it is prudent to prioritize contents with respect to their potential to cause hazards or losses. Research described in the following chapters evaluates the performance of critical contents and estimates the potential for damage and downtime.

2.6 COSTS OF ANCHORING LABORATORY CONTENTS

In order to develop an understanding of the costs and benefits of seismic anchorage of laboratory contents, estimates of costs on various retrofit schemes were produced. A PEER-sponsored study of the cost of seismic anchorage in five prototype laboratories on the UC Berkeley campus (Comerio and Stallmeyer, 2001) was used as the basis for estimating anchorage costs in the case study building. Estimates assumed union labor and retail pricing, but did not include contractor overhead markups. Cost reductions could be achieved if materials were purchased in quantity at wholesale prices.

The total cost to anchor all the equipment in the case study building would be \$25 per square foot of laboratory space (or \$20 per square foot of net useable building area). However, if anchorage were limited to the items in the three categories of critical factors—that is those tagged important, valuable, and life-safety category C and D⁸, then the number of items in need of anchorage would be about 4,000 (out of 10,500 total in the building). The cost to anchor these critical items would be \$16 per square foot of laboratory space or \$13 per net useable area. If a smaller subset of the critical items were anchored—those tagged important, with values over \$100,000, and life-safety category D—then the retrofit would be limited to about 1,300 items at a cost of \$9 per square foot of laboratory space (\$8 per square foot net).

2.7 REFERENCES

Comerio, M. C., 2003, *Seismic Protection of Laboratory Contents: The U.C. Berkeley Science Building Case Study*, IURD WP #2003-02, University of California, Berkeley, CA. Available at: http://www-iurd.ced.berkeley.edu/pub/abstract_WP200302.htm

Comerio, M. C., and Stallmeyer, J. C., 2003, Laboratory Equipment: Estimating Losses and Mitigating Costs, *Earthquake Spectra*, Vol. 19, No. 4, Nov. 2003.

Comerio, M. C., 2000, *The Economic Benefits of a Disaster Resistant University*, IURD WP #2000-02 University of California, Berkeley, CA. Available at: http://www-iurd.ced.berkeley.edu/pub/abstract_WP200002.htm

Comerio, M. C., and Stallmeyer, J. C., 2001, *Nonstructural Loss Estimation: The UC Berkeley Case Study*, Peer Report # 2002-01, Pacific Earthquake Engineering Research Center, University of California, Berkeley, CA.

Federal Emergency Management Agency (FEMA), 2003, *The Disaster Resistant University Guide*, Department of Homeland Security, Government Printing Office, Washington DC.

Filiatrault, A., and Christopoulos, C., 2002, *Guidelines, Specifications and Seismic Performance Characterization of Nonstructural Building Components and Equipment*, PEER Report # 2002-05, Pacific Earthquake Engineering Research Center, University of California, Berkeley.

⁸ It should be noted that life-safety category D included all items tagged as a chemical hazard.

Hamburger, R.E., Court, A.B., Soulages, J.R. (1995), "Vision 2000: A Framework for Performance Based Engineering of Buildings," Proceedings of SEAOC Annual Convention. Indian Wells, California.

Holmes, W. T., and Comerio, M. C., 2003. *Implementation Manual for the Seismic Protection of Laboratory Equipment: Format and Case Study Examples*. PEER Report, 2003/12, Pacific Earthquake Engineering Research Center, University of California, Berkeley, CA.

University of California, Berkeley. (1997), *Preliminary Seismic Evaluation*, Planning, Design and Construction, University of California, Berkeley, CA.

3 Hazard Analysis

Paul Somerville, URS Corporation, and Keith A. Porter, California Institute of Technology

After defining the facility to be examined, the first analytical step is the hazard analysis. The facility definition provides the site-location and site-soil information, as well as an estimate of any structural characteristics necessary to quantify the intensity measure (*IM*). The objectives of the hazard analysis are:

To select the hazard level(s) of interest;

To select the intensity measure (*IM*) to be used and to calculate the value(s) of *IM* corresponding to the selected hazard levels; and

To select or to simulate ground motion time histories that could reasonably occur at the facility, that match the calculated *IM* value(s), and that approximately match the magnitude, distance, and site classification. The ground motion time histories will be used in the structural analysis.

3.1 HAZARD LEVELS AND *IM* VALUES

In the present case, the hazard levels are selected as shaking with 50% probability of being exceeded in the next 50 years, 10% in 50 years, and 2% in 50 years to be consistent with scenario modeling already completed for the University of California (Somerville 2001). These hazard levels are commonly examined, but we offer no guidance on how to select hazard levels in general. The *IM* employed in the present study is the 5%-damped elastic spectral acceleration response at the estimated small-amplitude fundamental period, in this case, 0.45 sec (discussed in Chapter 4). Other *IMs* could be used; PEER is currently examining ten alternative *IMs*, with the objective of finding the *IM* that most strongly correlates with the decision variable, *DV*.

The S_a values for these hazard levels and this site were generated using the procedures described in URS Corporation (2000); see Table 3. They were calculated for rock site conditions using the average of the following three ground motion models, the first of which is most compatible with the site conditions at the UC Science Building site:

1. Abrahamson and Silva (1997), rock and shallow soil (up to 20 meters) over rock;
2. Idriss (1991), rock;
3. Sadigh et al. (1997), rock within about 1 meter of the surface; often weathered rock.

Table 3.1 Site uniform hazard spectra, 5% damping, S_a at 0.45 seconds

Hazard level	$S_a(0.45 \text{ sec}, 5\%)$	M mode	R mode	Dominant fault
50% in 50 years	0.710	5.5 – 6.0	1 km	Hayward
10% in 50 years	1.625	6.5 – 7.0	1 km	Hayward
2% in 50 years	2.740	6.5 – 7.0	1 km	Hayward

3.2 SELECTING GROUND MOTION RECORDINGS

The recordings listed in Tables 3.2 and 3.3 satisfy to the extent possible the magnitude and distance combinations listed in Table 3 for strike-slip earthquakes on site-class S_c sites. The time histories used to represent 50% exceedance probability of S_a at this site in 50 years are listed in Table 3.2. Three of the recordings are from sites that are classified as S_D . No attempt was made to adjust these recordings for S_c site conditions. Two of the recordings are from the abutment of the Coyote Lake Dam. The time histories used to represent 10% and 2% exceedance probability of S_a at this site in 50 years are listed in Table 3.3. The same set of time histories is used to generate the two sets. This is justified in part by the fact that the magnitude - distance combinations that dominate the hazard in each case are the same (Table 3). However, this ignores the fact that the 2%-in-50-yr time histories should be drawn from larger ground motion recordings than the 10%-in-50-yr time histories.

The issue here is the general agreement between the IM for each ground motion time-history and the earthquake that produces it. The acceleration amplitudes of any ground motion can be scaled to get any S_a value of interest, but if the amplitudes are scaled up or down too much, the scaled ground motion becomes unrealistic. Consider: one cause of a higher S_a value is

a high-magnitude earthquake. Higher magnitudes produce longer-duration motions, all else equal. Scaling the acceleration amplitudes of a ground motion, however, does not lengthen the duration of the motion. The greater the scaling, the more likely is the scaled ground motion to be unrealistic. It would be desirable to address this problem with one or both of the following: (1) simulation procedures that produce realistic ground motions for high magnitude or close fault distance and (2) well-defended limits for scaling ground motion amplitudes.

Table 3.2 Time histories representing 50% exceedance probability of S_a in 50 years

Earthquake	Mw	Station	Dist (km)	Site	Scale	Reference
Coyote Lake 8 Jun 1979	5.7	Coyote Lake Dam abutment	4.0	C	1.395	Liu and Helmberger (1983)
		Gilroy #6	1.2	C	0.999	
Parkfield 27 Jun 1966	6.0	Temblor	4.4	C	1.143	Cloud and Perez (1967)
		Array #5	3.7	D	0.978	
		Array #8	8.0	D	2.302	
Livermore 27 Jan 1980	5.5	Fagundes Ranch	4.1	D	1.644	Boatwright and Boore (1983)
		Morgan Territory Park	8.1	C	2.958	
Morgan Hill 24 Apr 1984	6.2	Coyote Lake Dam abutment	0.1	C	0.673	Hartzell and Heaton (1986)
		Anderson Dam Downstream	4.5	C	0.572	
		Halls Valley	2.5	C	1.362	

Table 3.3 Time histories representing 10% and 2% exceedance probability of S_a in 50 years

Earthquake	Mw	Station	Dist (km)	Site	Scale, 10/50	Scale, 2/50	Reference
Loma Prieta 17 Oct 1989	7.0	Los Gatos Presentation Center	3.5	C	1.016	1.713	Wald <i>et al.</i> (1991)
		Saratoga Aloha Ave	8.3	C	2.653	4.473	
		Corralitos	3.4	C	1.394	2.350	
		Gavilan College	9.5	C	2.097	3.535	
		Gilroy historic	?	C	2.319	3.910	
Kobe, Japan 17 Jan 1995	6.9	Kobe JMA	0.5	C	0.912	1.537	Wald (1996)
Tottori, Japan 6 Oct 2000	6.6	Kofu	10.0	C	1.039	1.751	K-net
		Hino	1.0	C	0.827	1.395	Kik-net
Erzincan Turkey 13 Mar 1992	6.7	Erzincan	1.8	C	2.455	4.139	EERI (1993)

3.3 REFERENCES

Abrahamson, N.A. and W.J. Silva, 1997, "Empirical response spectral attenuation relations for shallow crustal earthquakes," *Seismological Research Letters* 68, 94-127.

Boatwright, J. and D.M. Boore, 1982, "Analysis of the ground accelerations radiated from the 1980 Livermore Valley earthquakes for directivity and dynamic source characteristics," *Bulletin of the Seismological Society of America*, 72 (6), 1843-1865.

Earthquake Engineering Research Institute, 1993, "Erzincan, Turkey Earthquake of March 13, 1992: Reconnaissance Report, Chapter 2 – Geology and Geotechnical Effects," *Earthquake Spectra, Supplement to Volume 9*, Oakland, CA.

Hartzell, S.H. and T.H. Heaton, 1986, "Rupture history of the 1984 Morgan Hill, California, earthquake from the inversion of strong motion records," *Bulletin of the Seismological Society of America*, 76, 649- 674.

Idriss, I.M., 1991, *Procedures for Selecting Earthquake Ground Motions at Rock Sites*, Report to NIST.

KikNet website: www.kik.bosai.go.jp

K-Net website: www.k-net.bosai.go.jp

Liu, H.L. and D.V. Helmberger, 1983, "The near-source ground motion of the 6 August 1979 Coyote Lake, California, earthquake," *Bulletin of the Seismological Society of America*, 73, 201-218.

Sadigh, K., Chang, C.Y., Egan, J.A., Makdisi, F., Youngs, R.R., 1997, "Attenuation relationships for shallow crustal earthquakes based on California strong motion data," *Seismological Research Letters*, 68 (1), January.

Somerville, P.G., 2001, Ground Motion Time Histories for the UC Lab Building, URS Corporation, Pasadena, CA, 15pp.

URS Corporation, 2000, *Probabilistic Ground-Motion Analysis for the Central Campus*, Draft report prepared for the U.C. Berkeley Seismic Guidelines Project, June 8, 2000.

Wald, D.J., D.V. Helmberger and T.H. Heaton, 1991, "Rupture model of the 1989 Loma Prieta earthquake from the inversion of strong motion and broadband teleseismic data," *Bulletin of the Seismological Society of America*, 81, 1540-1572.

Wald, D.J., 1996, "Slip history of the 1995 Kobe, Japan, Earthquake determined from Strong Motion, Teleseismic, and Geodetic data," *J. Physics of the Earth*, 44, 489-503.

4 Structural Analysis

Tae-Hyung Lee and Khalid M. Mosalam, University of California, Berkeley

4.1 OBJECTIVE AND SCOPE

The objective of this component of the study is to create a state-of-the-art OpenSees (McKenna and Fenves 2001) model and to evaluate the seismic demands of the building. The model includes the superstructure system and the soil-foundation interface. The OpenSees modeling and analysis take benefit from all recent and ongoing PEER model development efforts improving the accuracy of the seismic response predictions. Seismic response is aimed at covering the range from near-elastic to near-collapse conditions. The probability distribution of the engineering demand parameter (*EDP*) is estimated based on a set of nonlinear time history analysis given a set of earthquake records. Deterministic sensitivity analysis of the building seismic demand is performed to evaluate uncertain parameters that significantly affect damage to the contents of the building. Detailed discussion on the whole study can be found in (Lee and Mosalam 2004).

4.2 DESCRIPTION OF STRUCTURAL SYSTEM

The gravity load-carrying system of the building consists of a reinforced concrete space frame, as shown in Figure 4.1 which includes the global geometry and span dimensions. On the other hand, the lateral load-resisting system consists of coupled shear walls in the transverse direction (east-west direction) and perforated shear walls in the longitudinal direction (north-south direction). The floors consist of waffle slab systems with solid parts acting as integral beams between the columns. The building foundation consists of a 38"-thick mat. Figure 4.2 presents the structural elevation view of the transverse frame (frame 8 in Fig. 4.1) and the longitudinal frame (frame H in Fig. 4.1) and indicates story heights. All interior columns are square with

dimensions 24" and transverse reinforcement #4@8" closed ties. The longitudinal reinforcing bars of the interior columns vary with the levels of the building: 12#11 between the foundation level and level 1, 12#10 between levels 1 and 3, and 8#8 between levels 3 and the roof. The coupling beams between the shear walls are 48" wide and 24-½" deep for all levels.

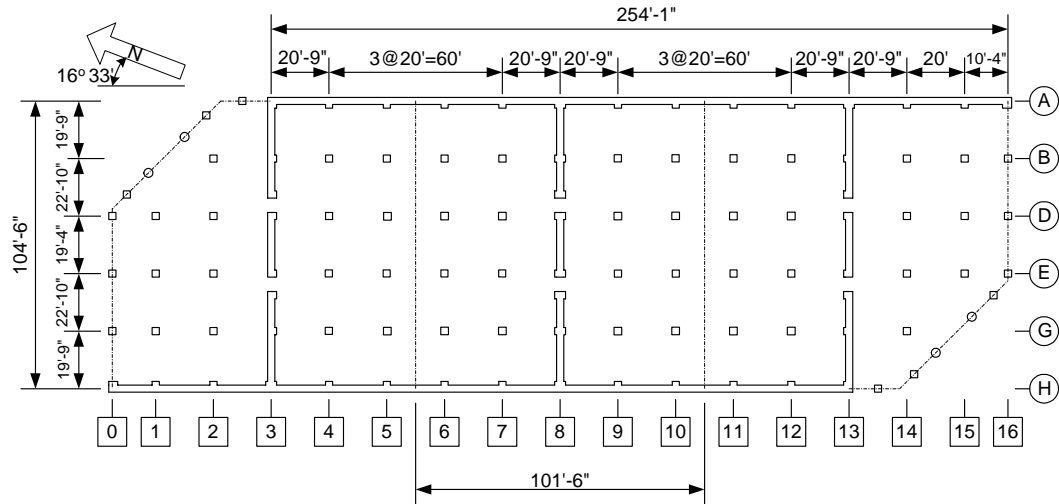


Fig. 4.1 Structural plan of UC Science Building

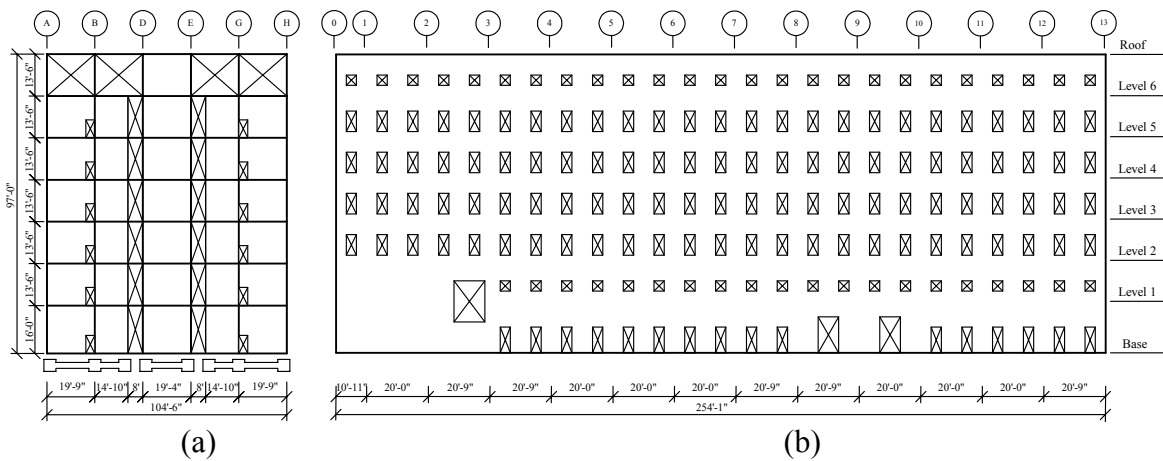


Fig. 4.2 Structural elevation of (a) transverse frame and (b) longitudinal frame

4.3 OPENSEES MODELING

Idealization of structural system. The modeling of the building is conducted on two levels. In the first, two-dimensional (2D) analysis is performed to investigate the seismic response of one of the transverse frames (frame 8 in Fig. 4.1) and one of the longitudinal frames (frame H in Fig. 4.1). The second analysis considers three-dimensional (3D) modeling of the entire building under multi-directional ground motion. In this report, only the 2D analyses are presented.⁹ The computational model of the building is developed using the modeling capabilities of OpenSees as shown in Figure 4.3 for the transverse and longitudinal frames. In this section, description of this modeling is presented together with a list of the adopted assumptions and the limitations of the modeling process.

⁹ For comparison to the two 2D models (the transverse and the longitudinal frames) of the building, the 3D model is analyzed in the transverse direction and in the longitudinal direction, separately. In other words, the middle transverse frame in the 3D model is monitored when a ground acceleration in the transverse direction is applied and the north longitudinal frame in the 3D model is monitored when a ground acceleration in the longitudinal direction is applied. Comparison is made in terms of the time history of the roof displacement.

The research considered two hazard levels, namely 50% in 50 yrs (low hazard) and 10% in 50 yrs (medium hazard) levels. In all, four cases were tested, i.e., transverse for low, transverse for medium, longitudinal for low, and the longitudinal direction for medium hazard. Comparison in the longitudinal directions (for both of the low and medium hazard levels) showed good matches between the response of the 3D model and that of the 2D longitudinal frame model. However, comparison in the transverse direction shows that the 3D model in the transverse direction is a lot stiffer than the 2D transverse frame. With the specific ground motion used, the stiffness ratio of 3D to 2D in the transverse direction is around 4. However, this ratio should not be generalized to UC Science Building or any other structural system.

The reason for the difference is as follows. There are two assumptions in the 2D transverse frame model that made the 2D model more flexible than the 3D model in the transverse direction:

1. The longitudinal shear walls are not considered in the modeling of the transverse frame as integrated parts of the transverse frames to act as flanges against the flexural behavior of UCS in the transverse direction. In the 3D model, the two longitudinal frames (perforated shear-walls) do act as significant resistance to lateral loadings in the transverse direction. In reality, the actual role of the longitudinal frame in terms of the stiffness in the transverse direction should be somewhere in the middle.
2. The stiffness of the waffle slab is not fully considered in the 2D model. In the 3D model, the waffle slab is acting almost as rigid in the transverse direction.

In conclusion, the stiffness of the 2D transverse frame model is underestimated relative to that of the 3D model in the transverse direction due to the effect of the rigidity of the waffle slab and the longitudinal frames. The actual stiffness of UCS in the transverse direction should fall between that of 2D transverse frame model and that of 3D model in the transverse direction. The stiffness estimations in the longitudinal direction by 2D and 3D models match well.

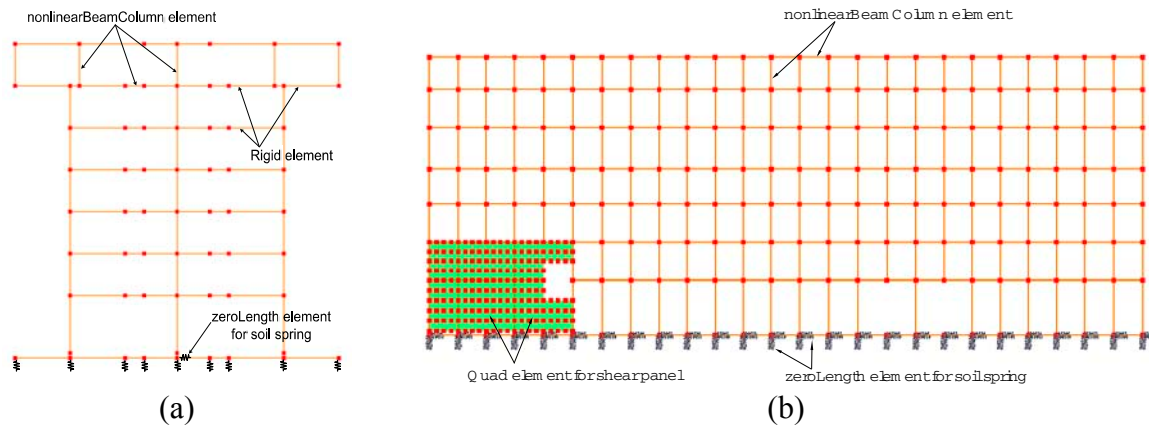


Fig. 4.3 OpenSees 2D models of (a) transverse frame and (b) longitudinal frame

Shear wall modeling. All shear wall elements are modeled using one-dimensional beam elements aligned with the centerline of the actual shear wall. For proper idealization of the geometry, the node at the shear wall centerline and the node at the boundary of the shear wall (representing one end of a coupling beam) are connected using rigid elements.

Beam-column elements. Most elements in the building model are based on flexibility formulation of beam-column elements (`nonlinearBeamColumn`). Each beam-column element has two nodes where each node has three degrees of freedom (two translations and one rotation). The beam element has several (usually four) monitoring sections with fiber element discretization. In this discretization, distinction is made between the constitutive models of the reinforcing bars, unconfined (cover) concrete, and confined (core) concrete.

Continuum elements. In Figure 4.2(b), the part enclosed by column line 0 and 3 between the base and Level 2 is a shear panel that cannot be modeled using a beam-column element and rigid elements as described in previous section. Thus, this part of the longitudinal frame is modeled using conventional four-node elements (`quad`) as shown in Figure 4.3(b).

Mass and gravity load. The dead load accounted for the self-weight of the waffle slab system and the supporting elements, i.e., shear walls and columns. The assumed unit weight of the concrete is 145 pcf. The computed dead load is 183 psf. Moreover, 25 psf representing building contents are included as a superimposed dead load. The live load of 100 psf is assumed according to the original design of the building. The mass of the building is modeled using lumped masses at the nodes. Nodal masses are directly computed from the dead load including

the superimposed dead load. The transverse frame has a tributary area with 101'-6" width as shown in Figure 4.1, while the longitudinal frame has a tributary area with 52'-3" width (half the dimension of the building in the transverse direction).

Boundary conditions and soil model. Flexible supports are used at the foundation level in the vertical and horizontal direction using spring-type elements (`zeroLength`). These elements represent soil having a modulus of subgrade reaction of 100 lb/in³. The same tributary areas as those of mass are used to consider the soil support in both frames. To simulate the characteristic of soil behavior, ENT material in OpenSees material library is adopted. An element with ENT material has elastic properties in compression and zero tensile strength.

Damping. The damping of the building is modeled using mass and stiffness proportional damping with 5% of critical damping for modes 1 and 2. These modes are estimated from the eigen solution using the initial elastic stiffness matrix as 0.62 and 0.28 seconds for the transverse frame and 0.26 and 0.14 seconds for the longitudinal frame, respectively.

Material properties and constitutive models. According to the design specifications, the concrete of the shear walls and the coupling beams has nominal 28-day compressive strength $f_c' = 5$ ksi. On the other hand, the concrete for the interior columns and the waffle slab systems has nominal strength $f_c' = 3$ ksi. The reinforcing steel is scheduled as ASTM A-615 Grade 40 for #4 and smaller bars and Grade 60 for #5 and larger bars. In OpenSees, concrete is modeled using uniaxial stress-strain relationships. Cover and core concrete materials are defined separately using the model `Concrete01` that is based on the modified Kent-Park model (McKenna and Fenves 2001). On the other hand, steel bars are modeled using `Steel01` that has a bilinear stress-strain relationship.

Assumptions and limitations. The 2D models of OpenSees are based on the following assumptions:

- A linear elastic shear force-deformation relationship is chosen for all the used elements in the transverse frame model relying on the fact that shear failure will not occur prior to flexure failure. However, elastic-hardening shear force-deformation relationship is used in the longitudinal frame model.
- Reinforcing bars are assumed to be fully bonded to the surrounding concrete.

Solution strategy. The Newmark β -method is used as the time integrator with coefficients $\gamma = 0.50$ and $\beta = 0.25$. In general, a time step of one half the ground motion time

interval is used, which implies a time step in the range of 0.0025 to 0.01 seconds. The Newton-Raphson solution algorithm is utilized for solving the nonlinear system of equilibrium equations.

4.4 INTENSITY MEASURE (*IM*)

Ground acceleration records selected for analyses (see Chapter 3), can be categorized by the hazard level as low, medium, and high with respective 50%, 10%, and 2% probability of exceedance of the elastic spectral acceleration (S_a) in 50 years, where S_a is obtained from the site uniform hazard spectra for a given damping and the fundamental period of the structure. Ten recorded ground motions are selected to represent a low hazard level and another 10 recorded ground motions are selected to represent both medium and high hazard levels. Most of the selected ground motions satisfy the magnitude and distance combinations and the soil type of the site. Different scaling factors are used for each ground motion to adjust *IM*.

4.5 ENGINEERING DEMAND PARAMETERS (*EDPs*)

Selected *EDPs* include (1) time histories of the relative floor acceleration and displacement (by relative, we mean relative to the ground), (2) time histories of absolute (or total) floor acceleration and displacement (an absolute response is the relative response added to the ground motion), (3) peak absolute floor acceleration and displacement, (4) peak transient interstory drift ratio (IDR). (1) and (4) are selected for estimating seismic demand on the structural system, and (2) and (3) are selected for estimating seismic demand on the building contents and for the purpose of conducting shaking table tests on these contents. Figure 4.4 shows sample time histories of various floor responses at the mid-point of the transverse frame due to the high hazard Erzincan (Turkey) earthquake. Peak absolute floor responses and IDR of the transverse frame are plotted in Figure 4.5(a) for the 10 low hazard earthquakes. Note that these values are not necessarily taking place at the same time for all floors. Statistics of these *EDPs* are computed and presented in Figure 4.5(b) in terms of the mean and mean \pm standard deviation bounds.

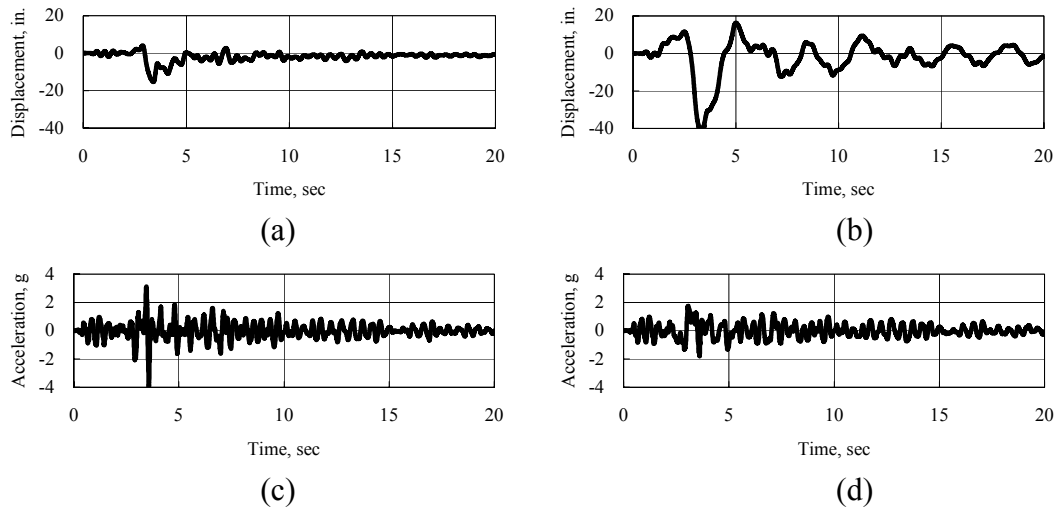


Fig. 4.4 Time history plots at midpoint of transverse frame due to high hazard Erzincan (Turkey) earthquake for (a) relative roof displacement, (b) absolute roof displacement, (c) relative roof acceleration, and (d) absolute roof acceleration

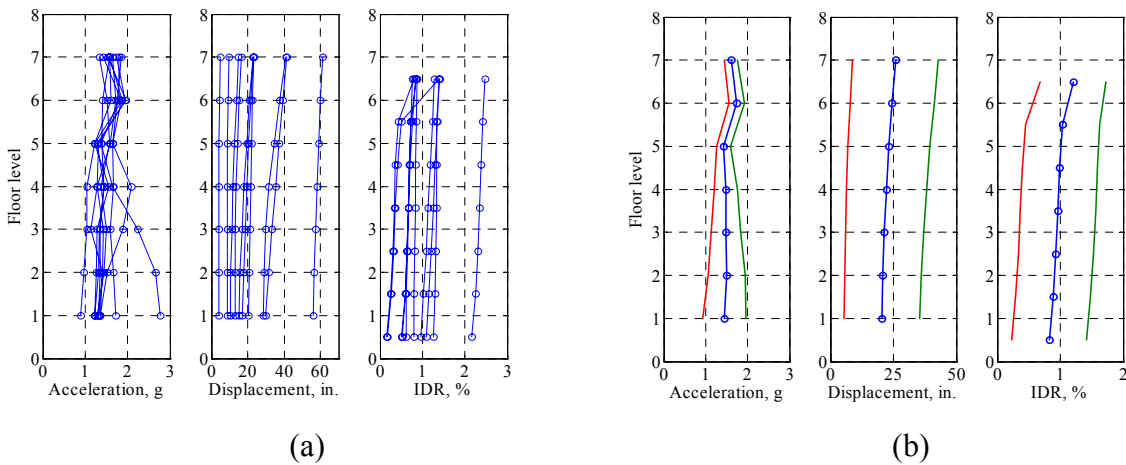


Fig. 4.5 (a) Peak absolute floor responses and IDR of transverse frame for 10 high hazard earthquakes and (b) mean and mean \pm standard deviation bounds of data shown in (a)

4.6 PROBABILITY DISTRIBUTION ESTIMATE OF *EDP/IM*

Uncertainty in ground motions causes any *EDP* to be random. The conditional probability distribution of *EDP* given *IM* is estimated based on the sample mean and standard deviation of the *EDP*. Figures 4.6 and 4.7 show the empirical CDF curves of peak absolute roof acceleration (PARA) and the 7th story IDR of the transverse frame and the longitudinal frame, respectively. Responses are monitored at the midpoint of columns D and E in the transverse frame (Fig. 4.2(a)) and at column 8 in the longitudinal frame (Fig. 4.2(b)). Normal and lognormal CDF curves based on the sample mean and standard deviation are added to each empirical CDF curve to estimate the probability distribution of the *EDP*. Correlations between the same *EDP* at different floors/stories are computed and a set of sample correlation matrices is given in Tables 4.1 and 4.2 for the transverse frame and the longitudinal frame, respectively.

4.7 DETERMINISTIC SENSITIVITY ANALYSIS

This section presents a deterministic sensitivity analysis of the UC Science Building subjected to seismic loading. It presents a simple methodology for investigating the relative importance of various variables to determine the *EDPs*. In this analysis, it is assumed that the output variable (*EDP* in this study) is a known deterministic computational model (e.g., using finite element analysis, FEA) of a set of input variables whose probability distribution is assumed by the analyst. For each input variable, the best estimate and two extreme values are selected corresponding to upper and lower bounds of its probability distribution. First, the deterministic model is used to evaluate the best estimate of the output variable using input variables set to their best estimates. Subsequently, for each input variable, the same computations are performed twice using one of the extreme values each time while the other input variables are set to their best estimates yielding two bounding values of the output variable for each input variable. The absolute difference of these two values, referred to as the *swing*, is used as an indicator of the “importance” of the given input variable to the output variable. One can rank input variables according to their swings, where a larger swing implies a more significant input variable to the uncertainty of the output variable.

Selected uncertain variables. The selection of input variables depends on the output variable of interest. In this study, we select PARA, peak absolute roof displacement (PARD), and

IDR as output variables. The ground motion profile, ground motion intensity, structural strength and stiffness, building mass, and viscous damping are selected as input variables. Other parameters not included in the study and that may contribute to the *EDP* uncertainty include soil flexibility, spatial distribution of the mass, and the modeling assumptions in the FEA.

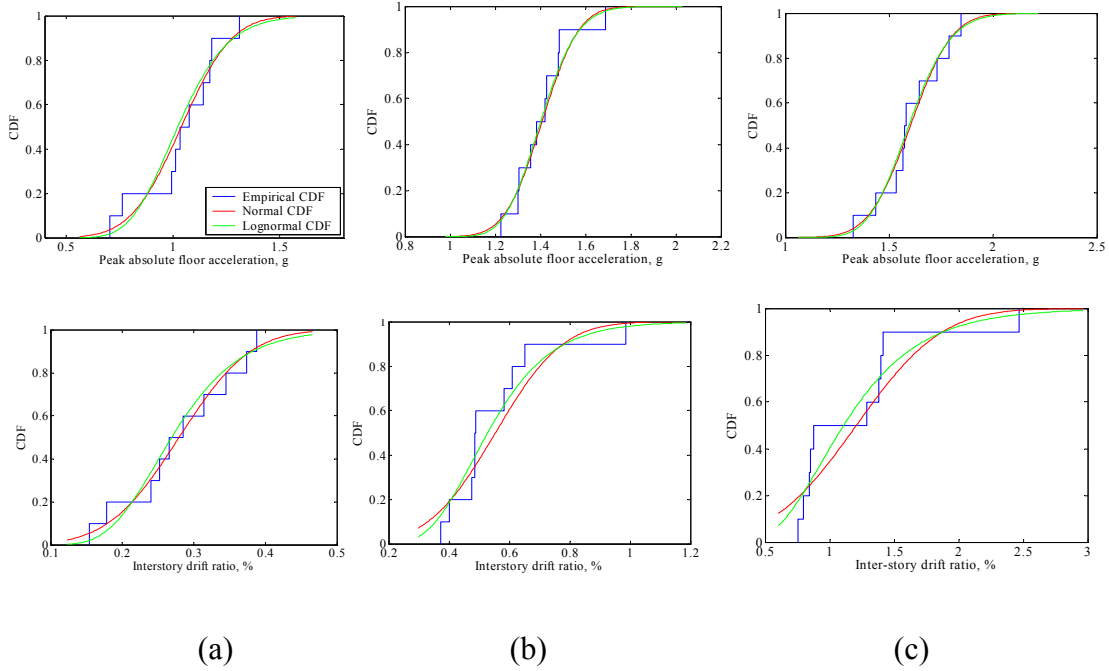


Fig. 4.6 Empirical CDF and probability distribution estimate by normal and lognormal distributions of transverse frame for PARA and IDR of 7th story for (a) low hazard, (b) medium hazard, and (c) high hazard

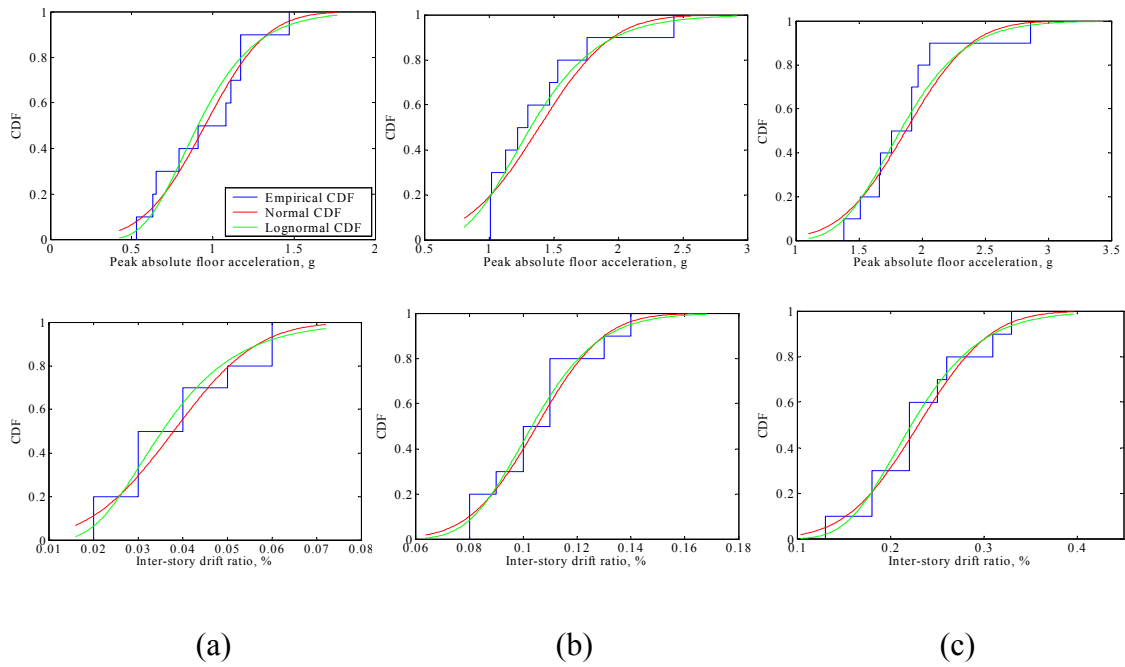


Fig. 4.7 Empirical CDF and probability distribution estimate by normal and lognormal distributions of longitudinal frame (column 8) for PARA and IDR of 7th story for (a) low hazard, (b) medium hazard, and (c) high hazard

Table 4.1 Correlation matrices of *EDPs* of transverse frame

	Low hazard							Medium hazard							High hazard						
	Peak absolute floor acceleration*																				
	L1	L2	L3	L4	L5	L6	R	L1	L2	L3	L4	L5	L6	R	L1	L2	L3	L4	L5	L6	R
L1	1	0.95	0.82	0.41	0.16	0.15	0.71	1	0.89	0.35	0.02	0.32	0.39	0.81	1	0.99	0.84	0.39	0.17	0.13	0.55
L2		1	0.95	0.66	0.42	0.35	0.83		1	0.39	0.16	0.09	0.26	0.65		1	0.88	0.43	0.22	0.14	0.47
L3			1	0.85	0.66	0.59	0.87			1	0.63	0.00	0.17	0.04			1	0.72	0.32	0.20	0.22
L4				1	0.93	0.78	0.77				1	0.65	-0.1	-0.2				1	0.49	0.30	-0.1
L5					1	0.89	0.57					1	0.03	-0.2					1	-0.2	-0.1
L6						1	0.57						1	0.69						1	0.3
R							1							1							1
	IDR**																				
	L1	L2	L3	L4	L5	L6	R	L1	L2	L3	L4	L5	L6	R	L1	L2	L3	L4	L5	L6	R
L1	1	1	0.98	0.97	0.94	0.85	0.67	1	0.99	0.99	0.99	0.98	0.97	0.95	1	1	1	1	0.99	0.99	0.83
L2		1	1	0.98	0.97	0.89	0.72		1	1	1	0.99	0.98	0.97		1	1	1	1	0.99	0.85
L3			1	1	0.98	0.92	0.77			1	1	1	0.99	0.98			1	1	1	1	0.86
L4				1	1	0.96	0.82				1	1	0.99	0.98				1	1	1	0.86
L5					1	0.98	0.87					1	1	0.99					1	1	0.87
L6						1	0.95						1	1						1	0.89
R							1							1							1

*: L1, ..., L6 indicate Level 1, ..., Level 6, respectively, and R indicates Roof
 **: L1, ..., L6 indicates 1st story, ..., 6th story, respectively, and R indicates 7th story

Table 4.2 Correlation matrices of *EDPs* of longitudinal frame (column 8)

	Low hazard							Medium hazard							High hazard						
	Peak absolute floor acceleration*																				
	L1	L2	L3	L4	L5	L6	R	L1	L2	L3	L4	L5	L6	R	L1	L2	L3	L4	L5	L6	R
L1	1	0.96	0.94	0.93	0.91	0.85	0.81	1	0.96	0.83	0.73	0.57	-0.2	-0.3	1	0.76	0.71	0.62	0.58	0.13	-0.4
L2		1	0.94	0.90	0.85	0.78	0.68		1	0.93	0.85	0.71	0.0	-0.2		1	0.97	0.86	0.75	0.26	-0.2
L3			1	0.99	0.93	0.89	0.85			1	0.97	0.88	0.16	-0.1			1	0.92	0.81	0.25	-0.2
L4				1	0.97	0.91	0.90				1	0.95	0.20	-0.2				1	0.94	0.21	-0.5
L5					1	0.94	0.90					1	0.28	-0.1					1	0.24	-0.5
L6						1	0.90						1	0.89						1	0.5
R							1							1							1

	IDR**																				
	L1	L2	L3	L4	L5	L6	R	L1	L2	L3	L4	L5	L6	R	L1	L2	L3	L4	L5	L6	R
	L1	1	0.92	0.58	0.72	0.55	0.64	0.69	1	0.64	0.51	0.56	0.55	0.52	0.56	1	0.76	0.64	0.66	0.64	0.66
L2		1	0.82	0.88	0.80	0.84	0.84		1	0.94	0.94	0.92	0.92	0.92		1	0.94	0.95	0.94	0.97	0.90
L3			1	0.91	0.92	0.93	0.91			1	0.99	0.99	0.99	0.90			1	1	0.99	0.96	0.80
L4				1	0.89	0.95	0.89				1	1	1	0.87				1	1	0.97	0.81
L5					1	0.87	0.74					1	0.99	0.84					1	0.97	0.81
L6						1	0.93						1	0.86						1	0.91
R							1							1							1

*: L1, ..., L6 indicate Level 1, ..., Level 6, respectively, and R indicates Roof
 **: L1, ..., L6 indicates 1st story, ..., 6th story, respectively, and R indicates 7th story

Uncertainty in ground motion intensity. For the purpose of the present study, the *IM* candidate must satisfy the following criteria: (1) it is a proper *IM* to the *EDP* of interest and (2) its probability function of occurrence is readily available. Satisfying these criteria, the elastic spectral acceleration S_a with 5% viscous damping is selected as an uncertain input variable representing earthquake *IM*. Frankel and Leyendecker (2001) provide probabilistic hazard information in terms of mean annual exceedance frequency of S_a for the UC Science Building site. Using this information and following the Poisson assumption for arrivals of earthquakes (Porter et al. 2002), the selected S_a values for the transverse frame are 0.15g, 0.40g, and 1.21g for the lower bound, median, and upper bound of ground motion *IM*, respectively, and 0.21g, 0.54g, and 1.56g for the longitudinal frame.

Uncertainty in ground motion profile. Different profiles of ground motion with the same earthquake *IM* may produce different outputs of a specific *EDP* of interest. Porter et al. (2002) discussed two ways of considering ground motion characteristics other than the primary *IM*, i.e., S_a . One of these methods is selected in the present study for its simplicity. In this method, one selects a set of ground motion profiles in which each is scaled according to the best estimate of *IM*. For a specific *EDP* of interest, one performs a set of structural analyses using the scaled ground motion profiles. The set of ground motion profiles can be sorted with respect to the obtained *EDPs* to determine the best estimate, the 10th and the 90th percentiles of the ground motion profile. Lee and Mosalam (2003a) present detailed steps for the methodology. Ground

motion profiles selected for the best estimate, the 10th and 90th percentiles are listed in Table 4.3 for the transverse and longitudinal frames. It should be noted that ground motion profiles in the transverse and longitudinal directions are different even if the profile name is identical.

Table 4.3 Ground motion profiles selected for best estimate, 10th and 90th percentiles, for transverse and longitudinal frames

EDP	10 th percentile	Best estimate	90 th percentile
Transverse frame			
PARA	Parkfield, Array #5	Tottori (Japan), Hino	Livermore, Morgan Territory Park
PARD	Parkfield, Temblor	Tottori (Japan), Hino	Loma Prieta, Lexington Dam abutment
IDR	Parkfield, Array #5	Coyote Lake, Coyote Lake Dam abutment	Parkfield, Array #8
Longitudinal frame			
PARA	Morgan Hill, Coyote Lake Dam abutment	Tottori (Japan), Kofu	Kobe (Japan), Kobe JMA
PARD	Loma Prieta, Corralitos	Coyote Lake, Coyote Lake Dam abutment	Morgan Hill, Halls Valley
IDR	Erzincan (Turkey), Erzincan	Coyote Lake, Coyote Lake Dam abutment	Loma Prieta, Gavilan College

Uncertainty in strength and stiffness. Uncertainties in the structural strength and stiffness are considered for the level of the constitutive models. Since the compressive strength of concrete f'_c and the yield stress of the reinforcement f_y dictate the structural strength, we considered them as uncertain variables at the same time. It is assumed that f'_c has a normal distribution with the mean as the nominal strength and COV of 0.175 according to Mirza et al. (1979). On the other hand, f_y is assumed to have a lognormal distribution with the mean as the nominal yield stress and COV of 0.1 according to Mirza and MacGregor (1979).

The initial tangent stiffness of the concrete constitutive model E_c and Young's modulus of the reinforcement E_s control the structural stiffness. They are considered as uncertain variables to represent the uncertainty of the structural stiffness. It is assumed that E_c has a normal distribution with the mean as the nominal initial tangent stiffness and COV of 0.08 (Mirza et al. 1979), while E_s has a normal distribution with the mean as the nominal Young's modulus and COV of 0.033 (Mirza and MacGregor 1979).

Uncertainty in building mass. Quantification of building mass in dynamic analysis depends on several factors: materials used in construction, building dimensions, locations of nonstructural elements, and structural model, e.g., nodal coordinates. We adopt a probability distribution model suggested by Ellingwood et al. (1980) for dead load. In this model, a normal distribution with the mean as the calculated nominal dead load and COV of 0.1 is assumed. Moreover, all nodal masses are assumed perfectly correlated. In other words, all nodal masses are increased or decreased together with the appropriate ratio.

Uncertainty in viscous damping. A comprehensive discussion of uncertainty in viscous damping is presented by Porter et al. (2002). In that regard, we assumed a normal distribution with the mean as 5% of critical damping and COV of 0.4 for damping following the recommendations in Porter et al. (2002).

Deterministic sensitivity result. According to the methodology and uncertain variables described in the previous section, the sensitivity of the peak absolute acceleration and displacement, and IDR to uncertain variables is investigated. The results are shown in Figure 4.8.

4.8 CONCLUDING REMARKS

Various outcomes for the OpenSees simulation of the UC Science Building contribute to the following research activities within PEER: (1) time histories of floor responses (acceleration and displacement) are used in the shake-table test of the building contents by UCI and UCB researchers; (2) estimates of conditional probability distribution of *EDP* given *IM* serve as inputs for the loss analysis by Caltech researchers; (3) sensitivity analysis using Tornado diagrams shows that the uncertainty in ground motions affects the variability of *EDP* more significantly than that in the structural properties.

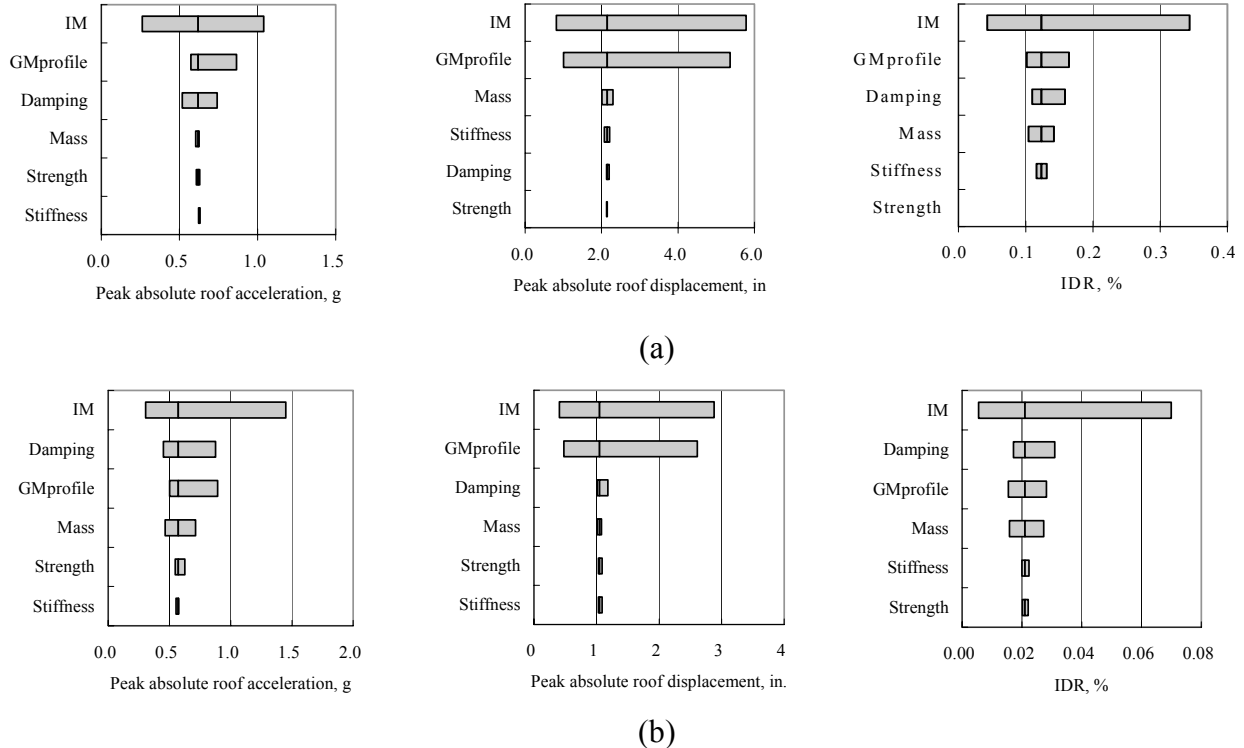


Fig. 4.8 Deterministic sensitivity results of different *EDPs* for (a) transverse frame and (b) longitudinal frame (column 8)

4.9 REFERENCES

- Ellingwood, B., Galambos, T.V., MacGregor, J.G., and Cornell, C.A. 1980. Development of a probability-based load criterion for American National Standard A58. *National Bureau of Standards*, Washington, D.C.: pp222.
- Frankel, A. and Leyendecker, E.V. 2001. Uniform hazard response spectra and seismic hazard curves for the United States, *US Geological Survey*, Menlo Park, CA.
- Lee, T.-H. and Mosalam, K.M. 2003a. Sensitivity of seismic demand of a reinforced concrete shear-wall building. *Proc. Ninth Int. Conf. on Applications of Statistics and Probability in Civil Eng.*, ICASP9, San Francisco, July 6-9, 2003.
- Lee, T.-H. and Mosalam, K.M. 2003b. Probabilistic fiber element modeling of reinforced concrete columns. *Proc. Ninth Int. Conf. on Applications of Statistics and Probability in Civil Eng.*, ICASP9, San Francisco, July 6-9, 2003.
- Lee, T.-H. and Mosalam, K.M. 2004, Probabilistic modeling of reinforced concrete structural systems subjected to seismic loading. *Pacific Earthquake Engineering Research center*, (PEER report in progress).

McKenna, F. and Fenves, G.L. 2001. OpenSees Manual. *PEER Center*, <http://opensees.berkeley.edu>.

Mirza, S.A. and MacGregor, J.G. 1979. Variability of mechanical properties of reinforcing bars. *J. of the Structural Div., ASCE*, **105**(ST5): 921-37.

Mirza, S.A., Hatzinikolas, M., and MacGregor, J.G. 1979. Statistical description of strength of concrete. *J. of the Structural Div., ASCE*, **105**(ST6): 1021-37.

Porter, K.A., Beck, J. L., and Shaikhutdinov, R.V. 2002. Sensitivity of building loss estimates to major uncertain variables. *Earthquake Spectra*, **18**(4): 719.

5 Performance Characterization of Bench- and Shelf-Mounted Equipment and Contents

Samit Ray Chaudhuri, and Tara. Hutchinson, University of California, Irvine

5.1 SMALL BENCH- AND SHELF-MOUNTED EQUIPMENT STUDIES

Motivation and technical approach. Equipment resting on bench surfaces in the UC Science Building laboratories include such things as analyzers, microscopes, centrifuges, monitors, and computer workstations. Many of these types of scientific equipment are fairly costly, and loss of functionality would result in total economic loss of the equipment itself. In addition, in hospital or other critical buildings, the failure of such equipment may hinder emergency response efforts immediately after an earthquake. However, in comparison with structural systems, there has been little fundamental research on the performance of these equipment and contents, particularly with respect to understanding the characteristics of the varied support (bench) conditions and their frictional behavior.

In general, these equipment and contents are observed to be short and rigid; therefore, imposed seismic excitation is likely to result in a sliding-dominated rather than a rocking-dominated response. Upon sliding, there is concern that the equipment may be damaged either by falling from the bench-top surface or through impact with neighboring equipment or surrounding side walls. The probability that either potential limit states will be exceeded is often expressed in the form of a seismic fragility curve. A seismic fragility curve associates the probability of exceedance of a defined limit state (a damage measure, DM) with an engineering demand parameter (EDP). An EDP may be considered as an input parameter to the fragility curve, for example, peak horizontal floor acceleration (PHFA) or peak interstory drift.

In this study, ten different bench-mounted equipment are considered and their fragility curves are determined. Based on the characteristics of these equipment, categories of small equipment are considered, and generalized curves are developed. Details of the equipment

considered are provided in Table 5.1. The selection of the equipment was based on review of the inventory of typical science laboratories (Comerio and Stallmeyer 2002). The equipment can be divided into three general categories: (1) scientific equipment, (2) computer monitors, and (3) Silicon Graphics Inc (SGI) computer workstations. In general, these elements are less than 40 kg, fairly short and squat, and thus dominated in response by their tendency to slide.

The approach adopted in this study involved conducting characterization experiments, large-scale shake table tests, and analytically developing a suite of seismic fragility curves for use by loss modelers (see Chapter 8). Subsequent sections describe the experimental and analytical studies conducted for the damage analysis of the small bench- and shelf-mounted equipment. It is assumed that the equipment response in this case is dominated by a sliding behavior as was generally observed in the shake table tests, and vertical seismic motion is not considered in the formulation.

Table 5.1 Summary details of equipment tested in this study

Category	Description	¹ Dimensions (cm)	Mass (kg)	μ_s		μ_k (average)	ϕ	
				Average	% Dev (+/-)		Average	% Dev (+/-)
Scientific Equipment	Small Microscope	41.9 x 38.1 x 20.3	10.5	0.70	7.91	0.61	0.87	10.50
	Large Microscope	45.7 x 55.9 x 39.4	21.7	0.35	7.25	0.31	0.89	4.50
	Technicon Autoanalyzer	35.6 x 48.3 x 40.5	17.8	0.66	6.06	0.62	0.94	2.50
	Eppendorf Centrifuge	28.6 x 27.9 x 21.0	5.9	0.72	0.70	0.70	0.97	-
Computer Monitors	38 cm (15" Standard) Diagonal CRT	38.1 x 36.8 x 35.6	14.1	0.50	5.05	0.52	1.04	-
	43 cm (17" Standard) Diagonal CRT	41.9 x 44.5 x 40.6	28.3	0.43	4.65	0.44	1.02	-
	48 cm (19" Standard) Diagonal CRT	44.5 x 58.4 x 45.7	31.1	0.86	8.77	0.92	1.06	-
Silicon Graphics Inc (SGI) Workstations	Indy	7.6 x 40.6 x 34.3	6.8	0.36	4.23	0.32	0.89	2.50
	Indigo	47.0 x 47.0 x 12.1	18.2	0.67	1.49	0.60	0.89	3.25
	Octane	29.8 x 40.6 x 27.9	24.5	0.66	6.87	0.64	0.97	5.00

¹ (depth x width x height)

5.2 EXPERIMENTAL STUDIES

The experimental investigation consisted of both system- and component-level testing. Component testing involved characterizing the individual components (bench-shelf and equipment-support interface). System-level testing involved recreating a mock-laboratory environment within which representative nonstructural systems were tested simultaneously. The

following sections will briefly discuss these experimental approaches. Additional reference may be found in Hutchinson and Ray Chaudhuri (2003) and Ray Chaudhuri and Hutchinson (2005).

Characterizing interface frictional behavior (μ_s and μ_k). The coefficients of static and kinetic friction (μ_s and μ_k) for each piece of rigid equipment were determined using repeated (horizontal) pull and inclined-base experiments (Ray Chaudhuri and Hutchinson 2004a). The coefficients of static and kinetic friction are calculated from these experiments and their variability is studied. Average values of μ_s and μ_k , and their maximum deviation determined by the horizontal pull and inclined-base tests for each of the equipment are provided in Table 1. Results in Table 5.1 indicate that μ_s for the equipment considered ranges from 0.35 to 0.86 and $\phi (= \frac{\mu_k}{\mu_s})$ ranges from 0.87 to 1.06. It should be mentioned that due to experimental limitations, the Eppendorf Centrifuge and the three CRT monitors could not be tested to determine μ_k using the inclined-base method. Therefore, no deviation is reported for these four items. Also it may be observed that the coefficient of kinetic friction is higher than the coefficient of static friction for the CRT monitors. This may be attributed to the uneven pressure distribution at the base and to the change in material (rubber) properties due to high load. The two values for each μ_s and μ_k , obtained by (horizontal) pull and inclined-base tests provide upper and lower limits with approximately $\pm 10\%$ maximum deviation from the average value (taken as the mean). Therefore, for the development of the fragility curves described in Section 1.4, a $\pm 10\%$ variation from the mean values are assumed for both μ_s and μ_k .

System-level shake table tests. The experimental setup for the system-level tests consisted of constructing four different integral bench-shelf configurations and assembling them within a mock-laboratory mounted on the 3.1 m x 3.7 m UC Irvine biaxial shake table. Transverse and longitudinal bench configurations, using both single and double (back-to-back) benches, were constructed. The mock-laboratory was constructed with two full-height timber walls at the rear of the configuration, providing support for a uni-strut frame system (which in turn supports the bench-shelving systems) and a rear enclosure for the room. At the front of the configuration, moment frames with stiffness comparable with the rear timber walls, were used to allow for an open viewing area of the specimens.

The bench-shelf system included continuous laboratory benches with two laterally placed rigid shelving systems stacked a single level high. These shelves were anchored to a horizontal channel system, which were supported by continuous vertical unistrut elements. Vertical uni-strut channels are anchored at the floor and ceiling. Layout and anchorage details for the integral laboratory bench and shelving system and supporting uni-strut elements were based on review of details within the UC Science Laboratory Building (Comerio and Stallmeyer 2002). A photograph of one of these configurations is shown in Figure 5.1. Equipment were mounted within each configuration (on the bench top and shelf) and measurements taken using a camera-based approach (Hutchinson et al. 2005).



Fig. 5.1 Photograph of bench-shelf system-level shake table tests conducted at UC Irvine

Ground Motions Selected. A total of ten earthquake motions were selected as input motions for the shake table testing (Table 5.2). These motions were prepared by Somerville (2002) and are described in Chapter 3. In addition, two of the motions provided by Somerville (2002) were acceleration-amplitude scaled by one-half to study the low amplitude response of the mock-laboratory and its contents. The range of peak ground accelerations (PGA) of the selected motions is broad (PGA = 0.13 g to 1.16 g). The selected range envelops the static friction coefficients of the equipment and contents as determined from static bench-top testing. Earthquake motions with large displacement magnitudes were considered, up to a peak ground displacement of PGD = 19 cm (GM-6). In addition, motions recorded in the near field, with large

velocity pulse characteristics were considered, with the strongest motion having a peak ground velocity of PGV = 64 cm/sec (GM-6).

Observations from shake table tests. Of particular importance in these experiments is the maximum sliding displacement experienced by the equipment, relative to the bench-top surface. Summary analyses of the measured response of the different scientific equipment considered in this study are shown in Figure 5.2(a)–(f). These results show the maximum displacement of the equipment (relative to the bench surface versus the maximum acceleration, taken at either the bench surface or the floor surface. Parts (a)–(c) are shown against the peak horizontal bench acceleration (PHBA), whereas parts (d)–(f) are shown against the peak horizontal floor acceleration (PHFA). The differences observed in PHBA (a–c) and PHFA (d–f) clearly illustrate the acceleration amplification provided by the bench-shelf system. Maximum values were taken as the average of multiple positions measured on the equipment. As anticipated, for these sliding-dominated, acceleration-sensitive equipment, increasing maximum relative displacement is observed with increasing input acceleration. Although there is some scatter in the data, generally below a PHFA of 0.8g, equipment resting in these three general configurations observed maximum relative sliding of less than 10 cm. In excess of 20 cm maximum relative sliding was observed for PHFA greater than 1.0g. It is interesting to note, that for a given PHFA, the maximum relative displacement experience by the equipment is not the same as between the different bench-system configurations, illustrating the sensitivity of response to the supporting system.

Table 5.2 Earthquake input motions selected for small equipment shake table tests

Input Motion	Earthquake Name and Location of Recording	Date M/D/YY	¹ Station	² PGA (g)	² PGV (cm/sec)	² PGD (cm)
GM-1	Morgan Hill	4/24/1984	Anderson Dam Down (T)	0.13	7	1.7
GM-2	Morgan Hill	4/24/1984	Hall valley (T)	0.18	24	4.8
50% in 50 Year Hazard Level						
GM-3	Morgan Hill	4/24/1984	Anderson Dam Down (T)	0.26	14	3.5
GM-4	Morgan Hill	4/24/1984	Hall valley (T)	0.36	47	9.3
10% in 50 Year Hazard Level						
GM-5	Kobe, Japan	1/17/1995	Kobe JMA (L)	0.44	50	11.0
GM-6	Loma Prieta	10/17/1989	Corralitos (T)	0.53	64	19.0
GM-7	Loma Prieta	10/17/1989	Gavilan College (T)	0.66	63	13.0
GM-8	Tottori, Japan	10/6/2000	Kofu (T)	0.69	33	6.0
GM-9	Loma Prieta	10/17/1989	Lexington Dam (L)	0.84	49	7.3
2% in 50 Year Hazard Level						
GM-10	Tottori, Japan	10/6/2000	Kofu (T)	1.16	55	10

¹ T=Transverse, L=Longitudinal

² PGA = peak ground acceleration, PGV = peak ground velocity, PGD = peak ground displacement

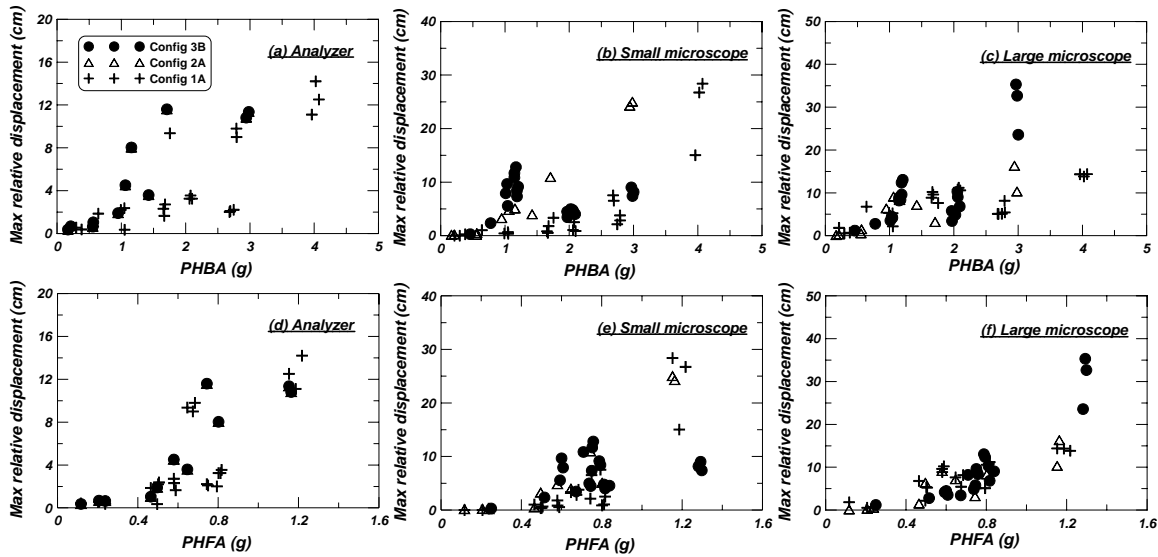


Fig. 5.2 Maximum equipment movement (relative to bench surface) versus peak horizontal bench acceleration (PHBA) for the (a) analyzer, (b) small microscope, and (c) large microscope, and maximum equipment movement (relative to bench surface) versus peak horizontal floor acceleration (PHFA) for the (d) analyzer, (e) small microscope, and (f) large microscope

Equally important is developing an understanding of the dynamic characteristics (frequency, damping, transmissibility) of the supporting bench-shelf systems.¹⁰ In this study, several methods were used to evaluate the dynamic characteristics of the various bench-shelf systems constructed. Techniques used include (1) low-amplitude, impulse-type (tap) experiments, (2) low-amplitude, band-limited white noise (base excitation), and (3) earthquake ground motion (base excitation). Each of these experiments was carried out on the representative configurations. Summary analysis of different characterizations illustrate that the natural

¹⁰ Shelf lips were included in the test-assembly; however, it is difficult to characterize their influence on equipment behavior. In general, we observed that when shaking was parallel to the lip direction, glassware tended to move along that axis and the lip restraint was not needed. However, when shaking was orthogonal to the lip direction, for nearly all cases, the 2"-tall lip did restrain the glassware from fully toppling and falling from the shelf. Only in cases where the glassware was significantly taller than the shelf lip, and for the strongest acceleration input motions considered, was the glassware observed to topple and fall completely from the shelf.

frequency of the system with relatively light mass is generally between 10–16 Hz, while the frequency of the system with relatively heavy mass (e.g., shelves full of books), is much less, between 4–6 Hz. Acceleration transfer functions were also calculated at the dominant frequencies, indicating that amplification as high as six times the input acceleration may occur [e.g., refer to Figs. 5.2(a)–(c)].

5.3 ANALYTICAL FORMULATION

Pure sliding under horizontal excitation. Considering the free body diagram of a rigid body resting on the top of a bench, the condition describing the onset of the movement of the body may be expressed as:

$$|m\ddot{x}(t)| \geq \mu_s mg \quad (5.1)$$

where, $\ddot{x}(t)$ = acceleration at the top of the bench, m = mass of the equipment, g = acceleration due to gravity, and μ_s = the static coefficient of friction between the bench-top surface and the body. Equation (5.1) assumes that the equipment has negligible height compared with the base width and the bench has negligible motions in other directions. It is clear from equation (5.1) that the body will start moving if the absolute maximum bench acceleration is greater than $\mu_s g$. Once the equipment begins sliding upon the bench, the equation of motion of the equipment may be expressed as (Shenton and Jones 1991):

$$m(\ddot{x}(t) + \ddot{u}(t)) = -S(\dot{u}(t))\mu_k mg \quad (5.2)$$

where, $S(\dot{u}(t))$ = signum function,

$$S(\dot{u}(t)) = 1; (\dot{u}(t) > 0) \quad (5.3)$$

$$S(\dot{u}(t)) = -1; (\dot{u}(t) < 0) \quad (5.4)$$

Thus, the sliding continues until the relative velocity of the mass equals to zero (i.e., $\dot{u}(t) = 0$). Therefore, the maximum relative displacement of equipment under a particular bench-top motion is function of μ_s and μ_k . Equation (5.2) may be solved numerically using, for example, the central difference method.

Effect of variability of μ_s and μ_k on sliding response. To account for the uncertainties associated with both the coefficients of static and kinetic friction, the problem can be cast in a probabilistic framework assuming an acceptable form of their probability distribution. For

simplicity, in this study, μ_s and ϕ ($= \frac{\mu_k}{\mu_s}$) are taken as two independent random variables with a uniform distribution. Assuming that the uncertainty in μ_s and ϕ can be expressed in terms of their upper limits U_{μ_s} and U_{ϕ} , respectively, and lower limits L_{μ_s} and L_{ϕ} , respectively, their probability density functions may be expressed as:

$$p(\mu_s) = \frac{1}{U_{\mu_s} - L_{\mu_s}}, \text{ for } L_{\mu_s} < \mu_s < U_{\mu_s} \quad (5.5)$$

$$= 0, \text{ elsewhere}$$

$$p(\phi) = \frac{1}{U_{\phi} - L_{\phi}}, \text{ for } L_{\phi} < \phi < U_{\phi} \quad (5.6)$$

$$= 0, \text{ elsewhere}$$

Since the coefficients of static and kinetic friction are uncertain, the maximum absolute relative displacement u_{\max} and the maximum absolute relative velocity \dot{u}_{\max} of the equipment are also uncertain. Therefore their mean and variance $m_{u_{\max}}$, $m_{\dot{u}_{\max}}$, $\sigma_{u_{\max}}$, $\sigma_{\dot{u}_{\max}}$, respectively, may be expressed as:

$$m_{u_{\max}} = E[U_{\max}] = \int_{-\infty}^{\infty} \int_{-\infty}^{\infty} u_{\max} p(\mu_s) p(\phi) d\mu_s d\phi \quad (5.7)$$

$$m_{\dot{u}_{\max}} = E[\dot{U}_{\max}] = \int_{-\infty}^{\infty} \int_{-\infty}^{\infty} \dot{u}_{\max} p(\mu_s) p(\phi) d\mu_s d\phi \quad (5.8)$$

$$\sigma_{u_{\max}} = \sqrt{E[U_{\max}^2] - m_{u_{\max}}^2} \quad (5.9)$$

$$\sigma_{\dot{u}_{\max}} = \sqrt{E[\dot{U}_{\max}^2] - m_{\dot{u}_{\max}}^2} \quad (5.10)$$

where,

$$E[\dot{U}_{\max}^2] = \int_{-\infty}^{\infty} \int_{-\infty}^{\infty} \dot{u}_{\max}^2 p(\mu_s) p(\phi) d\mu_s d\phi \quad (5.11)$$

$$E[U_{\max}^2] = \int_{-\infty}^{\infty} \int_{-\infty}^{\infty} u_{\max}^2 p(\mu_s) p(\phi) d\mu_s d\phi \quad (5.12)$$

5.4 DEVELOPMENT AND GENERALIZATION OF FRAGILITY CURVES

Data from the experiments described previously can be used to develop seismic fragility curves for use in design. Since the supporting bench plays a significant role in amplifying the input floor acceleration at the bench-top level, a cascade approach is used to generate the curves, whereby the bench is idealized as a single-degree-of-freedom system. Characterization data from the low amplitude hammer and shake table tests are used for input into the equations of motion and the bench-top response is determined. For the generation of the generalized fragility curves provided herein, the bench frequency and damping ratio are taken as $f_n = 10$ Hz and $\zeta_n = 10\%$, respectively.

Considering the 224 floor motions [from the 22 measured ground motions prepared at different hazard levels by Somerville (2002)] propagated through the UC Science Building (see Chapter 4), the amplification of the bench-top motions are obtained and, considering the uncertainty in μ_s and ϕ , seismic fragility curves are generated. Since the sliding of the equipment is acceleration sensitive and PHFA is more common in practice, for generation of these fragility curves PHFA is considered as the *EDP*.

To develop the fragility curves, the framework of probability theory is applied, with the underlying assumption that the probability of exceeding a particular limit state is a lognormal distribution. The probability of exceeding that particular limit state is therefore given by a lognormal distribution in the following form:

$$F(DM \geq b \mid EDP = a) = \Phi\left(\frac{\ln(a/\tilde{m})}{\tilde{\sigma}}\right) \quad (5.13)$$

where a = the input *EDP* (in this case, taken as PHFA), b = the value of damage measure (limit state of failure), and \tilde{m} and $\tilde{\sigma}$ are the median and log-standard deviation of the lognormal distribution, respectively. Provided that the median and log-standard deviations of the lognormal distribution are evaluated, for each a one may determine the probability that a particular limit state has been exceeded.

To determine \tilde{m} and $\tilde{\sigma}$, the maximum likelihood theory is used (Shinozuka et al. 2000). Considering, for any case i with the peak horizontal floor acceleration a_i , the probability of

exceeding a limit state is provided by $F(a_i)$, and for any case in which the limit state is not exceeded, the probability of exceeding that limit state is then provided by $(1 - F(a_i))$. The likelihood function $L(\tilde{m}, \tilde{\sigma})$ may then be expressed as:

$$L(\tilde{m}, \tilde{\sigma}) = \left(\prod_{i=1}^m F(a_i) \right) \left(\prod_{j=1}^{n-m} (1 - F(a_j)) \right) \quad (5.14)$$

where n = the total number of data points, and m = number of cases in which the limit state is exceeded, or $(n-m)$ = number of cases in which the limit state is not exceeded. To obtain the maximum values of $L(\tilde{m}, \tilde{\sigma})$, the following two conditions must be satisfied:

$$\frac{\partial \ln L(\tilde{m}, \tilde{\sigma})}{\partial \tilde{m}} = 0 \quad (5.15)$$

$$\frac{\partial \ln L(\tilde{m}, \tilde{\sigma})}{\partial \tilde{\sigma}} = 0 \quad (5.16)$$

Solving the above two-dimensional optimization problem numerically, \tilde{m} and $\tilde{\sigma}$ may be determined. After obtaining \tilde{m} and $\tilde{\sigma}$, the probability of exceeding a limit state for which \tilde{m} and $\tilde{\sigma}$ are determined and for any peak horizontal floor acceleration a_i may be determined using Equation (5.13).

Sample seismic fragility curves for bench-mounted equipment. An important consideration in the fragility curve description is the selection of a suitable damage measure. Two different damage measures are considered in this study: (1) sliding displacement and (2) sliding velocity, (maximum) relative to the bench top. Figure 3 illustrates a sample of the generated seismic fragility curves for the damage measure maximum relative sliding displacement = 5cm, considering different μ_s and ϕ values for the different equipment. Additional fragility curves for the different parameters studied may be found in Ray Chaudhuri and Hutchinson (2004b, 2006).

Although the fragility curves may be developed on a per-equipment basis as illustrated in Figure 5.3, the equipment considered in this study may be categorized by their frictional behavior into five broad categories. Table 5.3 shows the classification selected for these bench-mounted equipment, and lists the equipment, which has been tested, placed in their appropriate category. Thus, categorized equipment fragility curves are given in terms of their median \tilde{m} and coefficient of variation, cov (log-standard deviation/median i.e., $\tilde{\sigma}/\tilde{m}$) for the different displacements and equipment categories in Figure 5.4. It should be noted that for development of

the displacement fragility curves, an incremental displacement of 0.2 cm is selected, and for the velocity fragility curves, an incremental displacement of 1 cm/sec is selected in the calculations.

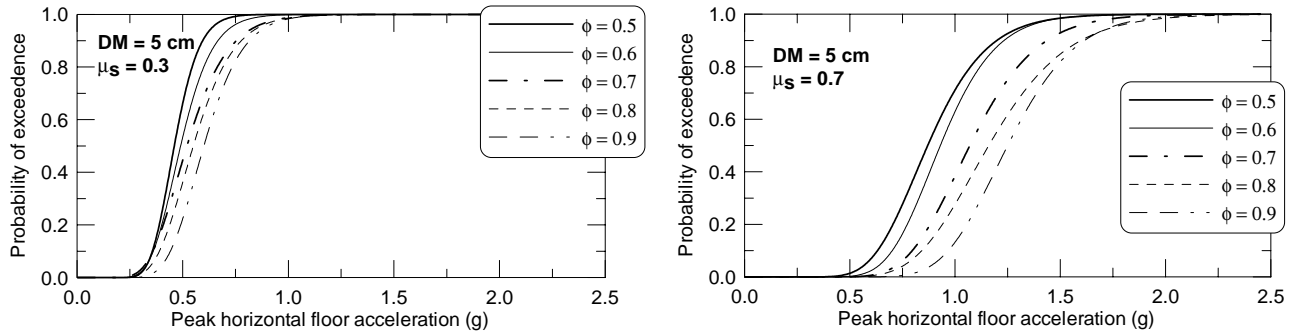


Fig. 5.3 Sample seismic fragility curves for small equipment, considering displacement = 5 cm, a range ϕ values, and: (a) $\mu_s = 0.3$ and (b) $\mu_s = 0.7$

*Using these curves to estimate $F(DM \geq b | EDP = a)$.*¹¹ These curves may be used as follows: (1) select a particular equipment and using Table 5.1, read the coefficients of static and kinetic friction for this equipment (or generalize a particular piece of equipment based on frictional resistance using Table 5.3); (2) select the fragility curves for the selected category: based on a selected damage measure (displacement or velocity) and its value (see Figs. 5.5 and 5.6); (3) find the values of the median \tilde{m} and coefficient of variation cov from the corresponding curves for that particular value of the damage measure; and (4) using the value of \tilde{m} , an assumed σ (=PHFA), the log-standard deviation ($\tilde{\sigma} = cov \cdot \tilde{m}$), determine the probability of exceedence for a given damage measure (b).

¹¹ Note that DM is used in the formula where the word “displacement” is used in the previous section.

Table 5.3 Generalized categories for small equipment

Category	Description	Items	Average μ_s	Average ϕ
1	Low base resistance	Large Microscope Indy	0.35	0.90
2	Low-medium base resistance	38 cm CRT 43 cm CRT	0.45	0.90
3	Medium base resistance	Technicon Autoanalyzer Indigo Octane	0.65	0.95
4	Medium-high base resistance	Eppendorf Centrifuge	0.70	0.90
5	High base resistance	48 cm CRT	0.85	0.95

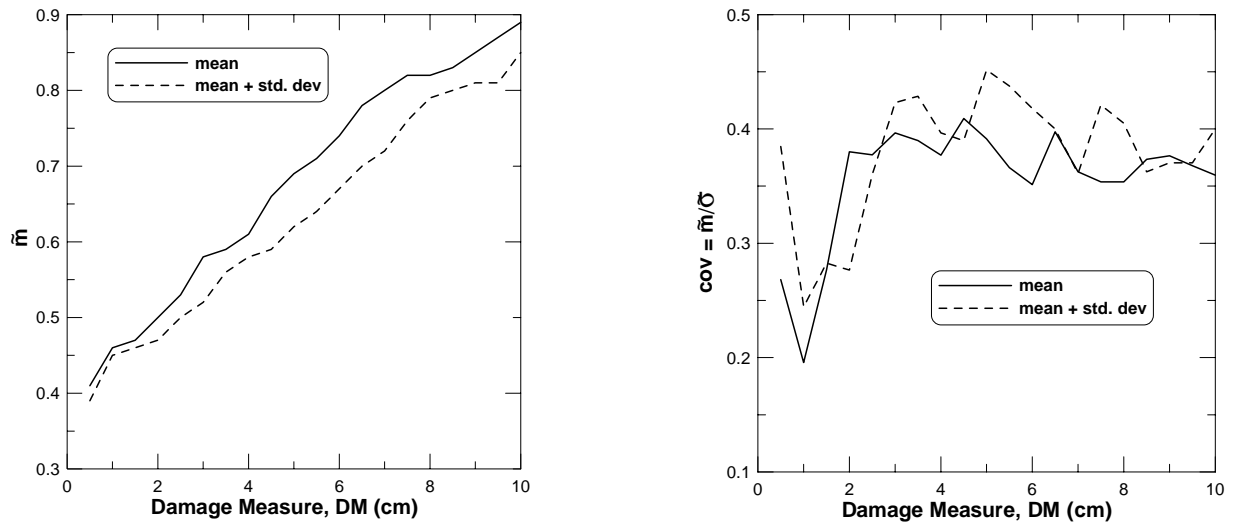


Fig. 5.4 Sample generalized lognormal parameters \tilde{m} and cov for $DM =$ maximum relative displacement, bench-mounted equipment category 1 ($\mu_s = 0.35$, $\mu_k = 0.90$)

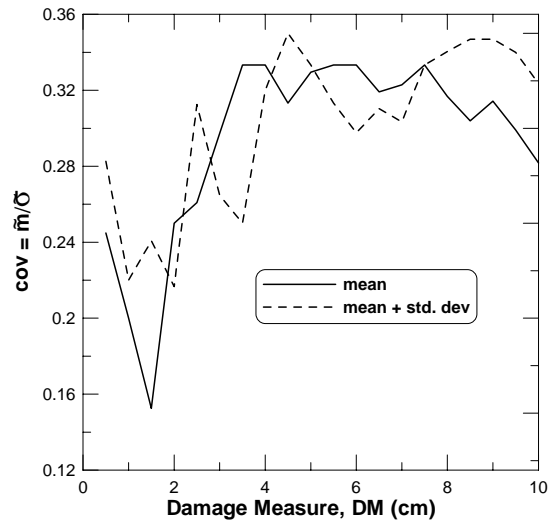
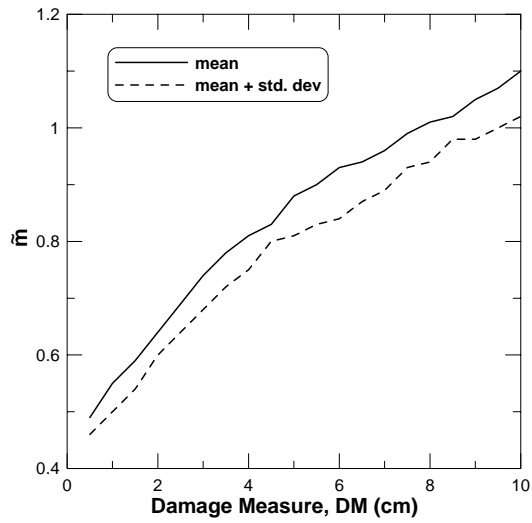


Fig. 5.5 Lognormal parameters \tilde{m} and cov for $DM =$ maximum relative displacement, bench-mounted equipment category 2 ($\mu_s = 0.45$, $\mu_k = 0.90$)

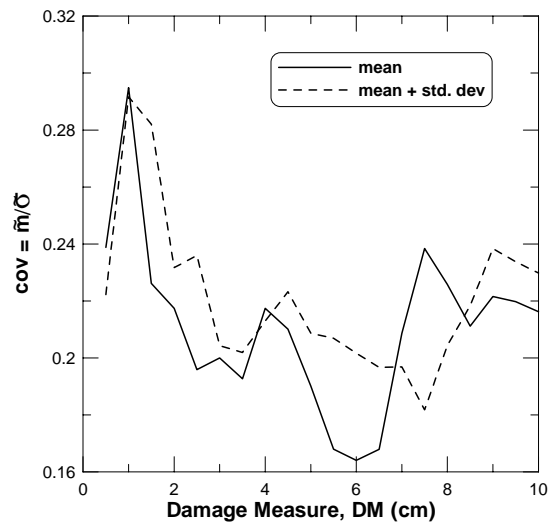
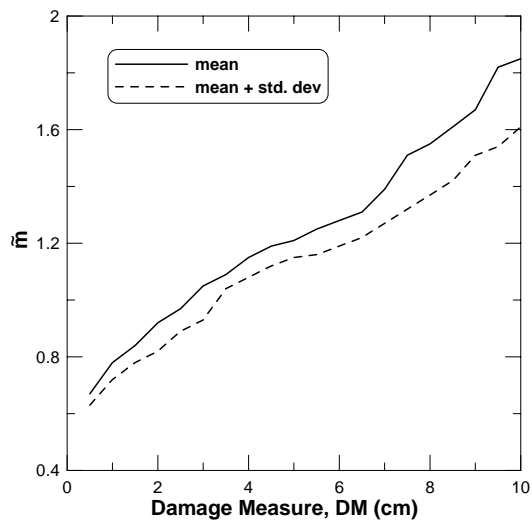


Fig. 5.6 Lognormal parameters \tilde{m} and cov for $DM =$ maximum relative displacement, bench-mounted equipment category 3 ($\mu_s = 0.65$, $\mu_k = 0.95$)

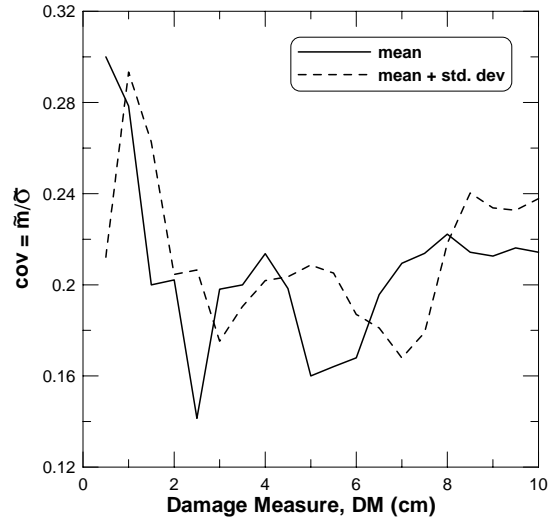
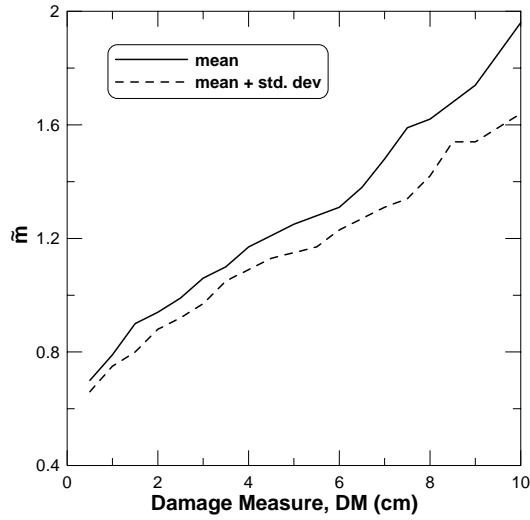


Fig. 5.7 Lognormal parameters \tilde{m} and cov for $DM =$ maximum relative displacement, bench-mounted equipment category 4 ($\mu_s = 0.70, \mu_k = 0.90$)

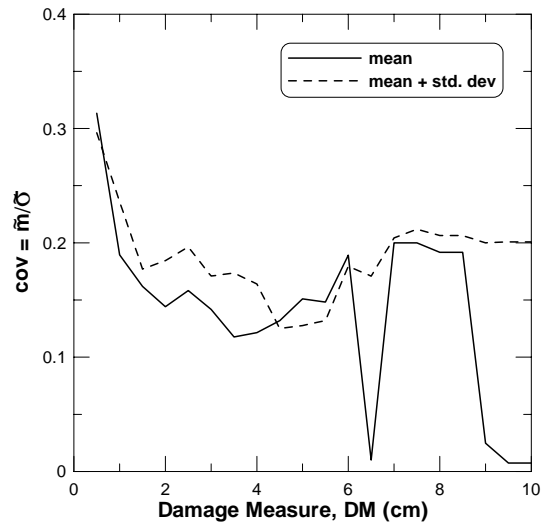
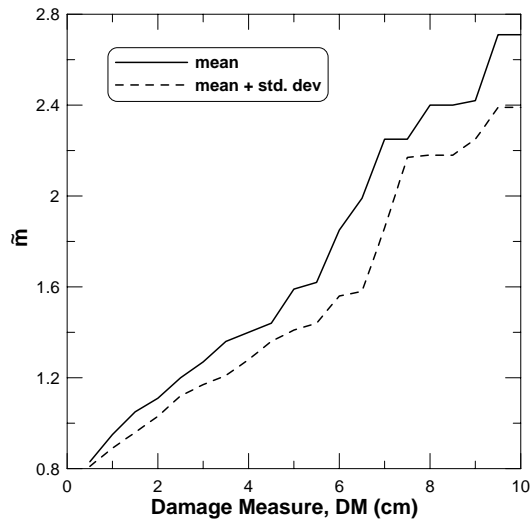


Fig. 5.8 Lognormal parameters \tilde{m} and cov for $DM =$ maximum relative displacement, bench-mounted equipment category 5 ($\mu_s = 0.85, \mu_k = 0.95$)

5.5 REFERENCES

- Comerio, M.C. and Stallmeyer, J.C. (2002). "Nonstructural loss estimation: the UC Berkeley case study." Pacific Earthquake Engineering Research (PEER) Center Report Number PEER-2002/01. 174 pp.
- Hutchinson, T.C., Ray Chaudhuri, S., Kuester, F., and Auduong, S. (2005). "Light-based motion tracking of equipment subjected to earthquake motions." *ASCE Journal of Computing in Civil Engineering* 19(3):293–303.
- Hutchinson, T.C. and Ray Chaudhuri, S. (2003). "Bench and shelf-mounted equipment and contents: shake table experiments." In the *Proceedings of the Applied Technology Council Seminar on Seismic Design, Performance, and Retrofit of Nonstructural Components in Critical Facilities*. ATC-29-2. Newport Beach, CA. 15 pp.
- Lee, T.H. and Mosalam, K. (2002). *OpenSees seismic analysis of the LSA Building*. Draft Report submitted to Pacific Earthquake Engineering Research (PEER) Center. 45 pp.
- Ray Chaudhuri, S. and Hutchinson, T.C. (2005). *Performance characterization of bench- and shelf-mounted equipment and contents*. Final report to Pacific Earthquake Engineering Research (PEER) Center Report 2005/05. (forthcoming).
- Ray Chaudhuri, S. and Hutchinson, T.C. (2004b). "Sliding Fragility of Bench-Mounted Unattached Scientific Equipment." In the *Proceedings of the 2nd International Conference on Structural Engineering, Mechanics, and Computation (SEMC)*. Cape Town, South Africa. 5 pp.
- Ray Chaudhuri, S. and Hutchinson, T.C. (2004a). "Characterizing Frictional Behavior for Use in Predicting the Seismic Response of Unattached Equipment." In the *Proceedings of the 11th International Conference on Soil Dynamics & Earthquake Engineering. (SDEE 2004)*. Berkeley, California. January. pp.368–375.
- Ray Chaudhuri, S. and Hutchinson, T.C. (2006). "Fragility of bench-mounted equipment considering uncertain parameters." Submitted to *ASCE Journal of Structural Engineering* (in press).
- Shenton, H.W. III and Jones, N.P. (1991). "Base excitation of rigid bodies. I: formulation." *Journal of Engineering Mechanics, ASCE*. 117: 2286–2306.
- Shenton, H.W. III. (1996). "Criteria for initiation of slide, rock, and slide-rock rigid-body modes." *Journal of Engineering Mechanics, ASCE*. 122(7): 690–693.
- Shinozuka, M., Feng, M.Q., Kim, H.K. and Kim, H.S. (2000). "Nonlinear static procedure for fragility curve development." *Journal of Engineering Mechanics, ASCE*. 126(12): 1287–1295.
- Sommerville, P. (2002). "Ground motion time histories for the UC lab building." Unpublished Pacific Earthquake Engineering Research (PEER) Center Report.

6 Experimental and Analytical Studies on the Seismic Response of Slender Laboratory Equipment

Nicos Makris, University of California, Berkeley (on leave at University of Patras, Greece 2003–2004) and Dimitrios Konstantinidis, University of California, Berkeley

6.1 MOTIVATION

During strong earthquake shaking, heavy equipment located at various floor levels of hospitals, university laboratories, and other critical facilities might slide appreciably, rock-slide, rock, or even overturn. While sliding is the favorable mode of response, excessive sliding displacements of sensitive/heavy equipment should be avoided, since the equipment may impact walls or neighboring equipment or it may block a doorway that serves for evacuation.

In the event that rocking response is realizable, the high acceleration spikes that develop during impact are a concern, since the sensitive contents of the equipment may be damaged. Furthermore, the re-centering mechanism during impact has a negative slope, while the energy dissipation during impact is minimal. Accordingly, rocking is in principle an undesirable response of equipment because it is often the cause of mechanical damage or total loss in the event of overturning.

6.2 OBJECTIVES OF THE RESEARCH

In this project, experimental and analytical studies were undertaken to examine the seismic vulnerability of freestanding and restrained equipment located in the UC Sciences laboratories within several floor levels. The equipment of interest included low-temperature refrigerators,

freezers, incubators, and other heavy equipment of the UC Science Laboratory Building at the UC Berkeley campus.

The dynamic behavior of either freestanding or restrained equipment is sensitive to many parameters but particularly to the characteristics of the base input (mainly peak base acceleration and duration of the predominant acceleration pulse of the excitation), the frictional characteristics of the equipment-base interface, and the slenderness of the equipment.

The experimental program concentrated on three heavy pieces of equipment of various sizes and slenderness (1) 90" x 38" x 31" (H x W x D), $\alpha=\tan^{-1}(H/D)=19^\circ$; (2) 71"x 32"x 26.5", $\alpha=20.5^\circ$; (3) 84" x 33"x 32.5" $\alpha=21^\circ$, that were obtained from the UC Science Building. After having experimentally identified the mechanical properties of their supports (flexibility of legs/pads and coefficient of friction), shake table studies were conducted to conclude on the response patterns of freestanding and anchored equipment. The experimental data were used to validate commercially available software (Working Model) that had been used during summer 2002 for simulation of the anticipated response. Upon validation of the Working Model software, fragility curves on the seismic response of building contents were produced.

6.3 SEISMIC HAZARD

This work is part of a wider study on the seismic response analysis of the contents of a laboratory on the main campus of UC Berkeley.

The seismic hazard on the Berkeley campus is dominated by potential ground motions generated from the Hayward fault, which is located less than one kilometer east of the central campus. The Hayward fault is a strike-slip fault that has a potential to generate earthquakes having magnitudes as large as $M_w = 7.0$. For a hazard level equal to 50% in 50 years, the largest contributions come from earthquakes in the magnitude range of $M_w = 5.5$ to 6.0. For hazard level equal to 10% in 50 years and to 2% in 50 years, the largest contributions come from earthquakes in the magnitude range of $M_w = 6.5$ to 7.0. The motions listed in Table 6.1 have been selected to satisfy (to the extent possible) the magnitude and the distance combination from a strike-slip earthquake on S_C soil type (Somerville 2001).

The interest of the UC Berkeley administration in the seismic response of the UC Science Laboratory Building has supported a comprehensive nonlinear dynamic analysis of the building which resulted in simulated floor motions (Lee and Mosalam 2002). Floor motions are of unique interest in assessing the seismic response of building contents, since they differ appreciably from ground motions.

Table 6.1 List of selected records

Earthquake	Record	M_w	Distance [km]	Hazard Level
Aegion, Greece (Ground)	OTE, FP	6.2	5.0	-
Coyote Lake, California (Ground)	Gilroy Array #6, FN	5.7	3.0	-
Parkfield, California (Ground and 6 th floor)	Cholome Array #8, FN	6.0	8.0	50% in 50yrs
Coyote, California (Ground and 6 th floor)	Gilroy Array #6, FN	5.7	3.0	50% in 50yrs
Tottori, Japan (Ground and 6 th floor)	Kofu, FN	6.6	10.0	10% in 50yrs
Loma Prieta (Ground and 6 th floor)	Gavilan College, FN	7.0	9.5	10% in 50yrs
Loma Prieta (Ground and 6 th floor)	Gilroy Historic Bldg. FN	7.0		2% in 50yrs
Loma Prieta (Ground)	Los Gatos PC, FP	7.0	3.5	2% in 50yrs
Loma Prieta (Ground)	Corralitos, FP	7.0	3.4	2% in 50yrs

6.4 FRICTION TESTS

The mechanical properties of the contact interface of the equipment and the laboratory floor have been determined by conducting slow pull tests on the equipment. The floors throughout the UC Science Laboratory are lined with vinyl tiles. In order to simulate the actual conditions, a 4ft. x 8ft. pressboard surface covered with vinyl tiles was constructed. Atop it rested the equipment specimens. Figure 6.1 shows a schematic of the experimental setup of the pull tests while Figure 6.2 shows a view of the three pieces of equipment of interest resting on the vinyl floor surface.

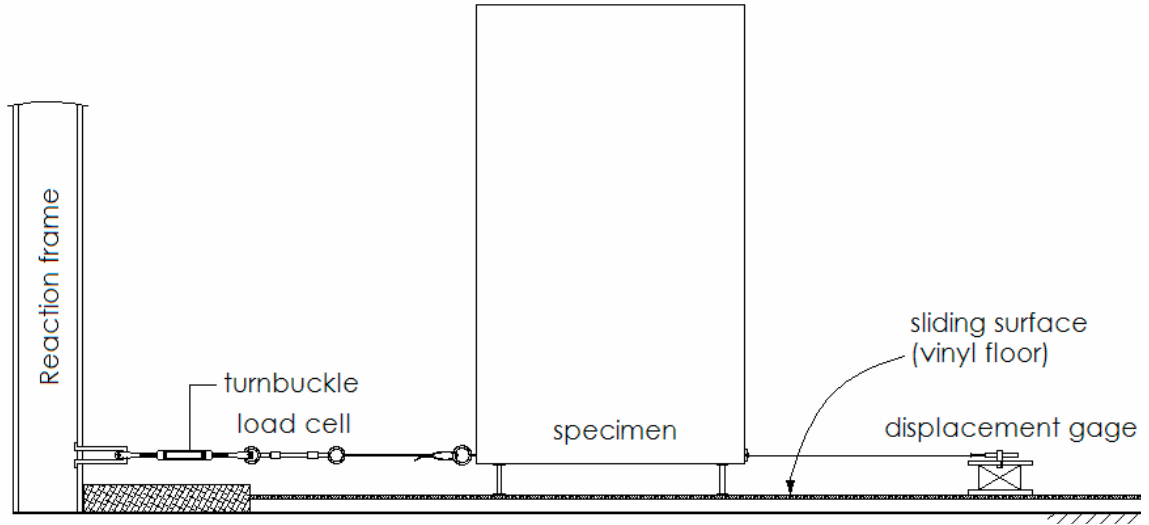


Fig. 6.1 Schematic diagram of experimental setup for friction tests

Figure 6.3 plots load-displacement curves recorded during the pull tests on the three pieces of equipment shown in Figure 6.2. All three sets of curves shown in Figure 6.3 exhibit a peak value when sliding initiates and subsequently a relatively constant friction force while sliding occurs.



FORMA Incubator



Kelvinator Refrigerator



ASP Refrigerator

Fig. 6.2 Three pieces of equipment of interest

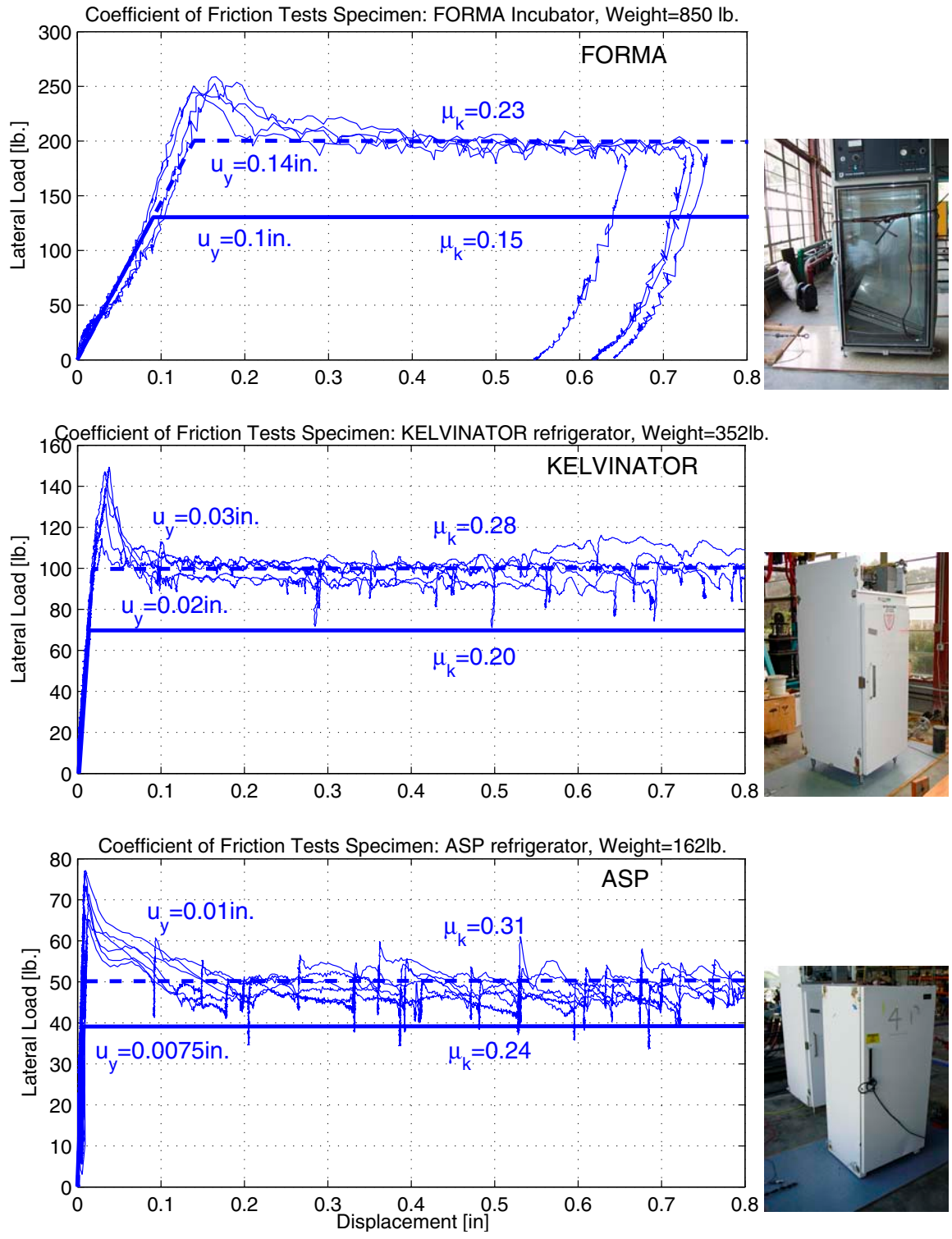


Fig. 6.3 Recorded load-displacement plots for three pieces of equipment obtained from pull tests (wavy lines); elastoplastic idealization with μ_k from pull tests (dashed lines); and elastic idealization with μ_k from best fit of shake table tests (solid lines)

The pre-yielding elasticity in the load displacement curves originates from the flexure of the legs of the equipment prior to sliding. This pre-yielding elasticity of the legs and the friction force that develops along the vinyl surface combine to a yielding mechanism of the interface. A simple idealization of the yielding mechanism of the interface is the elastoplastic model shown with a dashed line in Figure 6.3. The model parameters that define the elastoplastic idealization are the yield displacement, u_y , and the normalized strength, $\mu=Q/mg$.

Simulation studies on the sliding response of the equipment using the values of the coefficient of friction extracted from the pull tests yield results which are in fair agreement with the experimental data. The predicted response of all three pieces of equipment was appreciably improved when lower values of their respective coefficients of friction were used. These lower levels of friction coefficients are shown in Figure 6.3 with solid lines. Table 6.2 summarizes the values of the coefficients of friction and yield displacements that were obtained from the slow pull tests and from the best fit of the data obtained from shake table studies. The prediction of the recorded response using the values of the coefficients of friction shown in Figure 6.3 and Table 6.2 are offered in the next section following the presentation of the shake table studies.

In addition to sliding, rocking is a potential mode of response when a piece of equipment is freestanding. The parameters that govern the rocking response of a freestanding object are its *slenderness*, α , and the size of the block which is represented by the *frequency parameter*, p . For uniform-density, rectangular blocks with width $2b$ and height $2h$, $\alpha = \tan^{-1}(b/h)$ and $p = \sqrt{3g/4R}$, where $R = \sqrt{b^2 + h^2}$. Table 6.2 offers the slenderness α and the frequency parameter p along the most slender face of the equipment.

Table 6.2 Coefficients of friction and yield displacements obtained from slow pull tests and from best fit of shake table test data

Equipment	From slow pull tests			Values used to best fit experimental data from the shake table tests		weight [lb.]	α [rad]	p [rad/s]
	μ_s	μ_k	u_y [in.]	μ_k	u_y [in.]			
FORMA	0.30	0.23	0.14	0.15	0.09	850	0.27	2.49
KELVINATOR	0.37	0.28	0.03	0.20	0.02	352	0.29	2.57
ASP	0.43	0.31	0.01	0.24	0.008	162	0.31	2.79

6.5 SHAKE TABLE TESTS

The three pieces of equipment shown in Figure 6.2 were subjected to shake table tests. The same type of pressboard surface that was used as the base for the slow pull tests was positioned atop the shaking table to support the equipment. Figure 6.4 shows a photograph of one of the freestanding equipment resting on the shaking table.

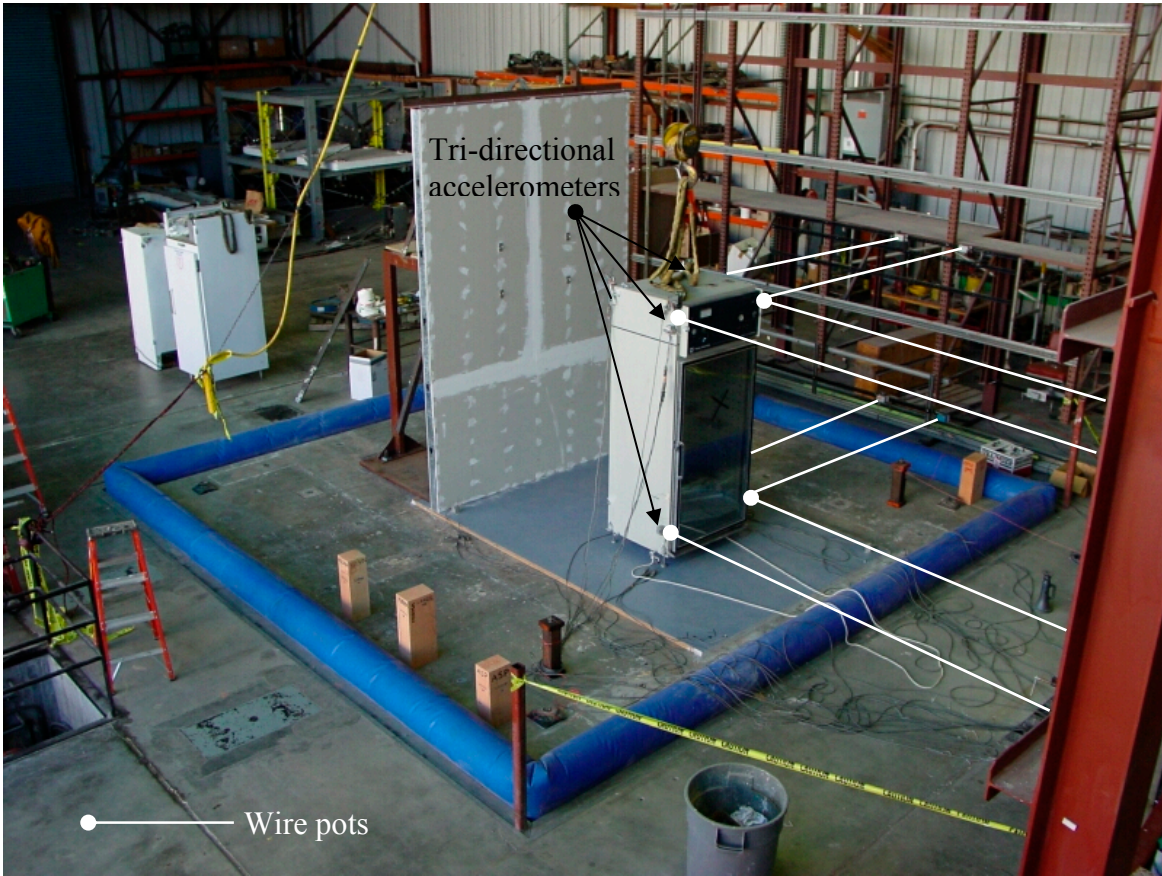


Fig. 6.4 FORMA incubator resting atop shaking table at Richmond Field Station earthquake simulation laboratory. Locations of wire pots are indicated with white lines, and locations of accelerometers indicated with dark arrows.

The displacement of the shaking table and the equipment were measured with wire pots attached to a frame fixed on the laboratory floor. Figure 6.4 shows the locations of the wire pots on the specimen. Accelerometers were also installed on the positions shown in Figure 6.4 in order to capture horizontal and vertical accelerations.

The horizontal displacement capacity of the shaking table at the Richmond Field Station earthquake simulation laboratory, UC Berkeley, is ± 6.0 inches. Given this constraint, we were able to run at full scale only the ground motions with hazard level equal to 50% in 50 years and 10% in 50 years. Shake table tests using the stronger ground motions with probability of occurrence equal to 2% in 50 years were conducted on scaled-down models by compressing the duration of the records.

Table 6.3 presents a list of the shake table tests conducted on the full-scale freestanding equipment shown in Figure 6.2. All the tests listed in Table 6.3 were one-directional tests and most of the motions of the equipment were along this direction. On several occasions, the equipment while shaken along the primary direction, exhibited rotations about the vertical axis. In some cases, these plane rotations were as small as 0.005 rad to as large as 0.33 rad, indicating that even when the excitation is one-directional, the response in reality is in three dimensions.

6.6 RESPONSE ANALYSIS OF FREESTANDING EQUIPMENT

Figure 6.5 (bottom) plots the OTE motion recorded during the 1995 Aegion, Greece, earthquake. The graph above the acceleration record plots the resulting table displacement and the third graph from the top plots the recorded sliding displacement of the Kelvinator refrigerator. The top graphs in Figure 6.3 plot the uplift of the equipment and the rotation about the vertical axis. The third graph from the top also plots the analytical predictions using the elastoplastic models shown in the middle graph of Figure 6.3. The dashed line is the analytical prediction that results with the values of the coefficient of friction $\mu = 0.28$ and the yield displacement $u_y = 0.03$ in. , which are suggested by the slow pull tests done on the Kelvinator refrigerator. The heavy line is the analytical prediction that results with $\mu = 0.20$ and $u_y = 0.02$ in. The superior performance of the elastoplastic model with these model parameters ($\mu = 0.20$ and $u_y = 0.02$ in.) is consistent with Figures 6.6 and 6.7 that plot response time histories for the Coyote Lake, Gilroy Array #6 ground motion and the corresponding motion that results in the 6th floor. The response histories from the remaining motions used in this experimental study are presented in a report by Konstantinidis and Makris (2004). Figure 6.8 plots the difference between the experimentally measured and the analytically predicted permanent displacement as a function of the rotation about the vertical axis.

The data points shown in Figure 6.8 suggest that when the rotation of the equipment about the vertical axis is small, the elastoplastic model with the calibrated parameters offers a very good prediction. The fidelity of the prediction diminishes when the rotation about the vertical axis increases. More on the fidelity of the results obtained with the calibrated elastoplastic model are offered in the report by Konstantinidis and Makris (2004).

6.7 ESTIMATION OF SLIDING DISPLACEMENT OF FREESTANDING EQUIPMENT

Within the context of earthquake engineering, an early solution to the response of a rigid-plastic system (rigid mass sliding on a moving base) subjected to a rectangular acceleration pulse was presented by Newmark (1965). Under a rectangular acceleration pulse with amplitude $a_p > \mu g$ and duration T_p , the maximum relative-to-the-base displacement is (Newmark 1965):

$$u_{\max} = \frac{1}{2} a_p T_p^2 \left(\frac{a_p - \mu g}{\mu g} \right) \quad (6.1)$$

Table 6.3 Input motions for shake table tests conducted on three laboratory specimens. Peak table accelerations and peak sliding displacements of freestanding equipment.

Earthquake	Record	Hazard Level	EQUIPMENT								
			FORMA			KELVIN		ASP		PROFILE	
			PGA	FACE PTA	FACE PSD	FACE PTA	FACE PSD	FACE PTA	FACE PSD	PROFILE PTA	PROFILE PSD
			[g]	[g]	[in.]	[g]	[in.]	[g]	[in.]	[g]	[in.]
Ægion, Greece 6/15/1995	OTE FP		0.50	0.75	6.87	0.76	6.00	0.86	3.16	0.73	2.41
Coyote Lake 8/6/1979	Gilroy Array #6 FN		0.47	0.68	2.57	0.69	2.13	0.73	1.61	0.70	1.02
Parkfield 6/27/1966	Cholome Array #8 FN GROUND	50% in 50 yrs	0.56	0.70	3.70	0.75	1.27	0.77	0.84	0.70	0.34
Parkfield 6/27/1966	Cholome Array #8 FN 6TH LEVEL	50% in 50 yrs	0.71	1.61	13.48	1.66	8.90	1.70	22.83	1.68	23.70
Coyote Lake 6/8/1979	Gilroy Array #6 FN GROUND	50% in 50 yrs	0.47	0.75	3.07	0.74	3.26	0.76	3.61	0.75	3.68
Coyote Lake 6/8/1979	Gilroy Array #6 FN 6TH LEVEL	50% in 50 yrs	0.78	0.43	0.76	0.76	7.37	0.77	9.35	0.80	8.01
Loma Prieta 10/17/1989	Gavilan College FN GROUND	10% in 50 yrs	0.66	0.73	3.79	0.76	2.26	0.77	1.85	0.79	2.59
Loma Prieta 10/17/1989	Gavilan College FN 6TH LEVEL	10% in 50 yrs	0.75	leg failure		0.64	5.06	0.67	7.03	0.67	6.70
Tottori, Japan 10/6/2000	Kofu FN GROUND	10% in 50 yrs	0.69			1.09	5.43	1.07	13.89	1.07	16.62
Tottori, Japan 10/6/2000	Kofu FN 6TH LEVEL	10% in 50 yrs	0.54			0.81	5.24	1.08	13.92	0.85	7.96

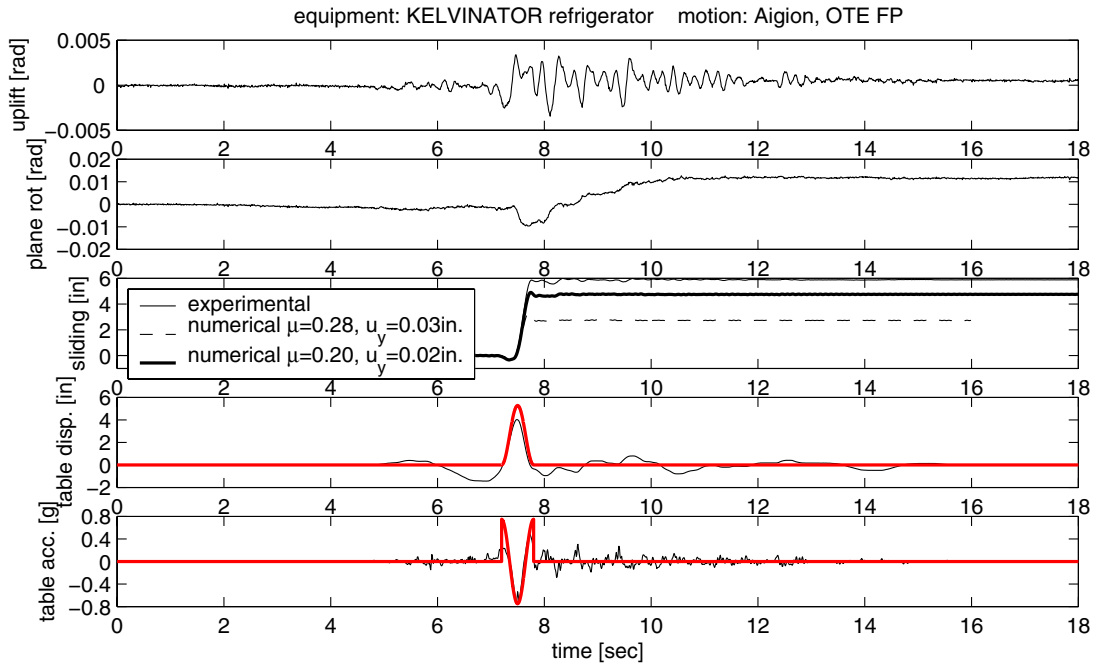


Fig. 6.5 Response time history for Kelvinator refrigerator plotted for Aigion earthquake record

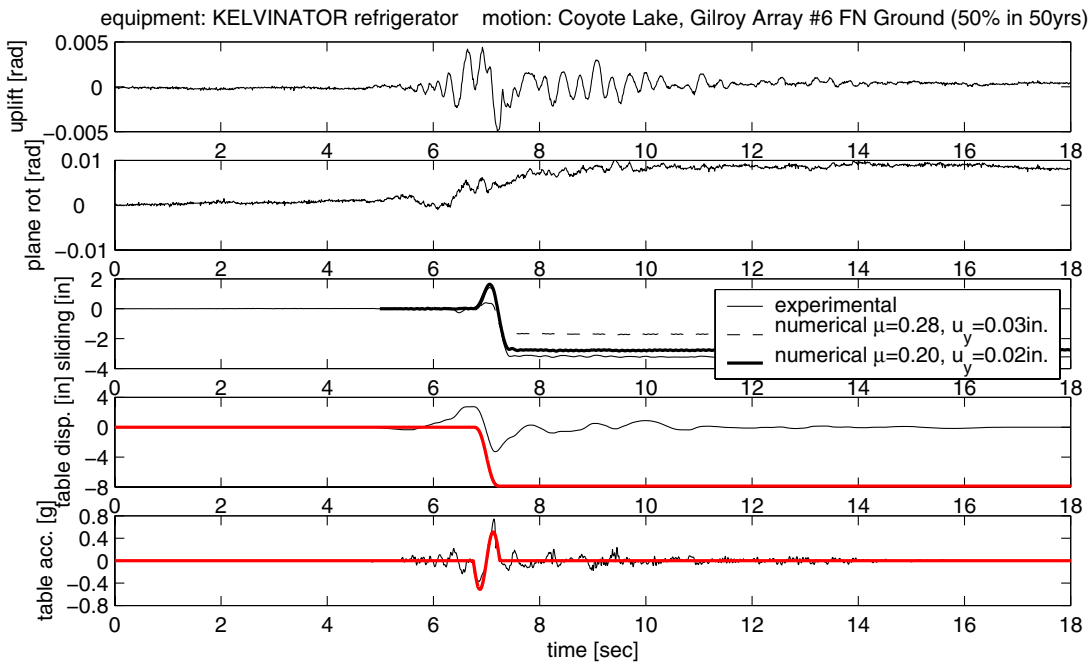


Fig. 6.6 Response time history for Kelvinator refrigerator plotted for Coyote Lake, Gilroy Array #6 earthquake record

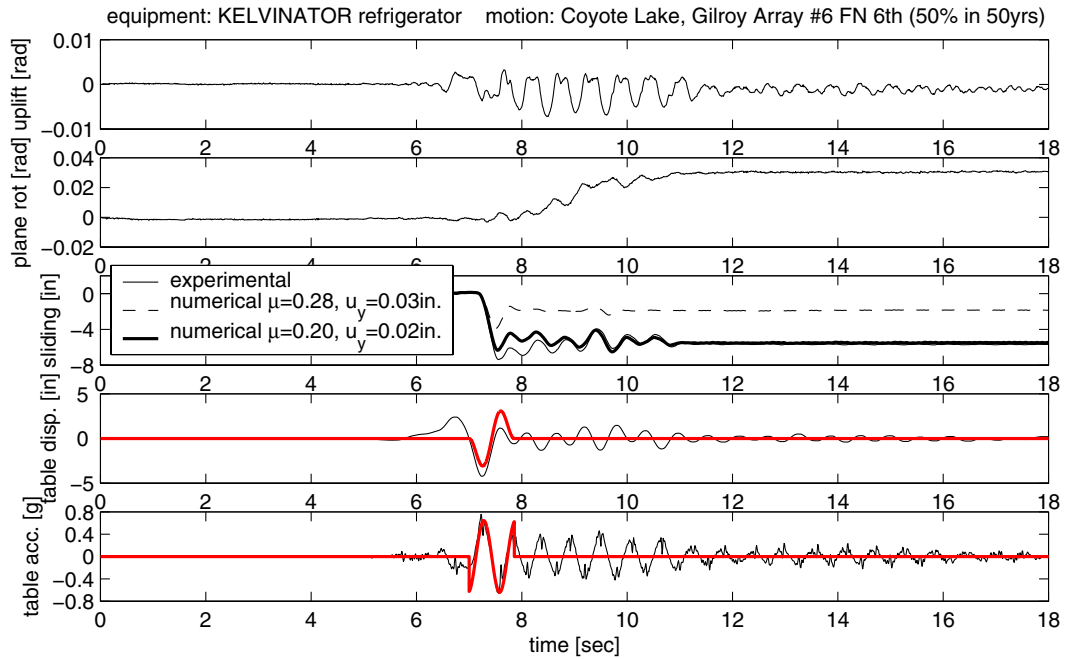


Fig. 6.7 Response time history for Kelvinator refrigerator plotted for Coyote Lake, Gilroy Array #6 earthquake record on 6th floor level

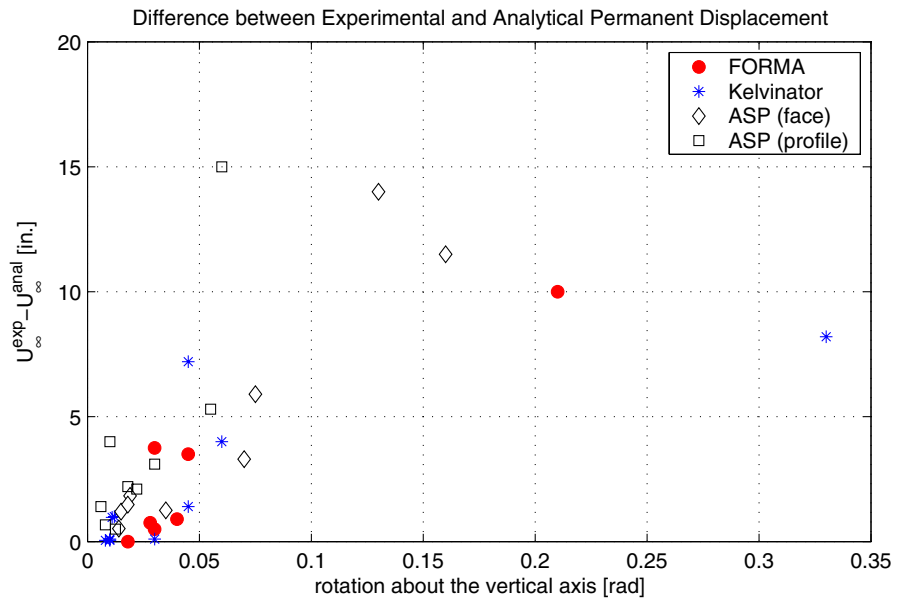


Fig. 6.8 Difference between experimental and analytically predicted permanent displacements as a function of rotation about vertical axis

Equation (6.1) suggests that the peak sliding displacement is proportional to the characteristic length scale of the excitation, $L_e = a_p T_p^2$, and the net strength of the pulse, $(a_p - \mu g)/\mu g$. The characteristic length, $L_e = a_p T_p^2$, is a measure of the energy induced by the dominant pulse of the excitation (Makris and Black 2003).

In the case of a rectangular or trigonometric pulse, the acceleration amplitude, a_p , and the duration of the pulse, T_p , are uniquely defined. When recorded ground motions or floor motion are of interest, the identification of the acceleration amplitude and duration of the most predominant pulse is a challenging task. Several near-source ground motions exhibit distinguishable acceleration pulses where the amplitude and duration are obvious. The bottom window of Figure 6.5 plots with a heavy line a one-cosine acceleration pulse that captures with fidelity many of the kinematic characteristics of the 1995 Aegion OTE record. The resulting displacement of the ground is plotted on the second window from the bottom. In the case of floor motions, the dominant period is the period of vibration of the building and the acceleration amplitude can be taken equal to the peak floor acceleration. The bottom window of Figure 6.7 plots with a heavy line a Type-C₁ (Makris and Roussos 2000; Makris and Chang 2000) that approximates the 6th floor motion which corresponds to the 1979 Coyote Lake Gilroy Array #6 ground motion. Figure 6.9 plots the experimental peak sliding displacement factored with the strength capacity over the inertial demand, $u_{\max} \mu g / PTA$, versus the intensity of the pulse, $(PTA - \mu g) / \omega_p^2$, for the three pieces of equipment; where ω_p^2 is the frequency of the predominant pulse of the excitation (in the case of ground motions) *or* the first modal frequency of vibration of the building (in the case of floor motions).

The variables appearing along the axes of Figure 6.9 which have dimension of length are selected after rearranging Equation (6.1); for a rectangular pulse with acceleration amplitude $a_p = PTA$ and duration $T_p = 2\pi / \omega_p$, (6.1) yields

$$u_{\max} \frac{\mu g}{PTA} = 2\pi^2 \frac{PTA - \mu g}{\omega_p^2} \quad (6.2)$$

which suggests a linear relation with a slope equal to $2\pi^2$. In the case of non-monotonic acceleration histories, we also adopt a linear relation, but one that has much smaller slope as determined from the best fit of the peak recorded values. Figure 6.9 plots with a solid line the linear relation. Our tests indicate that a good estimate of the peak sliding displacement of a piece

of equipment resting on a surface with coefficient of friction μ that is subjected to a ground motion with a predominant pulse with peak acceleration PTA and duration $T_p = 2\pi/\omega_p$ is given by the expression

$$u_{\max} \frac{\mu g}{PTA} = 1.58 \frac{PTA - \mu g}{\omega_p^2} \approx \frac{\pi}{2} \frac{PTA - \mu g}{\omega_p^2} \quad (6.3)$$

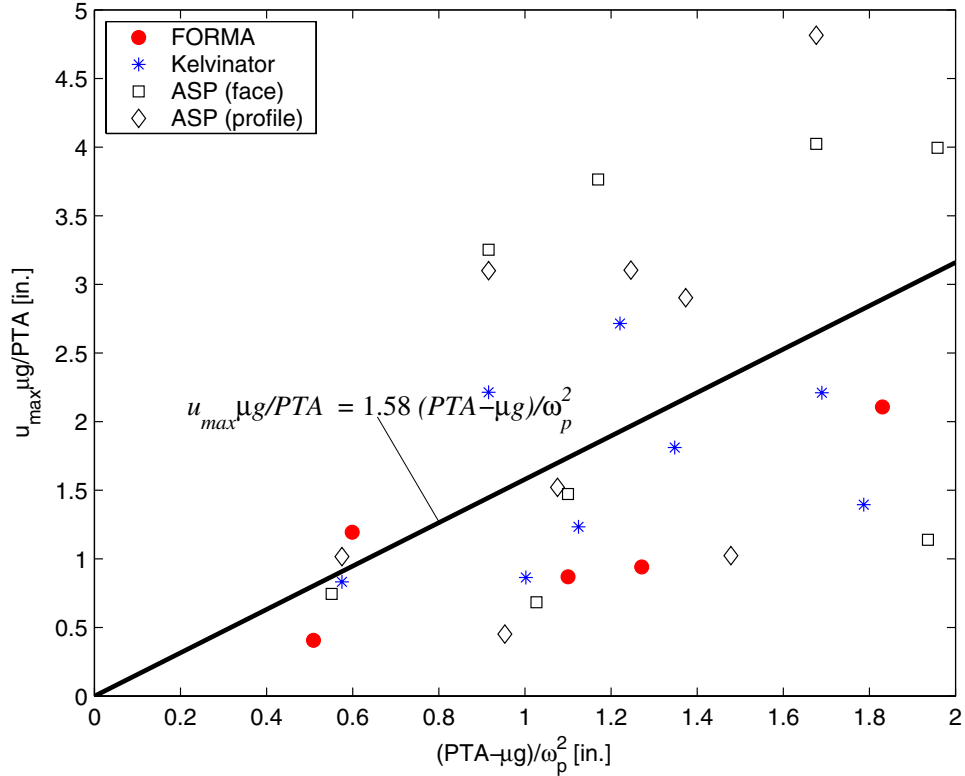


Fig. 6.9 Peak recorded sliding displacement of equipment as a function of strength of predominant pulse of excitation (points); and best linear fit of data (solid line)

The scattering of the data shown in Figure 6.9 suggests that the peak sliding displacement, u_{\max} , should be expressed as a random variable D

$$D = a_1 IM \cdot \varepsilon \quad (6.4)$$

where $a_1 = 1.58 \approx \pi/2$ is a coefficient (slope) determined by the best fit of experimental data, $IM = (PTA / \mu g)(PTA - \mu g) / \omega_p^2$ is an intensity measure of the pulse relative to the coefficient of

friction of a given interface, and ε is a lognormally distributed random variable with unit mean and standard deviation σ_1 . The probabilistic approach of this problem, together with a fragility analysis, is the subject of a separate study that will be presented in the report by Konstantinidis and Makris (2004)¹².

6.8 RESPONSE OF RESTRAINED EQUIPMENT

In order to simulate the conditions present in the UC Sciences Building laboratory a mock 12-ft-tall nonstructural wall was built (Fig. 6.4) onto which the equipment is anchored with chains. The chains are attached to the top of the equipment and are intended to restrain the equipment from exhibiting excessive displacement or possible overturning during a seismic event. The chains are connected to an anchor that is screwed into the light steel framing of the wall. No failure of this connection was observed in any of the shake table tests. Only minor damage was observed in the sheetrock from direct impact with the equipment.

When the same excitations with which the freestanding equipment was tested were applied to the restrained equipment, the peak equipment accelerations recorded were higher in all occasions but one. Figure 6.10 shows a comparison of the recorded peak equipment accelerations of the equipment in the two tested configurations. The horizontal axis indicates the peak table acceleration of the input excitation. It is obvious that typically the restrained equipment experienced significantly larger accelerations, in one instance even exceeding 800% that of the freestanding equipment.

¹² The fragility analysis was prepared as part of the tested research and incorporated into the loss analysis. The work completed for the testbed is documented in a report by Giorgio Lupoi, Dimitrios Konstantinidis and Nicos Makris, titled, "Fragility Analysis on the Seismic Response of Freestanding Equipment," available on the testbed website.

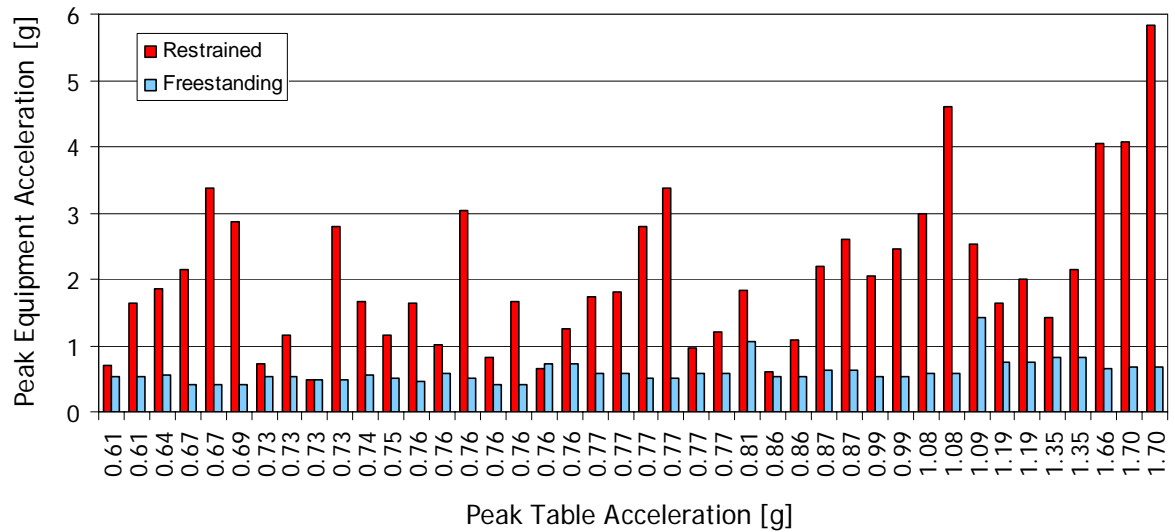


Fig. 6.10 Comparison of recorded peak equipment accelerations of restrained and freestanding equipment

6.9 SHAKE TABLE TESTS OF SCALE MODELS

Because of the limited displacement capacity of the shaking table, full-scale tests were only run for the 50% and 10% in 50 years excitations. In order to access the possibility of overturning of the equipment subjected to stronger excitations (2% in 50 years), experiments were performed on 1/4-scale wooden block models of the equipment.

The mechanical properties of the actual interfaces between the equipment and lab floors were very difficult to replicate for the wooden model shake table tests. The measured coefficient of friction of the wood model-base interface was 0.68, which is significantly higher than the measured coefficients of friction of the interfaces between the actual equipment and lab floors (Fig. 6.3 and Table 6.2). This resulted in overturning being the predominant mode of response for the wood models. Numerical simulations with the Working Model confirmed this overturning for the full-scale equipment with the coefficient of friction of 0.68. On the other hand, numerical simulations with the actual values of the coefficients of friction of the equipment-floor interfaces resulted in pure sliding being the mode of response. Therefore, equipment with coefficients of friction within the same range (or lower) as the ones tested does not seem to pose an overturning threat.

6.10 CONCLUSIONS

In this study, a full experimental program investigating the response of freestanding and restrained slender laboratory equipment was undertaken. In this brief report, we first presented and discussed experimental results from shake table studies on freestanding equipment subjected to ground and floor motions. Simulation studies concluded that the better agreement with the recorded response histories is achieved when the coefficients of friction determined with slow pull tests are reduced by approximately 20–35%. Subsequently, this report proposes a simple linear relation between the peak sliding displacement, u_{max} , and the intensity of the base excitation, $(PTA/\mu g)(PTA - \mu g)/\omega_p^2$. This linear relation emerges from the theory of dimensional analysis (Makris and Black 2003) and sets the stage for a simple yet effective fragility analysis.

The results obtained from the freestanding equipment shake table tests in conjunction with the results obtained from the wooden block model shake table tests were used to validate the numerical software Working Model, confirming its ability to capture with good accuracy overturning response or sliding response under a range of coefficients of friction.

From the experiments performed on the restrained equipment, it is concluded that the peak accelerations recorded are significantly larger than those recorded during the freestanding equipment tests. Such high accelerations may pose a threat to the sensitive contents of laboratory equipment.

6.11 REFERENCES

Choi, B., and Tung, C.C.D., 2002,. “Estimating Sliding Displacement of an Unanchored Body Subjected to Earthquake Excitation,” *Earthquake Spectra*, v.18 no.4, pp. 601-613.

Konstantinidis, D. and Makris, N. “Experimental and Analytical Results on the Seismic Response of Slender Laboratory Equipment.” *Proceedings of the ATC-29-2 Seminar on Seismic Design, Performance, and Retrofit of Nonstructural Components in Critical Facilities*. Newport Beach, California, October 23-24, 2003.

Konstantinidis, D. and Makris, N. (2004), *Experimental and Analytical Seismic Response of Building Contents*, Report No. PEER 2005/07, Pacific Earthquake Engineering Research Center, University of California, Berkeley, CA (forthcoming).

Lopez Garcia, D. and Soong, T.T., 2003 (1), "Sliding Fragility of Block-Type Non-Structural Components. Part 1: Unrestrained Components," *Earthquake Engineering and Structural Dynamics*, v.32, pp. 111-129.

Lopez Garcia, D. and Soong, T.T., 2003 (2), "Sliding Fragility of Block-Type Non-Structural Components. Part 2: Restrained Components," *Earthquake Engineering and Structural Dynamics*, v.32, pp. 131-149.

Makris, N. and Black, C.J., 2003, *Dimensional Analysis of Inelastic Structures Subjected to Near-Fault Ground Motions*, Report No. EERC 2003-05, Earthquake Engineering Research Center, University of California, Berkeley, CA.

Makris, N. and Chang, S.-P., 2000, "Effects of Viscous, Viscoplastic and Friction Damping on the Response of Seismic Isolation Structures," *Earthquake Engineering and Structural Dynamics*, v.29 no.1, pp. 85-107.

Makris, N. and Roussos, Y., 2000, "Rocking Response of Rigid Blocks under Near-Source Ground Motions," *Géotechnique*, v.50 no.3, pp. 243-262.

Lee, T.-H. and Mosalam, K., 2002. Personal Correspondence.

Newmark, N.M., 1965, "Effects of Earthquakes on Dams and Embankments." Fifth Rankine Lecture, *Géotechnique*, v.15, pp. 139-160.

Somerville, P., 2001. "Ground Motion Time Histories for the UC Lab Building." PEER Testbed Project. Pacific Earthquake Engineering Research Center, University of California, Berkeley, CA.

7 Damage Analysis

Keith A. Porter and James L. Beck, California Institute of Technology

7.1 ROLE OF DAMAGE ANALYSIS IN PBEE ANALYSIS

This chapter summarizes the damage analysis methodology and results presented in Porter et al. (in progress). As shown in Figure 1.1, the purpose of the damage analysis is to estimate physical damage at the component or system level, as a function of structural response. The response is parameterized via one or more engineering demand parameters, *EDP*, which are estimated in the structural-analysis phase of the evaluation, as discussed in Chapter 4. Damage is parameterized via a vector of damage measures (*DM*), which quantifies physical damage to the system (e.g., collapse) and to facility components (individual structural, architectural, mechanical, electrical, or plumbing components, furnishings, fixtures, equipment, or other contents). *DM* contains only quantitative, concretely defined engineering parameters, as opposed to qualitative measures such as “light damage.” To estimate *DM* requires *EDP* and a damage model, i.e., a probabilistic relationship $P[DM | EDP]$. (This relationship is implicitly conditioned on the facility definition, *D*, discussed in Chapter 2.)

7.2 ASSEMBLIES AND OPERATIONAL UNITS

The damage and loss analysis presented here can be performed at either of two levels of aggregation. The finer of the two is the level of individual components or assemblies. The coarser is at the level of an entire laboratory, office, suite, etc. (generically referred to here as an “operational unit”). The finer level of analysis can be used to create a generic damage model at the operational-unit level, which can then be re-used for simplified damage and loss evaluation. We present the finer level of analysis here, and in the next chapter offer generic damage and loss models for entire operational units of various sizes.

Definition of components and assemblies. For the damage and loss analysis, a facility is modeled as comprising a number of damageable assemblies or components. A component is a structural member, architectural element, a mechanical, electrical, or plumbing fixture (often referred to as “MEP”), or an item of contents (referred to as “furnishings,” “fixtures,” and “equipment,” or “FFE”), defined according to a standard taxonomy such as RS Means’s line items extended from CSI’s MasterFormat classification (e.g., RS Means Co. Inc. 2000). A microscope or a countertop is an example of a component. An assembly is a more aggregated set of components, assembled and in place, and defined according to a standard taxonomic system such as the assembly-numbering system of RS Means’s assembly-numbering system extended from CSI’s UniFormat classification (e.g., RS Means Co. Inc. 1997). A segment of wallboard partition is an example of an assembly. We use the term “assembly” hereafter to refer generically to the unit of analysis at which damage and loss are assessed, whether that unit is an assembly such as a segment of wallboard partition or a component such as a microscope. A limited taxonomy of structural, architectural, MEP, and FFE assemblies is offered in Porter et al. (in progress).

Definition of operational unit. An operational unit is defined as a distinct portion of a facility whose seismic performance (e.g., operational or life-safety failure) is of interest. An operational unit could be a laboratory, an office suite, an assembly line, etc., within a facility. The UC Science Building contains approximately 50 operational units, all of which are laboratories.

7.3 ASSEMBLY-LEVEL DAMAGE-ANALYSIS METHODOLOGY

Assembly fragility functions and the cumulative distribution function of DM . In the damage analysis, one first evaluates the probability distribution of DM for each assembly via one or more fragility functions. A fragility function in general gives the probability that some undesirable event will occur, given some excitation. Here, we refer to assembly fragility functions, by which we mean the probability that an assembly subjected to an engineering demand measured by EDP will reach or exceed some predefined damage state, measured by DM .

That is, after an assembly is subjected to a certain EDP , it will be in an uncertain damage state DM , indexed by $dm = 0, 1, 2, \dots, N_{DM}$, where $dm = 0$ indicates the undamaged state and N_{DM}

is the number of damage states for the assembly. Each assembly type has a fragility function for each damage state $dm = 1, 2, \dots, N_{DM}$. We assume that the damage states can be sorted in increasing order, either because an assembly in damage state $dm = i + 1$ must have passed through damage state i already, or because the effort to restore an assembly from damage state $dm = i + 1$ necessarily restores it from damage state $dm = i$. The threshold level of EDP causing an assembly to reach or exceed damage state dm is uncertain (we refer to it as the assembly's *capacity* with respect to dm), and is denoted by X_{dm} . The cumulative distribution function (CDF) of capacity X_{dm} evaluated at x gives the probability that $X_{dm} \leq x$, and is equivalent to the probability that the assembly will reach or exceed damage state dm when subjected to $EDP = x$. Thus, the CDF of X_{dm} evaluated at a particular value x , denoted here by $F_{X_{dm}}(x)$, is the fragility function for that assembly and damage state.

Many fragility functions (although not necessarily all) are approximated by the cumulative lognormal distribution, in which case one needs only two parameters of the capacity X_{dm} : a central value such as the median, which for consistency with Chapter 5 is denoted here by m , and a measure of dispersion such as the logarithmic standard deviation (the standard deviation of $\ln X_{dm}$), which for consistency with Chapter 5 is denoted here by σ . In such a case, the fragility function is given by

$$\begin{aligned}
 F_{X_{dm}}(x) &\equiv P[X_{dm} \leq x] \\
 &= P[DM \geq dm \mid EDP = x] \\
 &= \Phi\left(\frac{\ln(x/m)}{\sigma}\right)
 \end{aligned} \tag{7.1}$$

where $P[A|B]$ denotes the probability that A is true given that B is true, and where Φ denotes the cumulative standard normal distribution, readily evaluated by common spreadsheet applications and other software. Each fragility function would have its own distribution (lognormal or otherwise) and relevant parameters. (Equation 7.1 also requires that EDP not depend on the damage state of the assembly, which is reasonable for nonstructural assemblies but can cause problems for structural elements when the structural analysis to compute EDP does not reflect the damage to them. The interested reader is referred to Shaikhutdinov et al. (2004) for discussion.)

For cases of $N_{DM} = 1$, the failure probability conditioned on $EDP = x$ is simply $F_{X1}(x)$. Where $N_{DM} \geq 2$, it is necessary to evaluate the CDF of DM , conditioned in $EDP = x$, using all of the assembly's fragility functions. This CDF is denoted by $F_{DM|EDP=x}(dm)$, and is given by:

$$\begin{aligned}
F_{DM|EDP=x}(dm) &\equiv P[DM \leq dm \mid EDP = x] \\
&= 1 - P[DM > dm \mid EDP = x] && 0 \leq dm < N_{DM} \\
&= 1 - P[DM \geq dm + 1 \mid EDP = x] && 0 \leq dm < N_{DM} \\
&= 1 - F_{X_{dm+1}}(x) && 0 \leq dm < N_{DM} \\
&= 1 && dm = N_{DM}
\end{aligned} \tag{7.2}$$

As an aside, the conditional probability mass function of the damage state is denoted by $p_{DM|EDP=x}(dm)$ and is given by

$$\begin{aligned}
p_{DM|EDP=x}(dm) &\equiv P[DM = dm \mid EDP = x] \\
&= 1 - F_{X1}(x) && dm = 0 \\
&= F_{X_{dm}}(x) - F_{X_{dm+1}}(x) && 1 \leq dm < N_{DM} \\
&= F_{X_{N_{DM}}}(x) && dm = N_{DM}
\end{aligned} \tag{7.3}$$

Fragility functions for laboratory equipment. Ideally, the DM s for laboratory equipment would be breakage of individual pieces of equipment. PEER researchers did not test for equipment breakage, but rather maximum sliding distance (for countertop- and shelf-mounted equipment, as described in Chapter 5) and overturning of floor-standing equipment (as described in Chapter 6). We therefore rely on a proxy for breakage, namely, overturning of floor-standing equipment or falling of countertop- or shelf-mounted equipment from their countertop or shelf. Thus, for each piece of equipment, $N_{DM} = 1$, and each DM is binary variable: $DM = 1$ (“true”) indicates that the equipment has overturned or fallen, $DM = 0$ (“false”) otherwise. Since in the present case we do not need the subscript for multiple damage states, we denote a piece of equipment's capacity to resist falling or overturning simply as $F_X(x)$.

In the present study, we do not have fragility functions for overturning of floor-standing equipment. As explained in Chapter 6, none of the test specimens overturned during the tests, aside from one specimen whose overturning was attributed to fatigue induced by earlier tests. To deal with this problem, we conclude that while it is possible that such equipment can overturn in earthquakes, the probability is low for the excitation levels considered here, and is low compared with the failure probability of countertop- and shelf-mounted equipment.

Furthermore, as shown in Chapter 5, we do not have an explicit expression of $F_X(x)$ for countertop- or shelf-mounted equipment, where X is the capacity to resist falling in terms of EDP . Rather, the laboratory experiments described in Chapter 5 produced parameters for Equation 5.13, which gives the probability that equipment of category c , when subjected to $EDP = x$, will slide at least some distance b . This can be thought of as a conditional fragility function, i.e., the failure probability (with failure defined as the object sliding off a surface), given that it falls when it slides distance b :

$$\begin{aligned} F_{X|B=b}(x) &\equiv P[\text{failure} | EDP = x, \text{category} = c, B = b] \\ &= \Phi\left(\frac{\ln(x/m_c(b))}{\sigma_c(b)}\right) \end{aligned} \quad (7.4)$$

where B denotes the uncertain distance of the center of gravity of the object from the edge of the shelf or countertop, b denotes a particular value of that distance, Φ denotes the cumulative standard normal distribution function, and $m_c(b)$ and $\sigma_c(b)$ denote parameters of the conditional fragility function, which as shown in Chapter 5 are functions of b and depend on c .

To overcome this latter problem, we first assume that displacement is isotropic, i.e., that during the course of the shaking, an object that moves distance b from its initial position in one unconstrained direction will also move b in any other unconstrained direction. Second, we estimate a probability density function for the uncertain distance that the object must slide before it falls, which we denote by $f_B(b)$. Finally, we apply the theorem of total probability and Equation 5.13 to produce the fragility function for these assemblies, i.e., the probability that an object of category c will fall from a shelf or countertop when subjected to $EDP = x$:

$$\begin{aligned} F_X(x) &\equiv P[\text{failure} | EDP = x, \text{category} = c] \\ &= \int_{b=0}^D \Phi\left(\frac{\ln(x/m_c(b))}{\sigma_c(b)}\right) f_B(b) db \end{aligned} \quad (7.5)$$

where D denotes the depth of the shelf or countertop. We assume that the parameters for the CDF can be approximated as linear functions of b (as is apparent in the present case from Chapter 5); that is,

$$\begin{aligned} m_c(b) &= a_1 b + a_2 \\ \sigma_c(b) &= a_3 b + a_4 \end{aligned} \quad (7.6)$$

where different sets of a_1 through a_4 are available for each c . We assume B depends on the location of the equipment (e.g., countertop or shelf) and is uniformly distributed between a_5 and a_6 , i.e.,

$$\begin{aligned} f_B(b) &= 0 & b < a_5 \\ &= \frac{1}{a_6 - a_5} & a_5 \leq b < a_6 \\ &= 0 & b \geq a_6 \end{aligned} \quad (7.7)$$

Equivalently, the CDF of B is given by

$$\begin{aligned} F_B(b) &\equiv P[B \leq b] \\ &= 0 & b < a_5 \\ &= (b - a_5)/(a_6 - a_5) & a_5 \leq b < a_6 \\ &= 1 & b \geq a_6 \end{aligned} \quad (7.8)$$

Combining Equations 7.5 and 7.7 yields the fragility function for countertop- or shelf-mounted equipment:

$$P[\textit{failure} \mid EDP = x, \textit{category} = c, \textit{location} = l] = \int_{b=a_5}^{a_6} \Phi\left(\frac{\ln(x/(a_1 b + a_2))}{a_3 b + a_4}\right) \frac{1}{(a_6 - a_5)} db \quad (7.9)$$

where parameters a_1 through a_4 depend on c , and a_5 and a_6 depend on the location l of the equipment. This fragility function is difficult to evaluate in closed form.

Propagating uncertainty, general case. There are several ways to propagate uncertainty through a PBEE analysis: Monte Carlo simulation (MCS, e.g., Beck et al. 2002), first-order, second-moment method (FOSM, Baker and Cornell 2003), moment matching (Ching et al. 2004), and possibly others. The latter two are problematic to apply when DV is not solely a function of continuous random variables, as in the present case. MCS, by contrast, is versatile, intuitive, and easy to apply here, as will be shown.

Under an MCS approach, damage to each assembly is simulated by inverting Equation 7.2 at a random probability value. For each structural analysis and each assembly, one draws an independent sample u from a random number uniformly distributed between 0 and 1—denoted here by $u \sim U(0,1)$ —and determines the simulated assembly damage state DM from

$$DM = F_{DM|EDP=x}^{-1}(u) \quad (7.10)$$

A simple algorithm for evaluating DM. In a simple case, if $N_{DM} = 1$ and X_1 is lognormally distributed, given $EDP = x$, failure occurs ($DM = 1$) if

$$u < \Phi\left(\frac{\ln(x/m)}{\sigma}\right)$$

Otherwise, the assembly is undamaged. To evaluate Equation 7.10 given $EDP = x$ for the more general case, i.e., $N_{DM} \geq 1$ and any form of $F_{Xdm}(x)$, evaluate the fragility functions $F_{Xdm}(x)$ for $dm = 1, 2, \dots, N_{DM}$. Use these to calculate $F_{DM|EDP=x}(dm)$ per Equation 7.2. Use a random-number generator (e.g., “=rand()” in Microsoft Excel) to draw an independent sample u from $U(0,1)$ and test u against $F_{DM|EDP=x}(dm)$ as follows:

$$\begin{aligned} &\text{if } [u > F_{DM|EDP=x}(1)] \text{ then } DM = 0 \text{ (undamaged)} \\ &\text{if } [(F_{DM|EDP=x}(dm+1) < u \leq F_{DM|EDP=x}(dm)) \text{ and } (1 \leq dm < N_{DM})] \text{ then } DM = dm \quad (7.11) \\ &\text{if } [u \leq F_{DM|EDP=x}(N_{DM})] \text{ then } DM = N_{DM} \end{aligned}$$

For each sample value of EDP and each assembly, draw a sample value u and apply Equation 7.11. (One must exercise care in selecting and using a random number generator to ensure that samples u are independent.) The result is a sample damage state for each assembly and each structural analysis. Denoting by N_S the number of simulations of ground motion, EDP , and DM per IM value, one can estimate the failure probability for an individual assembly conditioned on $IM = im$ as

$$P[\text{failure}|IM=im] = n/N_S \quad (7.12)$$

where n denotes the number of simulations at $IM = im$ in which the assembly fails.

Evaluating DM for countertop- or shelf-mounted equipment. In the case of a falling failure of a piece of equipment that is an uncertain distance B from the edge of its counter or shelf, where the probability of falling is of the form shown in Equation 7.9, failure is readily simulated using MCS, as follows. First simulate B by drawing $u_1 \sim U(0,1)$ and inverting Equation 7.8 at u_1 :

$$b = a_5 + u_1 \cdot (a_6 - a_5) \quad (7.13)$$

Now given $EDP = x$, $B = b$, and the equipment category c , simulate failure by drawing a second sample $u_2 \sim U(0,1)$ independent of u_1 , and checking:

$$\begin{aligned} &\text{if } u_2 \leq \Phi\left(\frac{\ln(x/(a_1 \cdot b + a_2))}{(a_3 b + a_4)}\right) \rightarrow DM = 1 \text{ (failed by falling)} \\ &\text{if } u_2 > \Phi\left(\frac{\ln(x/(a_1 \cdot b + a_2))}{(a_3 b + a_4)}\right) \rightarrow DM = 0 \text{ (undamaged)} \end{aligned} \quad (7.14)$$

Again, u_1 , u_2 , b , and hence DM , are sampled as appropriate once per assembly and structural analysis. Equation 7.12 again gives the failure probability for an individual assembly conditioned on IM .

Evaluating average failure probability for countertop- or shelf-mounted equipment. In some cases, it may be unnecessary to simulate DM , but only to simulate failure probability, in which case one simulates B by drawing $u \sim U(0,1)$ and applying Equation 7.13, and then by calculating failure probability by Equation 7.4. The process is repeated N_S times for each level of IM , and the average failure probability given $EDP = x$ is taken as the sample average of the failure probabilities from each sample $i = 1, 2, \dots, N_S$:

$$b = a_5 + u \cdot (a_6 - a_5)$$

$$P[\text{failure} \mid EDP = x, \text{category} = c, B = b] = \Phi\left(\frac{\ln(x/(a_1b + a_2))}{(a_3b + a_4)}\right) \quad (7.15)$$

$$\bar{P}[\text{failure} \mid EDP = x, \text{category} = c] = \frac{1}{N_S} \sum_{i=1}^{N_S} \Phi\left(\frac{\ln(x_i/(a_1b_i + a_2))}{(a_3b_i + a_4)}\right)$$

This approach converges much faster than simulation by Equations 7.12–7.14.

7.4 APPLICATION TO UC SCIENCE BUILDING TESTBED

Define the DVs of interest. The purpose of the damage analysis is to estimate the DMs that, once known, determine the decision variables (DV) of interest. Consequently, it is necessary to know the DVs before selecting the DMs , compiling the component fragility functions ($P[DM|EDP]$), and performing the damage analysis. In general, DVs might include repair costs, loss of life-safety, or number of casualties, and loss of operability or repair duration. In the present study, as will be discussed in Chapter 8, the DVs are:

- Loss of post-earthquake operability, DV_{Op} , a binary variable: 0 for operational, 1 otherwise.
- Occurrence of life-threatening damage, DV_{LS} , a binary variable: 0 for life safe, 1 otherwise.

Define critical equipment. A component is considered critical if it is (1) operationally critical or (2) life-safety critical. It is operationally critical if when it ceases to function, it could cause the operational unit to cease to produce its principal product until the component is

repaired or replaced. We define a life-safety-critical component as one that, if it overturned, fell, or broke, could either (2a) directly cause an injury that would require emergency medical treatment (“emergency department treat and release,” or greater, according to the injury-severity scale presented by Shoaf et al. 2001) or (2b) is part of a life-safety equipment system, such as fire detection or suppression, medical equipment, or equipment necessary to the operation of a 911 telephone service (see Porter et al. 1993 for illustrations of such systems).

Regarding criterion 1, the investigators who operate the laboratories of the UC Science Building identified those pieces of laboratory equipment that were deemed operationally critical (see Chapter 2). It is difficult to determine which pieces of laboratory equipment precisely meet criterion 2. We include under criterion 2a any equipment that poses a chemical hazard, according to the university’s environmental health and safety department. We also include tall and heavy or high and heavy objects, using the life-safety hazard-rating system proposed by the engineering practitioners who inventoried the facility equipment. They rated equipment life-safety threat on an A to D scale, with D being worst, based on weight and location of the equipment of five feet or more above the floor. We interpret this measure of urgency as an assessment of the hazard of blunt-force trauma; see Table 7.1 (also Table 2.2). Inadequate research has been performed to distinguish which of these four classes of components can cause blunt-force trauma sufficient to meet criterion 2; we somewhat arbitrarily selected only class D of Table 7.1 as doing so. We ignore life-safety threats associated with penetrating-trauma, as no data are available either to identify objects in the facility that are capable of inflicting penetrating-trauma injuries, nor does a model exist to relate their possible *DMs* to the potential for injury. Criterion 2b is ignored here, since these systems are outside the scope of the present study.

Identify operational units to be examined. The operational units considered here are the laboratories of individual investigators. We focus on the performance of the equipment within a few sample operational units, and measure seismic performance by the probability that damage to critical equipment produces failure of an operational unit. We examine four operational units to test sensitivity of operational-unit failure to the quantity of critical components:

1. Lab S: relatively small number of critical components, both in terms of life-safety and operations.
2. Lab M: a laboratory with a medium quantity of critical components. The inventory of lab M is shown in Table 7.2.

3. Lab LO: a laboratory with a large quantity of operationally critical components.
4. Lab LL: a laboratory with a large quantity of life-safety-critical components.

We ignore some components deemed operationally critical by laboratory investigators because these component are readily replaceable, particularly computer monitors. Furthermore, we ignore restrained equipment, as well as a few components whose fragility function were not produced for this study (breakage of objects inside of fume hoods). Total component counts by sample laboratory are shown in Table 7.3.

Select fragility functions. Component fragility functions for the damage analysis were developed by testing of heavy floor-mounted equipment and smaller bench-top equipment as part of our collaborative effort and are described in Chapters 5 and 6, respectively. In the laboratory tests of full-scale floor-standing equipment, no overturning was observed, and so no fragility functions for overturning were available to us. Floor-standing equipment are therefore assumed to be rugged, meaning that the probability of failure is low compared with that of countertop- or shelf-mounted equipment, whose failure will therefore dominate DV .

The probability that a piece of countertop- and shelf-mounted equipment will slide off its surface is as calculated in Equation 7.4. Reading Figures 5.4–5.8, and referring to the categories listed in Table 7.3, we estimate the parameters a_1 through a_4 as shown in Table 7.4. We observe that parameters a_1 – a_4 are very similar for categories 1 and 2, and for categories 3–5, so we aggregate 1 and 2 to category L (lower base resistance, defined as $\mu_s < 0.5$), and 3 through 5 as category H (higher base resistance, defined as $\mu_s \geq 0.5$), with displacement parameters shown at the bottom of Table 7.4.

We observe from photos of equipment on shelves and countertops that they are packed together up to the front edge of shelves, and within about 4 cm of the edge of countertops. We also observe that shelf-mounted equipment are small, with a base on the order of 4–10 cm, while equipment on countertops have a base on the order of 4–45 cm. Comerio indicates that the critical equipment are typically those at the front of the shelf or countertop. Thus, equipment are taken as having

$$B \sim U(2 \text{ cm}, 5 \text{ cm}) \text{ shelf}$$

$$B \sim U(6 \text{ cm}, 26 \text{ cm}) \text{ countertop}$$

and thus, a_5 and a_6 are as shown in Table 7.5.

Calculate DM. Chapter 4 gives the distribution of *EDP* at each hazard level. For a more robust damage estimate, we simulated 100 sets of *EDP* for each *IM* value, based on the data from Chapter 4. For each such simulation, we applied the algorithm shown in Equations 7.15. Table 7.2 presents results for laboratory M. This simulation took only a few moments using a Microsoft Excel add-in (Savage 1998). We observe from Table 7.2 that high-base-resistance equipment have relatively low failure probability, even at high hazard levels, compared with low-base-resistance equipment, suggesting that equipment with rubber feet contribute little to operational-unit fragility if there are a comparable or greater number of pieces of equipment with low base resistance.

7.5 CONCLUDING REMARKS

This chapter presents a methodology for calculating the probabilistic damage state of critical laboratory equipment as a function of peak diaphragm acceleration, accounting for base resistance and uncertainty in the distance of the equipment from the edge of the surface. We offer a simplified equipment categorization scheme that enables one to characterize fragility of small equipment in terms of location (countertop or shelf) and base-resistance category (low or high, L or H, distinguished by the coefficient of static friction, μ_s , being less than or greater than 0.5). We offer a Monte Carlo simulation method for quantifying equipment *DM* at the level of individual pieces of equipment. In Chapter 8 we will present a further simplification that allows one to estimate the fragility of an entire laboratory by counting the number of pieces of unrestrained critical equipment in it.

7.6 REFERENCES

- Baker, J.W. and Cornell, C.A., 2003, *Uncertainty Specification and Propagation for Loss Estimation Using FOSM Methods*, PEER Report 2003/07, Pacific Earthquake Engineering Research (PEER) Center, Richmond, CA, http://www.stanford.edu/~bakerjw/Baker_Cornell_PEER_Uncertainty_Report.pdf
- Beck, J.L., K.A. Porter, R. Shaikhutdinov, S. K. Au, K. Mizukoshi, M. Miyamura, H. Ishida, T. Moroi, Y. Tsukada, and M. Masuda, 2002, *Impact of Seismic Risk on Lifetime Property Values, Final Report*, Consortium of Universities for Research in Earthquake Engineering, Richmond, CA, <http://resolver.caltech.edu/caltechEERL:2002.EERL-2002-04>

Ching, J.Y., K.A. Porter, and J.L. Beck, 2004, *Uncertainty Propagation and Feature Selection for Loss Estimation in Performance-Based Earthquake Engineering*, California Institute of Technology, Pasadena, CA

Copes W.S., W.J. Sacco, H.R. Champion, and L.W. Bain, 1990, “Progress in Characterizing Anatomic Injury,” *Proceedings of the 33rd Annual Meeting of the Association for the Advancement of Automotive Medicine*, Baltimore, MA, USA, 205-218

Porter, K.A., J.L. Beck, and R.V. Shaikhutdinov, in progress, *PEER Damage and Loss Analysis of a Laboratory Facility*, for Pacific Earthquake Engineering Research Center, Richmond, CA

Porter, K.A., G.S. Johnson, M.M. Zadeh, C.R. Scawthorn, and S.J. Eder, 1993, *Seismic Vulnerability of Equipment in Critical Facilities: Life-Safety and Operational Consequences*, NCEER-93-0022, Multidisciplinary Center for Earthquake Engineering Research, State University of New York, Buffalo, NY, 364 pp.

RS Means Co., Inc., 1997, *Means Assemblies Cost Data*, Kingston, MA.

RS Means Co., Inc., 2000, *Repair and Remodeling Cost Data*, Kingston, MA

Savage, S.L., 1998, *Insight.xls Business Analysis Software for Microsoft Excel*, LINDO Systems, Chicago, IL

Shaikhutdinov, R.V., J.L. Beck, and K.A. Porter, 2004, “Comparative study of different methods of structural damage assessment,” *13th World Conference on Earthquake Engineering, Vancouver, B.C., Canada, August 1-6, 2004*, Paper 1678

Shoaf, K., H. Seligson, C. Peek-Asa, and M. Mahue-Giangreco, 2001, *Standardized Injury Categorization Schemes for Earthquake Related Injuries*, UCLA Center for Public Health and Disasters, Los Angeles, CA, 43 pp., <http://www.cphd.ucla.edu/pdfs/classificationScheme.pdf>

Table 7.1 Blunt-force trauma hazard

Weight	Location		
	Low	Medium	High
< 20 lb	A	B	C
20-400 lb	B	C	C
> 400 lb	C	C	D

Table 7.2 Inventory and fragility functions for critical components in laboratory M

Room, key	Equipment	Manufacturer	Safety	Ops	Location	DM	Category	$P_{50/50}$	$P_{10/50}$	$P_{2/50}$
x43a-I	Computer	Silicon Graphics	N	Y	Counter	Fall	L	0.041	0.189	0.474
x43a-M	Computer	Silicon Graphics	N	Y	Counter	Fall	L	0.041	0.189	0.474
x43-C	Incubator		N	Y	Counter	Fall	H	0.003	0.015	0.084
x41c-WS1	On shelving		Y (Ch)	N	Shelf	Fall	L	0.238	0.742	0.973
x41c-WS2	On shelving		Y (Ch)	N	Shelf	Fall	L	0.238	0.742	0.973
x45-WB2	On work bench		Y (Ch)	N	Counter	Fall	L	0.043	0.189	0.473
x45-WS3	On shelving		Y (Ch)	N	Shelf	Fall	L	0.238	0.742	0.973
x45-WS4	On shelving		Y (Ch)	N	Shelf	Fall	L	0.238	0.742	0.973
x43-G	Refrigerator		Y (T)	N	Floor	Overturn	L	***	***	***
x43-J	Incubator	Percival	Y (T)	Y	Floor	Overturn	L	***	***	***
x43-K	Freezer	Coldspot	Y (T)	Y	Floor	Overturn	L	***	***	***
x43-L	Centrifuge	DuPont/Sorvall	Y (T)	N	Floor	Overturn	L	***	***	***
x43-M	Refrigerator	Kenmore	Y (T)	N	Floor	Overturn	L	***	***	***
x45-B	Refrigerator	Philco	Y (T)	N	Floor	Overturn	L	***	***	***
x45-E	In fume hood		Y (Ch)	N		Break	L	?	?	?
x45-M	Refrigerator	Kenmore	Y (T)	N	Floor	Overturn	L	***	***	***
x45-N	Refrigerator	Fisher Scientific	Y (T)	N	Floor	Overturn	L	***	***	***

Notes:

Safety: N = not critical for life safety; Y (Ch) = chemical hazard; Y (T) = blunt-force-trauma hazard

Ops: N = not operationally critical; Y = operationally critical

Category: base resistance. See Table 7.4.

Failure probabilities $P_{a/b}$: a = exceedance probability, %; b = period, yr; *** = very small; ? = unknown

Table 7.3 Quantity of critical equipment in operational units (labs) examined here

Lab	Floor	Operability		Life safety	
		Total	Non-rugged*	Total	Non-rugged *
S	1	1	1	2	1
M	3	5	3	14	5
LO	4	24	14	21	6
LL	4	1	1	31	12

* Large floor-mounted objects are treated as rugged; objects in fume hoods are ignored for lack of laboratory test data.

Table 7.4 Simplified equipment categories and displacement parameters

Category	Base resistance	a_1	a_2	cov	a_3	a_4
1	Low	0.05	0.4	0.38	0.019	0.15
2	Medium-low	0.06	0.5	0.3	0.018	0.15
3	Medium	0.12	0.6	0.2	0.024	0.12
4	Medium-high	0.14	0.6	0.2	0.028	0.12
5	High	0.16	0.8	0.15	0.024	0.12
L (1 or 2)	Lower ($\mu_s < 0.5$)	0.06	0.4		0.018	0.15
H (3, 4, or 5)	Higher ($\mu_s \geq 0.5$)	0.15	0.7		0.026	0.12

Table 7.5 Failure distance parameters for shelf and countertop equipment

Location	a_5 (cm)	a_6 (cm)
Shelf	2	5
Counter	6	26

8 Loss Analysis

Keith A. Porter and James L. Beck, California Institute of Technology

8.1 DECISION VARIABLES AND PERFORMANCE METRICS

Decision variables. As shown in Figure 1.1, the purpose of the loss analysis is to estimate system performance (parameterized via one or more system-level decision variables, DV) as a function of physical damage at the component or system level. The damage is parameterized via one or more damage measures, DM , which are estimated in the damage-analysis phase of the evaluation, as discussed in Chapter 7. DV measures performance in terms of direct interest to the facility stakeholders. The DV s examined here for the UC Science testbed are:

1. **Loss of post-earthquake operability (DV_{Op}).** The event that facility damage causes significant interruption of normal operations in an operational unit. In this case, $DV_{Op}=1$; otherwise, $DV_{Op}=0$. This DV is examined in the present study by considering damage to laboratory equipment.
2. **The occurrence of life-threatening damage (DV_{LS}).** The event that facility damage endangers life safety, either through blunt-impact trauma, penetrating trauma, chemical, biological, or nuclear hazard release, fire, blocking of egress, or operational failure of a facility system intended to protect life safety. In this case, $DV_{LS}=1$; otherwise, $DV_{LS}=0$. This DV is examined in the present study by considering the potential for blunt-impact trauma and chemical hazard release resulting from damage to laboratory equipment.

Other DV s of interest in PBEE, but not examined here, include:

3. **Repair cost (DV_s).** The cost to restore the facility to its pre-earthquake state, or if required by regulation, to a (potentially higher) post-earthquake performance level. Not examined here. See Beck et al. (1999), Porter et al. (2001), and the companion study of the PEER Van Nuys testbed for illustration.

4. **Deaths (DV_X)**. Number of fatal injuries as a direct result of facility damage. See the companion study of the PEER Van Nuys testbed facility for illustration.
5. **Injuries (DV_I)**. Number of injuries, whether treated or not, not fatal within 30 days, directly resulting from facility damage.
6. **Repair duration (DV_T)**. Time between earthquake occurrence and completion of repairs. See Porter et al. (2001) for illustration.

Performance metrics. The loss analysis produces a probability distribution of DV . It may be conditioned on the occurrence of some scenario level of IM , or it may be the probability distribution of a single-event maximum value of DV during some planning period t , or it may be a probability distribution of the cumulative value of DV considering all events occurring during a planning period t . It is difficult however to use such a probability distribution directly in a decision-making situation. It common for facility stakeholders to use only one or two scalar metrics of the probability distribution of DV , whose values directly inform a risk-management decision. We refer to these as *performance metrics*. (“Performance metric” is not a standard PEER term; we advocate its inclusion in PEER terminology, with the foregoing definition.) Some possible performance metrics include:

- **Scenario mean DV** . A mean or other central value of DV conditioned on some scenario event such as shaking with intensity IM that has P_e exceedance probability in time t . Examples considered in this chapter are the operational and life-safety failure probabilities in 50%/50-yr, 10%/50-yr, and 2%/50-yr shaking. Another example is the mean repair cost conditioned on a value of IM with stated exceedance probability such as 10% in a stated planning period such as 50 years. (This is one way to measure loss in “the” earthquake.)
- **Mean failure frequency or mean failure recurrence period**. Used here as metrics of DV_{Op} and DV_{LS} , these are the frequencies with which $DV_{Op} = 1$ and $DV_{LS} = 1$ for an operational unit, in events per unit time, and the mean time between failure, which might be a more intuitive measure of risk.
- **Risk of ruin**. The probability that a single-event DV will exceed some intolerable level during a planning period t . Examples examined here are $P[DV_{Op} = 1 \mid t = 10 \text{ yr}]$ and $P[DV_{LS} = 1 \mid t = 50 \text{ yr}]$, i.e., the probability that a lab will experience operational failure at least once during an operational planning period of 10 years or that it will experience life-

safety failure at least once during a life-safety planning period of 50 years. Other examples include $P[DV_X \geq 1 \mid t = 50 \text{ yr}]$ and $P[DV_S \geq \text{owner equity} \mid t = 10 \text{ yr}]$.

- **Probability of y failures within a planning period t .** One failure may be tolerable where two or more might not.
- **Upper fractile of a scenario DV .** A common example is the 90th percentile of repair cost conditioned on the occurrence of the value of IM with 10% exceedance probability in 50 years. (This is a common definition of probable maximum loss, often used by commercial lenders to decide whether to require earthquake insurance for high-value properties located in California.)
- **Present value of cumulative DV for a stated planning period.** An example is the present value of repair costs during the design life of a facility, often used by the Federal Emergency Management Agency (FEMA 2000) in the cost-benefit analysis of hazard mitigation grant applications. Another is the value of statistical deaths and injuries avoided. FEMA (2000) routinely considers these benefits in awarding mitigation grants. The Federal Highway Administration (FHWA 1994) and Federal Aviation Administration (FAA 1998) include them in benefit-cost assessments of new regulations. This is important: while old and new buildings can be code compliant, that does not ensure avoidance of deaths and injuries. Additional safety can often be bought at the cost of above-code design or mitigation. Quantifying the value of casualties avoided can help to answer the question of whether the cost is justified by the additional safety.
- **Certainty equivalent of cumulative DV for a stated planning period.** Relevant to formal decision analysis of mitigation decisions, this is the amount of money the decision maker would accept (or pay) in exchange for the uncertain cumulative value of DV (especially DV_S), considering his or her risk tolerance and the time value of money. See Beck et al. (2002).

8.2 LOSS MODEL

EDP-DV relationship. Chapter 7 presented and illustrated a methodology for calculating the probabilistic damage state of various assemblies (here, the assemblies in question are pieces of laboratory equipment) subjected to structural response, i.e., for calculating $P[DM = 1 \mid EDP = x]$,

where $DM = 1$ indicates assembly failure in terms that are meaningful to DV . In cases where DV is the failure of an operational unit where system failure occurs if any critical assembly fails (as in the present case), one can readily relate EDP to DV . First,

$$[DV_{Op} = 1 | EDP = x] = \bigcup_i ([DM_i = 1 | EDP = x]) \quad (8.1)$$

$$[DV_{LS} = 1 | EDP = x] = \bigcup_i ([DM_i = 1 | EDP = x]) \quad (8.2)$$

where

$[X | Y]$ = the event that X is true given that Y is true

DM_i = the uncertain damage measure for assembly i

EDP = the engineering demand parameter to which assembly i is subjected

x = a particular value of EDP

$\bigcup_i ()$ = the union of events i inside parentheses, i.e., true if at least one event is true

Equation 8.1 considers only those assemblies that are critical for operations, and Equation 8.2 considers only those assemblies that are critical for life safety.

If events on the right-hand sides of Equations 8.1 and 8.2 are conditionally independent (i.e., the failure of assembly i is independent of the failure of component $j \neq i$, conditioned on the structural response x), then one can express the failure probability conditioned on $EDP = x$ by

$$P[DV_{Op} = 1 | EDP = x] = 1 - \prod_i (1 - P[DM_i = 1 | EDP = x]) \quad (8.3)$$

$$P[DV_{LS} = 1 | EDP = x] = 1 - \prod_i (1 - P[DM_i = 1 | EDP = x]) \quad (8.4)$$

where

$P[X | Y]$ = the probability that event X is true given that Y is true

$\prod_i ()$ = the product of the terms inside the parentheses

Equation (8.3) considers only those components that are critical for operations, and

Equation (8.4) considers only those components that are critical for life safety.

Operational-unit fragility function. Observe that Equations 8.3 and 8.4 produce a relationship between EDP and DV for the operational unit in question at a given value of $EDP =$

x . One could evaluate these equations at multiple values of x to create a functional relationship between failure probability and EDP , for a particular operational unit. This would be equivalent to calculating a probability distribution of the value of EDP at which failure occurs—that is, the capacity of the operational unit in terms of EDP . We refer to such a relationship or capacity distribution as an operational-unit fragility function. Such a function could be created for prototypical operational units, and then archived and re-used in later studies, thereby avoiding the detailed effort required to assess a facility on an assembly-by-assembly basis. Depending on the result of this analysis, it may be possible to fit an idealized probability distribution (such as a lognormal) to operational-unit capacity, and merely archive and disseminate the parameters of the capacity distribution.

IM-DV relationship. Equations 8.3 and 8.4 produce a relationship between EDP and DV . As shown in Chapter 4, structural analysis produces $P[EDP = x | IM = im]$. Using the theorem of total probability, one can combine these to relate DV to IM :

$$P[DV = 1 | IM = im] = \int_{x=0}^{\infty} P[DV = 1 | EDP = x] f_{EDP|IM=im}(x) dx \quad (8.5)$$

where $f_{EDP|IM=im}(x)$ denotes the probability density function of EDP conditioned on $IM = im$. Equation 6.5 is evaluated by MCS as follows:

1. Select IM level(s) of interest, e.g., by inverting the mean seismic hazard function $\lambda[im]$ at a frequency level of interest.
2. Create a stochastic structural model. As shown in Chapter 4, uncertainty in damping can account for as much or more uncertainty in EDP as can the detailed ground motion time history for a given IM level.
3. Pair a ground motion time history with a realization of the stochastic structural model, perform a nonlinear time-history structural analysis, and tabulate EDP .
4. Use assembly fragility functions as described in Chapter 7 to determine $P[DM_i = 1 | EDP = x]$ for each critical assembly.
5. Evaluate 8.3 or 8.4 as appropriate to determine $P[DV = 1 | EDP = x]$.
6. Repeat steps 3 through 5 several times (let us denote by N_S the number of simulations at a given level of IM). Calculate

$$P[DV = 1 | IM = im] = \frac{1}{N_S} \sum_{i=1}^{N_S} P[DV = 1 | EDP = x_j, IM = im] \quad (8.6)$$

where the subscript j indexes the iteration of steps 3–5. Note that as EDP is a state vector, adding the conditioning $IM = im$ in Equation 8.6 does not affect the result.

In cases where the analyst has an operational-unit fragility function, skip Equations 8.3 or 8.4 (step 5 of the algorithm) and use the pre-evaluated $P[DV = 1 | EDP = x]$ instead. In cases where structural analysis is computationally expensive, one can use a few structural analyses (the number of analyses denoted by N_{S1}) to create a joint PDF of EDP conditioned on $IM = im$, as shown in Chapter 4. One then simulates a vector of EDP at the beginning of step 4, and iterates steps 4 and 5 a larger number of times ($N_S \gg N_{S1}$).

D-DV relationship. One can integrate over IM to calculate the mean failure frequency (i.e., the frequency with which $DV = 1$), as follows:

$$\lambda[DV = 1] = \int_{im=0}^{\infty} P[DV = 1 | IM = im] |\lambda'[im]| d im \quad (8.7)$$

where $|\lambda'[im]|$ denotes the absolute value of the first derivative of the mean hazard function evaluated at $IM = im$. Note that conditioning on facility design, D , is implicit; D can be relevant to the seismic hazard, e.g., because IM depends on the estimated fundamental period of the facility. Since $P[DV = 1 | IM = im]$ can be calculated at a number of discrete IM values, and $\lambda[im]$ is also readily available at discrete values of IM , Equation 8.7 can be evaluated numerically.

To do so, let us assume that both $P[DV = 1 | IM = im]$ and $\ln(\lambda[im])$ vary linearly between values of IM at which failure probability is calculated. Let us denote by im_i ($i = 0, 1, \dots, n$) the values of IM at which failure probability and mean hazard are evaluated. Let us also denote by p_i and G_i the values $P[DV = 1 | IM = im_i]$ and $\lambda[im_i]$, respectively. Then we can evaluate Equation 8.7 numerically as:

$$\begin{aligned} \lambda[DV = 1] &= \sum_{i=1}^n \left(\int_0^{\Delta im_i} \left(p_{i-1} + \frac{\Delta p_i}{\Delta im_i} \tau \right) (-m_i G_{i-1} \exp(m_i \tau)) d \tau \right) \\ &= \sum_{i=1}^n \left(-p_{i-1} G_{i-1} \exp(m_i \tau) \Big|_{\tau=0}^{\Delta im_i} - \frac{\Delta p_i}{\Delta im_i} G_{i-1} \left(\exp(m_i \tau) \left(\tau - \frac{1}{m_i} \right) \right) \Big|_{\tau=0}^{\Delta im_i} \right) \\ &= \sum_{i=1}^n \left(p_{i-1} G_{i-1} (1 - \exp(m_i \Delta im_i)) - \frac{\Delta p_i}{\Delta im_i} G_{i-1} \left(\exp(m_i \Delta im_i) \left(\Delta im_i - \frac{1}{m_i} \right) + \frac{1}{m_i} \right) \right) \end{aligned} \quad (8.8)$$

where a small remainder term for $IM > im_n$ is ignored and where

$$m_i = \frac{\ln(G_i/G_{i-1})}{\Delta im_i} \quad i = 1, 2, \dots, n \quad (8.9)$$

$$\Delta im_i = im_i - im_{i-1} \quad i = 1, 2, \dots, n \quad (8.10)$$

$$\Delta p_i = p_i - p_{i-1} \quad i = 1, 2, \dots, n \quad (8.11)$$

Alternatively, one could take $P[DV = 1|IM = im]$ as linear with $\ln(\lambda[im])$, i.e., where, piecewise,

$$\begin{aligned} p &= a \ln(G) + b \\ &\geq 0 \\ &\leq 1 \end{aligned} \quad (8.12)$$

$$a_i = \frac{p_{i+1} - p_i}{\ln G_{i+1} - \ln G_i} \quad (8.13)$$

$$b_i = p_i - a_i \ln(G_i) \quad (8.14)$$

Then

$$\begin{aligned} \lambda[DV = 1] &= -\sum_{i=0}^{n-1} \left(\int_{G_i}^{G_{i+1}} (a_i \ln G + b_i) dG \right) \\ &= -\sum_{i=0}^{n-1} \left(\int_{G_i}^{G_{i+1}} a_i \ln G dG + \int_{G_i}^{G_{i+1}} b_i dG \right) \\ &= -\sum_{i=0}^{n-1} \left((a_i G \ln G - a_i G + b_i G) \Big|_{G_i}^{G_{i+1}} \right) \end{aligned} \quad (8.15)$$

8.3 CALCULATING PERFORMANCE METRICS

Not all of the performance metrics discussed in Section 8.1 are relevant to the present study. We consider only three.

Scenario failure probability. Section 8.2 presented a methodology for calculating $P[DV_{Op} = 1|IM = im]$.

Mean failure frequency and mean failure recurrence period. Equation 8.7 presented a methodology for calculating the mean failure frequency of an operational unit, $\lambda[DV = 1]$. The mean failure recurrence period is $1/\lambda[DV = 1]$.

Risk of ruin. Denoted here generically by $P[DV = 1 | t = \hat{t}]$, where DV is a binary variable and \hat{t} denotes a selected planning period. To calculate the risk of ruin, we assume that failures follow a Poisson process with mean failure frequency $\lambda[DV = 1]$ per Equation 8.7, denoted here simply by λ :

$$P[DV = 1 | t = \hat{t}] = 1 - \exp(-\lambda\hat{t}) \quad (8.16)$$

8.4 APPLICATION TO THE UC SCIENCE TESTBED BUILDING

Operational-unit fragility functions. We prepared operational-unit fragility functions for the four sample labs considered here. Figures 8.1(a)–(d) show operational and life-safety fragility for labs S, M, LO, and LL, respectively. The solid lines show calculated fragility. The dashed lines show a lognormal approximation of these, i.e., where

$$P[failure | EDP = x] = \Phi\left(\frac{\ln(x/m)}{\sigma}\right) \quad (8.17)$$

where

EDP = uncertain peak floor acceleration

x = particular value of EDP

m = median capacity of the operational unit, i.e., the value of EDP at which there is a 50% probability that the operational unit will fail

σ = logarithmic standard deviation of operational-unit capacity

In several of the curves, the lognormal approximation is so close to the calculated capacity that the dashed line cannot be distinguished behind the solid. The resulting median and logarithmic standard deviations are summarized in Table 8.1. In the table, n refers to the number of non-rugged pieces of critical equipment in each lab, relevant to each DV . A modest trend relates n to both m and σ , as plotted in Figure 8.2.

Note that there is some residual uncertainty in median capacity (i.e., scatter about the trendline). This uncertainty can be accounted for by treating the operational-unit capacity as compound lognormally distributed, i.e., lognormal with logarithmic standard deviation s as indicated in Figure 8.2b and uncertain median m . The uncertain median is treated as having a

lognormal distribution, whose median value is the same as m indicated by Figure 8.2a, and with logarithmic standard deviation $\sigma_m = \sqrt{\text{Var}[\ln m_i - \ln m(n)]}$, where m_i reflect the individual data in Figure 8.2a, and $m(n)$ is the value of the trendline evaluated at n . The two sources of uncertainty can be combined, creating an ordinary lognormally distributed capacity with median value m as indicated in Figure 8.2a, and with logarithmic standard deviation $\sigma_c = \sqrt{\sigma^2 + \sigma_m^2}$. From these data, $\sigma_m = 0.5$. Thus, for an operational unit with n pieces of non-rugged critical equipment (i.e., unrestrained countertop- or shelf-mounted equipment), the operational-unit capacity, denoted here by X_{OU} , is given by Equation 8.18. Its CDF is equivalent to the operational-unit fragility function.

$$\begin{aligned}
 X_{OU} &\sim LN(m, \sigma_c) \\
 P[DV = 1 | EDP = x, n] &= P[X_{OU} \leq x | n] \\
 &= \Phi\left(\frac{\ln(x/m)}{\sigma_c}\right) \\
 m &= 1.2 \cdot n^{-0.4} \\
 \sigma_c &= \sqrt{0.18n^{-0.8} + 0.25}
 \end{aligned} \tag{8.18}$$

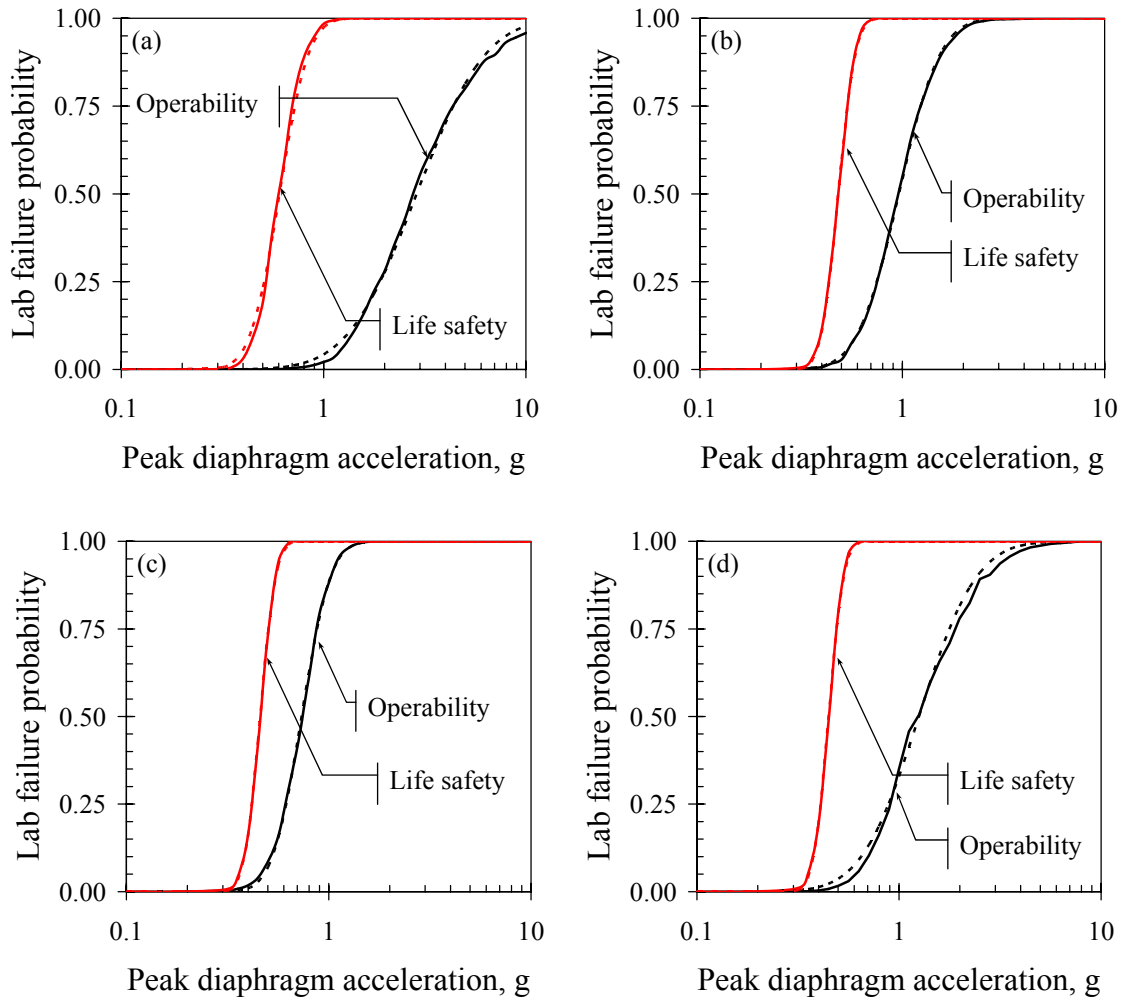


Fig. 8.1 Lab fragility functions (a) lab S; (b) lab M; (c) lab LO; (d) lab LL

Table 8.1 Parameters of operational-unit lognormal fragility functions

Lab	DV	n	m	σ
S	DV_{Op}	1	2.89	0.62
S	DV_{LS}	1	0.61	0.26
M	DV_{Op}	3	0.96	0.37
M	DV_{LS}	5	0.48	0.15
LO	DV_{Op}	14	0.73	0.26
LO	DV_{LS}	6	0.46	0.14
LL	DV_{Op}	1	1.26	0.52
LL	DV_{LS}	12	0.45	0.13

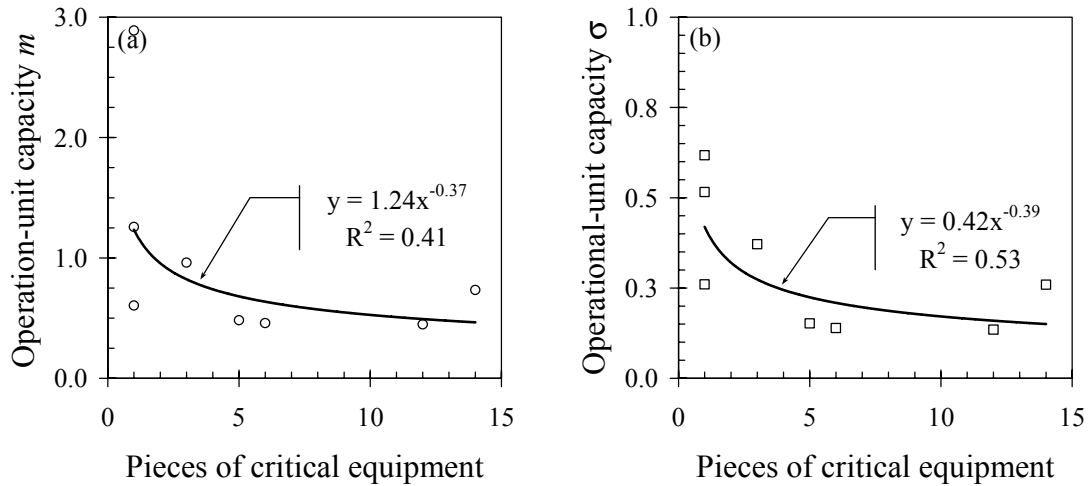


Fig. 8.2 Laboratory capacity as a function of number of critical components (a) median; (b) logarithmic standard deviation

IM-DV relationship; scenario mean DV. Equation 8.5 was evaluated for each operational unit considered here at each of three levels of *IM*. Table 8.2 presents the results, showing the failure probability of each lab conditioned on *IM*. In the table, n_{Op} indicates the number of pieces of operationally critical, non-rugged components (an indicator of the size of the post-earthquake operability problem); n_{LS} indicates the number of pieces of life-safety-critical, non-rugged components. Each row corresponds to one of the example labs. Columns depict the probability of operational or life-safety failure, conditioned on a scenario level of *IM*.

The data can be depicted graphically in at least two interesting ways: as lab fragility functions conditioned on *IM* rather than *EDP* (Fig. 8.3) and as mean frequency with which earthquakes occur producing a given failure probability (Fig. 8.4). The latter can be seen as a *DV*-hazard curve, that is, depicted the same way *IM* hazard is often shown, with the *y*-axis measuring mean exceedance frequency and the *x*-axis measuring of severity (S_a in the case of *IM* hazard, failure probability in the case of *DV* hazard). Figures 8.3(a) and 8.4(a) show the fragility and hazard, respectively, for operability failure, while Figures 8.3(b) and 8.4(b) show the fragility and hazard for life-safety failure.

Table 8.2 UC Science Building lab failure probabilities at three hazard levels

Lab	Floor	n_{Op}	n_{LS}	Hazard level					
				$S_a = 0.71g$ 50%/50 yr (0.0139 yr ⁻¹)		$S_a = 1.62g$ 10%/50 yr (0.0021 yr ⁻¹)		$S_a = 2.74g$ 2%/50 yr (0.0004 yr ⁻¹)	
				Operability	Safety	Operability	Safety	Operability	Safety
S	1	1	1	0.2%	20.4%	1.2%	74.2%	7.2%	94.1%
M	3	3	5	7.8%	48.4%	41.6%	93.7%	73.3%	99.5%
LL	4	1	12	4.7%	56.2%	14.2%	95.9%	44.8%	100.0%
LO	4	14	6	11.8%	43.2%	45.0%	95.3%	91.8%	100.0%

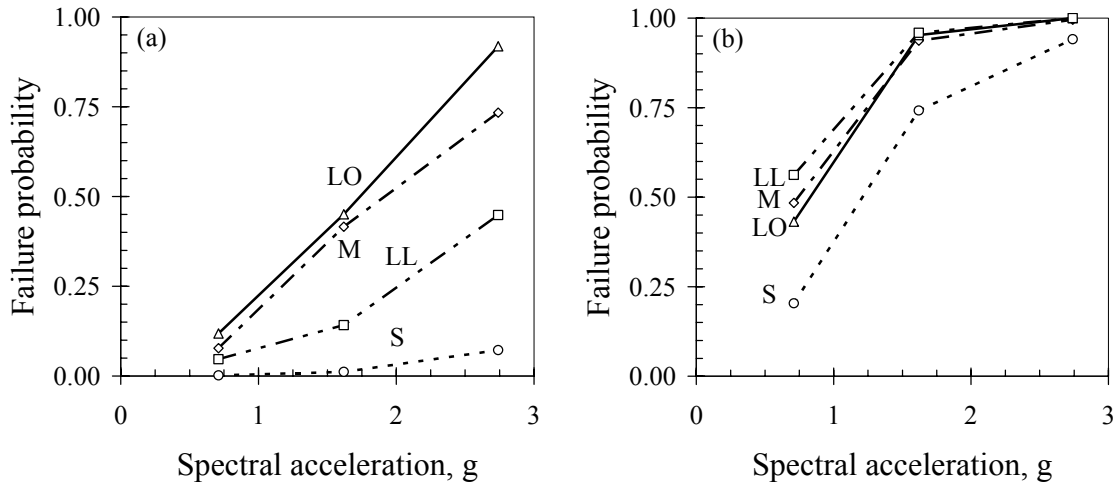


Fig. 8.3 Lab fragility as a function of *IM* (a) operability, (b) life safety

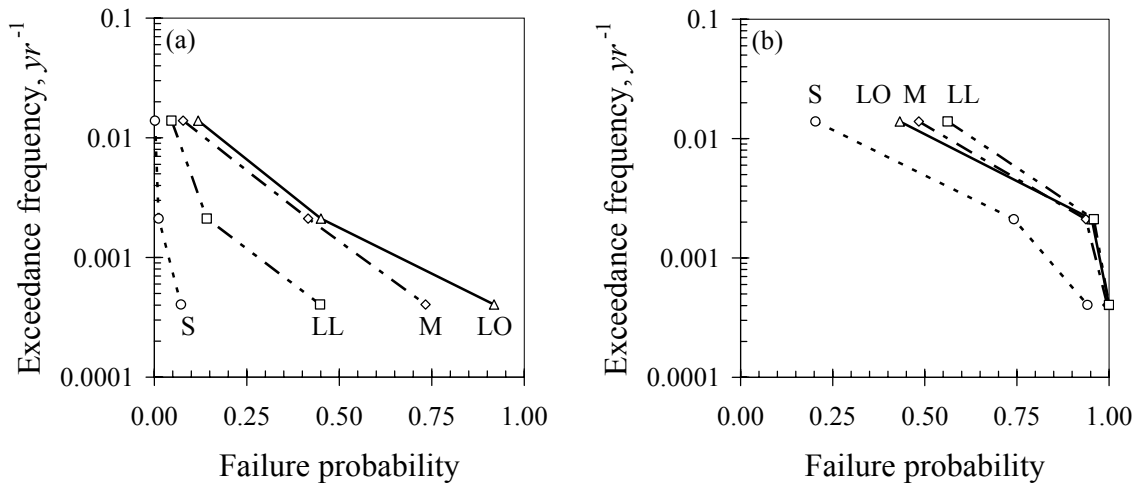


Fig. 8.4 Lab failure hazard (a) operability and (b) life-safety

Table 8.2 shows that in 9 of 12 cases examined here, life-safety failure is more likely than not. This is entirely because of chemical hazards. Even at the lowest hazard level, probability of life-safety failure exceeds 20% for all four labs examined here. The table also shows that operability failure only exceeds 20% probability in the 10%/50-yr event and then only for the M and LO labs. One can conclude from Table 8.2 and Figures 8.3 and 8.4 that:

1. Life-safety mitigation efforts at this facility should focus on mitigating chemical hazards.
2. Post-earthquake operability is less of a concern, but should be mitigated in the large labs if the investigators want reasonable assurance of post-earthquake operability in the 10%/50-yr earthquake.

Mean failure frequency, mean failure recurrence period, risk of ruin. From Figure 8.4, it is clear that there is probability of life-safety and operational failure at intensities below the 50%/50-yr *IM*. To evaluate Equation 8.15 accurately, it is necessary to extrapolate back the hazard curves in Figure 8.4 to $p = 0$. Evaluating Equation 8.15 over $0.0004 \leq \lambda[im] \leq 0.2$, the mean failure frequencies and mean failure recurrence periods are given in Table 8.3. The table also shows the risk of ruin (probability of at least one failure) within a planning period of 20 years, calculated according to Equation 8.16.

In performing the integration of Equation 8.15, we noticed that in several cases, the hazard below the 50%/50-yr exceedance level dominates the risk, accounting for 76% of the total estimated failure frequency in the last of life-safety failure of lab LL, 62% of the life-safety

failure frequency for lab M, and 49% of the life-safety failure frequency for lab LO. One implication is that it is necessary to evaluate seismic performance at shaking intensities below the 50%/50-yr hazard level.

The mean failure recurrence periods shown in Table 8.3 may make the case more clearly than do Figures 8.2 and 8.3 that life-safety risk is fairly high, especially in lab LL, where one would expect an earthquake-induced life-threatening chemical hazard on average once every 24 years, or on average at least once within a reasonably long career of the investigator in charge of the lab.

The recurrence periods for operability failure may suggest that post-earthquake operability failure is a fairly minor risk, more than likely not happening within the career of the investigators in charge of these labs. The risk of ruin, however, may counter that perception. It may be that a 5–10% probability of operational failure during a 20-year period may be unacceptably high. The 20-year risk of ruin for life safety also highlights a possibly intolerably high probability of life-threatening damage.

Table 8.3. Mean failure frequencies and failure recurrence periods

Lab	Operability			Life safety		
	λ, yr^{-1}	T, yr	$P[\text{ruin}]$	λ, yr^{-1}	T, yr	$P[\text{ruin}]$
S	0.0001	>1000	0.2%	0.0073	140	14%
M	0.0035	290	6.8%	0.0242	41	38%
LO	0.0045	220	8.7%	0.0174	57	29%
LL	0.0018	560	3.5%	0.0414	24	56%

8.5 RISK-MANAGEMENT DECISION MAKING

How should a university or lab decision maker interpret the results presented in the previous section? The answer depends in large part on how the decision maker prefers to think about risk. For a decision maker who is concerned with “the” earthquake, the scenario failure probabilities depicted in Table 8.2 might be most informative, especially those for the 10%/50-yr or 2%/50-yr events. For a decision maker more comfortable with probabilities, the risk-of-ruin data or possibly the mean-recurrence-period data shown in Table 8.3 might be more meaningful. We

doubt that risk-management decision makers would find the graphics of Figures 8.3 or 8.4 particularly useful.

8.6 CONCLUDING REMARKS

This chapter has presented a methodology for evaluating probabilistic relationships between DV and DM , DV and EDP , DV and IM , and the marginal probability distribution of DV for a planning period t (all of course conditioned on facility design, D), for the case of a laboratory facility where DV is evaluated in terms of life-safety or operational failure probability.

We have presented the concept of an operational unit, a subset of a facility at which DV can be evaluated and risk-management decisions can be made. In the present case, we have suggested that in the case of a laboratory facility, a reasonable operational unit might be a portion of the facility operated by an individual laboratory investigator. We have illustrated each of these DV relationships for four sample operational units (laboratories) of the UC Science Building testbed: one small, one medium, and two large-sized labs, where size is measured in terms of the number of pieces of equipment critical either to life safety or to operability.

We have presented the concept of an operational-unit fragility function, by which we mean a relationship between DV and EDP for an entire operational unit, where the operational unit is characterized solely by n , the number of non-rugged pieces of critical equipment. We have presented equations for parameters for the fragility function in terms of mean and logarithmic standard deviation of a cumulative lognormal distribution, where both parameters are functions of n . These equations would only be appropriate for facilities like the UC Science Building, i.e., with unrestrained countertop- or shelf-mounted equipment.

We have also discussed the concept of a performance metric, by which we mean a scalar measure of probabilistic DV for direct use in risk-management decision making. We have discussed several particular performance metrics, presenting the mathematics required to evaluate them, and illustrating three of them using the sample operational units. We found that the appearance of risk depends significantly on the performance metric used to characterize it. A decision maker considering scenario operability failure might conclude that the probability is small. The same DV information, when depicted in terms of risk of ruin (failure probability

during a reasonable planning period such as 20 years), makes a different case, suggesting possibly intolerable risk of operational failure.

We found that risk in this facility can be dominated by shaking at less than the 50%/50-yr level of *IM*, suggesting that PBEE evaluations of facilities of this type should examine lower hazard levels. Finally, we found that life-safety risk at this facility is high, and results primarily from chemical hazards.

8.7 REFERENCES

Beck, J.L., A. Kiremidjian, S. Wilkie, A. Mason, T. Salmon, J. Goltz, R. Olson, J. Workman, A. Irfanoglu, and K. Porter, 1999, *Decision Support Tools for Earthquake Recovery of Businesses, Final Report*, CUREe-Kajima Joint Research Program Phase III, Consortium of Universities for Earthquake Engineering Research, Richmond, CA.

Beck, J.L., K.A. Porter, R. V. Shaikhutdinov, S.K. Au, K. Mizukoshi, M. Miyamura, H. Ishida, T. Moroi, Y. Tsukada and M. Masuda, 2002, *Impact of Seismic Risk on Lifetime Property Values*, Report No. EERL 2002-04, California Institute of Technology, Pasadena, CA.

Federal Aviation Administration (FAA), 1998, *Economic Values for Evaluation of FAA Investment and Regulatory Decisions*, Report FAA-APO-98-8, <http://apo.faa.gov/economic/toc.htm>

FEMA, 2000, *Benefit-Cost Analysis of Hazard Mitigation Projects, Earthquake, Ver 5.1a* Washington, DC

Federal Highway Administration, 1994, *Technical Advisory: Motor Vehicle Accident Costs, Technical Advisory #7570.2*, U.S. Department of Transportation, Washington, D.C. <http://fhwa.dot.gov/legsregs/directives/techadv/t75702.htm>.

Porter, K.A., A.S. Kiremidjian, and J.S. LeGrue, 2001, "Assembly-based vulnerability of buildings and its use in performance evaluation," *Earthquake Spectra*, **17** (2), 291-312.

9 Stakeholders and Decision Issues

Stephanie E. Chang, University of Washington

9.1 OVERVIEW

This section discusses stakeholder concerns and potential issues relevant to the UC Science testbed (“Decision-Making” element of Fig. 1). This provides background on the decision-making context for earthquake hazard mitigation at the University of California at Berkeley in the case of nonstructural mitigation issues. Related PEER research has examined the decision-making process and identified relevant decision makers in the prioritization of buildings for structural mitigation (DeVries et al. 2000; Pannor 2002). However, these studies have not considered nonstructural decision making. In addition, there has not been any explicit focus on either performance-level decisions associated with an individual building such as the UC Science testbed or the ways in which various decision makers conceptualize “downtime.” A finer-scale analysis, which focuses on a single building, will permit the inclusion of a wider array of stakeholders than has been previously considered. Research at the campus scale considers only a limited number of stakeholders, namely university administrators and design professionals (DeVries et al. 2000; Pannor 2002). However, it has also been suggested that constituent groups may become more important once a particular building has been selected (DeVries et al. 2000). This is especially true at UC Berkeley, where the diffuse decision structure allows for the involvement of an array of stakeholders.

This section aims to address the following questions: For nonstructural mitigations, who are the stakeholder groups and what are their roles? What types of decisions do they make? How do the decision makers conceptualize seismic performance? What kinds of information do they need? How is nonstructural mitigation funded? And what are the barriers to implementing these mitigations? To address these questions, a series of interviews was conducted with managers and researchers associated with the UC Science Building case.

Briefly, we found the following:

- While there are numerous stakeholder groups involved in nonstructural mitigation, ultimately, it is the faculty-researchers who use the laboratory space that decide whether or not to undertake this mitigation.
- How the mitigations are implemented is largely the responsibility of crafts professionals in campus support offices.
- Nonstructural mitigations are primarily funded by individual faculty-researchers.
- An important lesson from a former program known as Q-Brace, which provided matching funds for nonstructural mitigations, was the need to recognize that campus crafts offices have capacity limitations. There is a need for appropriate standardized mitigation solutions that can be readily implemented.
- Stakeholders generally conceptualize performance in terms of both life safety and downtime. However, they need more information if they are to translate this concept into performance-based decision making. For example, many faculty-researchers currently conceptualize nonstructural mitigation in binary (“yes/no”) terms.
- Potential downtime in the laboratories due to earthquake damage could range from 6 months to 3 years, and is related to data preservation and access to specialized equipment.

Research was undertaken through in-person interviews that utilized an open-ended structured survey. Preliminary discussions with PEER and DRU researchers and administrators helped identify relevant stakeholders and critical issues. A total of 12 formal interviews were conducted during the late spring and early summer of 2003—6 with faculty-researchers, 3 with crafts professionals, 2 with campus administrative and safety offices, and 1 with the UC Science Building operations staff. Interview questions focused on (1) identifying the manner in which stakeholder groups are involved in the seismic decision-making process and (2) understanding the ways in which various aspects of performance, especially downtime, are conceptualized. Further details of the study can be found in Falit-Baiamonte and Chang (2003).

9.2 NONSTRUCTURAL RETROFIT DECISION MAKING FOR UC SCIENCE TESTBED

In the UC Science Building, nonstructural seismic mitigations are usually undertaken during the renovation or upgrading of laboratories. In general, they take place under one of three scenarios: retrofit of an existing lab; mitigation of a lab that is being reconfigured for a new research grant; or startup of a lab for a newly hired researcher. Nonstructural mitigation decisions can be classified into three main types: whether or not to mitigate; how to design and implement; and how to fund. Each of these involves a different set of stakeholders.

The decisions associated with the process of nonstructural mitigation in the UC Science Building involve a variety of stakeholders, the most important of whom are: faculty-researchers who use the laboratory space in the UC Science Building, UC crafts professionals who design, implement, and inspect nonstructural mitigations, the UC Science Building operations staff, and the UC campus administration and safety offices. The crafts professionals work out of a variety of offices, the most relevant of which are: the Academic Facilities Office (AFO), the Physical Plant Campus Services (PPCS), and Capital Projects. Table 1 summarizes the roles of major stakeholder groups in each of the main decision-making contexts.

Table 9.1 Stakeholder roles in nonstructural mitigation decision making

Stakeholder group	Type of Decision		
	Undertake Mitigation	Design and Implementation	Funding
Faculty-researchers <i>Crafts professionals</i> - Academic facilities office - Physical plant campus services - Capital projects Operations staff for building Campus admin. and safety offices - Vice provost for planning/facil. - Environmental health and safety	Make final decision Consult Facilitate safety self-inspection	Make final decision Design/implement (minor projects) Design/implement (major projects) Inspect Provide information (Q-Brace program)	Provide finance Finance when part of start-up costs Provide matching funds (Q-Brace)

The faculty-researchers who use the laboratory space in the UC Science Building make the final decision on whether or not to undertake nonstructural mitigations. In practice, these decisions are undertaken in consultation with the UC Science Building operations staff. Since nonstructural mitigations are neither funded nor mandated by the state, the entire cost of labor and materials is borne by individual faculty-researchers. Existing labs finance these mitigations using their research funds, while new faculty are provided start-up funding from the Office of the Executive Vice Chancellor and Provost.

Most nonstructural mitigations are performed by AFO, which is responsible for simple and semi-complex mitigations such as the storage of dangerous chemicals, the bracing of hazardous gas tanks, and the restraining of furniture. PPCS also performs nonstructural mitigations. They are most often involved with more complex mitigations, which can involve “semi-structural” elements, such as the restraining of large equipment and the supporting of free standing walls. In deciding how to implement these more complex mitigations, PPCS often requires information pertaining to the “generic structural details” of the building. Both AFO and PPCS are responsible for deciding how to implement the mitigations. At this point, neither unit has standardized the process to the point that would allow the Construction Inspection Services unit of the Capital Projects division to inspect the work.

Stakeholder interviews highlight several important concerns related to the implementation of nonstructural mitigations. The issue of capacity is of central importance. While each of the crafts units have specialized skills that they bring to bear on different aspects of the nonstructural mitigation process, time schedules and finance can limit their practical participation. Successful nonstructural mitigation also depends on the information available about both the specific building and the equipment being installed. This was demonstrated not only in the Q-Brace program, which provided matching funds to be used to implement basic nonstructural mitigations, but also in the everyday experiences of PPCS and Capital Projects. While interviewees indicated that the information about the UC Science Building is more than adequate, this level of detail is not available for most buildings on campus.

The issue of standardized versus individualized mitigation solutions is a capacity-related concern that was raised in every interview conducted with craft and safety professionals. Each of these stakeholders preferred standardized solutions that utilized mass-produced materials. Such an approach is thought to minimize the cost and time needed to implement a mitigation, as

well as provide a standard against which to inspect a completed project. Presently, PEER's technical manual for retrofitting laboratories (Holmes and Comerio 2003) provides both the generic structural details and specific work processes required for this approach, although this information is lacking for many other buildings. However, a standardized approach is most applicable to macro-scale mitigations such as the storage of dangerous chemicals, the bracing of hazardous gas tanks, the restraining of large equipment and furniture, and the supporting of freestanding walls. Micro-scale mitigations that aim to protect the contents of furniture and equipment (e.g., test tubes on a shelf or in a refrigerator) are thought to be an insurmountable task requiring individually engineered solutions, which are prohibitive in terms of cost and time.

9.3 CONCEPTUALIZATIONS OF PERFORMANCE

Each of the stakeholders interviewed in some way conceptualized performance in terms of both life-safety and downtime. All agreed that life-safety was by far the overriding concern. Downtime concerns, on the other hand, while recognized, do not seem to be a priority. In fact, an AFO project manager reported that making a lab "as safe as possible" requires large, cumbersome bracing that is prohibitive in terms of both cost and installation time.

While all of the faculty-researchers interviewed in some way recognized the importance of downtime, none had ever been informed of the full range of options available for implementing nonstructural mitigations. Most thought that their options were to either "brace for seismic" or to do nothing. They were unaware of the possibility of specifying performance levels that exceeded life-safety criteria.

Faculty-researchers conceptualized downtime in terms of damage to critical equipment and data loss. While access to the UC Science Building and their specific lab is a concern, all interviewees felt that they could continue their research in any basic science lab on campus, given the preservation of their data and specialized equipment. Downtime is thought to be a function of data preservation and access to specialized equipment. Every faculty-researcher reported that ordering and calibrating specialized equipment would take anywhere from 6~12 months. Downtime related to data loss was more variable. Some researchers predicted that data could be replaced in as little as two weeks, while others reported that lost data would be irreplaceable. Others predicted downtime in the range of 6 months, 1–2 years, and 2–3 years.

9.4 IMPLICATIONS FOR PERFORMANCE-BASED EARTHQUAKE ENGINEERING

This research has found that the promotion of nonstructural retrofits needs to focus on the dissemination of information in order to inform the stakeholders, especially the faculty-researchers, of their full range of options. While all of the faculty-researchers interviewed in some way recognized the importance of downtime, none had ever been informed of the full range of options available for implementing nonstructural mitigations. For example, most conceptualized nonstructural mitigations in binary (“yes”/”no”) terms. In this scenario, the array of options is reduced to “brace for seismic” or do nothing.

Given the concerns expressed by the stakeholders that were interviewed, it is suggested that information provided should associate various performance levels with estimates of the cost and time required for implementation, potential damage state of data and critical equipment, and a prediction of how mitigations could impact the work flow of the lab. This information will not only serve to inform the faculty-researchers of their full range of options, but also draw their attention to the ways in which a seismic event might damage their research infrastructure.

9.5 REFERENCES

- DeVries, F. and K. Mannen, M. Comerio, J. Ellwood, R. MacCoun. 2000. “Decision fault-lines: Seismic safety at four California universities.” PEER Discussion Paper.
- Falit-Baiamonte, A. and S. E. Chang. 2003. “Background on non-structural seismic mitigation decision-making at UC Berkeley.” PEER Discussion Paper.
- Holmes, W. and M. Comerio. 2003. “Implementation Manual for the Seismic Protection of Laboratory Contents: Format and Case Studies.” PEER Center Technical Report, PEER, University of California, Berkeley, CA.
- Pannor, M. (2002). “Differences in seismic risk perception among decision-makers and technical experts.” PEER Discussion Paper.

10 Practitioners Use of Testbed Data and Methods

William T. Holmes, Rutherford & Chekene, Oakland, CA

There is a growing concern about the seismic life-safety risks to occupants of laboratories. Attention was drawn to the laboratory setting by the presence of chemicals and storage tanks for various gases, but concern has expanded to the potential risks from large unanchored equipment such as refrigerators, freezers, and incubators. Studies by Comerio and others at University of California at Berkeley have identified the importance and value of much of the contents of research laboratories and the significant losses that could occur in an earthquake, but most seismic protection programs to date have been directed toward life-safety issues. Other than chemical spills, little is known about the fragility of lab contents and the level of life-safety risk actually presented. This testbed demonstrates the difficulty and creates serious questions about the viability of establishing definitive individual fragilities and potential losses for the wide variety of contents, configurations, and other conditions in labs.

The summaries contained in this test-bed report do not always completely describe the assumptions and results of the various studies. Some of the issues noted here might be resolved and documented in the full individual reports, but it is doubtful that the overall conclusions of this chapter will change.

10.1 DIRECT USE OF EXPERIMENTAL RESULTS

Previous studies of the contents of the testbed building (see Chapter 2) identified several issues regarding the fragility of items, the resulting need to retrofit, and the effectiveness of various retrofit techniques. Although the primary purpose of the laboratory experiments was to enable a

testbed use of the PEER PBEE methodology, it was hoped that some of the practical issues could also be resolved.

Practical issues related to bench- and shelf-mounted contents included:

- Under what circumstances will contents overturn or fall to the floor (presumably resulting in damage)?
- Vertical “lips” are standard at the perimeter of lab shelving. How high must these lips be to be effective?
- Will glassware and other fragile contents on shelves be broken even with a lip that will prevent falling, or within cabinets with closed doors?

A useful relationship was developed between peak horizontal floor motion and probable maximum sliding displacement dependent on the frictional properties of the contents. However, based on the summary descriptions in this report, the significance of the following effects are unclear:

- Are the relationships equally valid for the much larger floor displacements expected in buildings? Is an intensity measure for a potential pulse, similar to that used for the large lab equipment, needed to completely describe the problem?
- Is overturning an issue for bench and shelf equipment with high friction bases?
- Is there a practical method to determine the dynamic characteristics of benches and shelves of various configurations and support conditions?
- The issues of restraining lips and fragility of restrained, brittle contents were not systematically studied in this series of experiments.

Practical issues related to tall and heavy laboratory equipment included:

- Is this equipment likely to overturn?
- Is this equipment likely to slide in such a way to create a life-safety hazard or to block a doorway?
- If restrained in various ways, will anchorage forces or high accelerations damage the equipment or contents?

A useful relationship was developed that relates peak sliding displacements to an intensity measure of the governing input pulse and friction characteristics of the base. However,

based on the summary descriptions in this report, the significance of the following effects are unclear:

- Is there a practical method to predict the probability of various pulse intensities?
- Can more than one pulse occur in one ground motion, resulting in larger movements? Are there permanent displacements caused by “walking” or incremental sliding without the presence of a significant pulse (perhaps related to maximum floor accelerations similar to benchtop equipment)?
- Can the single case of overturning be overlooked? Many instances of equipment with fully extended leveling feet can be found. Does linoleum or other floor material dimple under the leveling feet over time, creating the equivalent of high initial friction that would increase the probability of overturning?
- The existing restraint detail of loose tethers (actually chains) to the adjacent steel stud walls apparently was successful in limiting movement of the equipment without failing the connections or the wall itself. However the restrained equipment experienced extremely high accelerations. It is unknown if the equipment or its contents would be damaged by such accelerations to create losses from interrupted operation or from loss of valuable experimental products.
- It was not within the scope of the experiment to develop or test any other restraint details.

10.2 GENERAL REVIEW OF TESTBED PROJECT

Successful trial of methodology. The series of testbed projects related to the UC Science Building demonstrates that development of information to populate the PEER PBEE framing equation is possible. However, many simplifications and assumptions were needed to complete the process even for the single set of overall conditions associated with the Science Building. For example, as pointed out in Chapter 8, “None of the necessary information on laboratory equipment costs and repairs, nor on content-induced injury, is currently available.” Without this data and a more refined consideration of individual conditions (as described below), the Safety and Operability failure probabilities may not be adequate for risk management decision making by practitioners.

Apparent oversimplifications. The following assumptions and simplifications may not be appropriate. Many of these issues are already pointed out in other chapters.

- Movement of bench-top and shelf-mounted equipment and supplies being limited to sliding.
- Breakage of glassware on shelves or in cabinets is not considered.
- Lips on shelving are not considered.
- Partial damage to contents is not considered.
- Casualty rates for life-safety “failures” are not used.
- Time for repair or replacement is not considered.
- Overturning of heavy tall equipment is not considered (limits of test data).
- Sliding of heavy tall equipment is judged to not present a life-safety risk.
- The loose tether restraints for tall heavy equipment that exists in a extensive array of configurations in the building are not considered. It is unclear if these tethers result in risk reduction (smaller sliding distances) or risk increase (damage to the equipment and contents, and possibly partitions, due to high accelerations).

Need for data on retrofit. To complete the use of this methodology for risk management decision making, complete data are also needed for realistic mitigation measures. Even more than for seismic risk reduction in other fields, “retrofit” of laboratory contents does not imply prevention of damage.

As previously mentioned, reasonable and economical methods to provide protection for valuable contents of freezers or incubators that prevents unwanted movement of the equipment without damaging the equipment or contents are not developed. On the other hand, there are insufficient data from this project to justify leaving this category of equipment unrestrained. In addition to the issue of structural capacity of threaded leveling bolt supports, much of this equipment is mounted on wheels (sometimes locked, sometimes not), and laboratory floor finishes vary greatly.

Commercially available restraint for bench-top equipment typically consists of tethers attached with double-backed tape. Although these products have been developed to be easily installed and moved and generally to satisfy users, their reliability to provide protection against damage is unclear. As mentioned previously, the effectiveness of the standard restraint lips used on laboratory shelves is unknown. There is no apparent backup for the normal height of 1.375–

1.5" and the extent of damage to contents with various height lips or tray-type holders on shelving is unknown.

10.3 PRACTICAL USE OF TESTBED METHODOLOGY

Despite the extensive effort of the participants in the Life Science Building Testbed Project, it appears that the methodology would require considerable additional refinement to produce loss data in sufficient detail for risk management decision making by practitioners. This additional effort, combined with the pre-testbed effort of collecting detailed laboratory inventory, indicates that an element-by-element fragility approach to performance based engineering, at least for contents, may be impractical. Similar attempts to produce element-by-element fragility and loss data for nonstructural systems in HAZUS were quickly abandoned due to lack of data and complex interaction between systems. However, these efforts may provide an invaluable lesson for planning the future of performance-based engineering for both building contents and nonstructural building systems.

The attempt to develop a simplified lab-wide fragility function described in Chapter 8 is laudable but based on assumptions that are oversimplified as described above. However, either this concept must be pursued and refined or a completely different more global, floor or room-based methodology developed.

On the other hand, use of the PEER methodology to shed light on difficult individual issues regarding lab contents (or contents and nonstructural elements of all buildings) may be appropriate and valuable. For example, the appropriate height and strength of a shelf lip may be determined based only on the probabilities of various failures. This information could then be adopted as an industry standard (similar to the current, but undocumented, standard lip designs). Similarly, appropriate and economical restraint for tall, heavy floor mounted-equipment could also be developed based on risks of various movements or internal damage (if, indeed, any restraint is required). Continuing with these examples, given sufficient fragility data, different lip heights, and equipment restraint could be determined for different levels of seismicity, and an appropriate cutoff determined for any consideration of seismic protection. Although more extensive testing may be required to answer these questions, it is far less daunting than providing

data for *all* contents. Proceeding on this path would require prioritization of issues and careful targeting of the limited research resources.

11 Lessons and Future Research Directions

Mary C. Comerio, University of California, Berkeley, and Keith A. Porter, California Institute of Technology

The review of the testbed in Chapter 10 provides a discussion of the practical issues for engineering design that are needed to improve contents testings and loss modeling. The questions raised by our Business and Industry partner are the kinds of questions which are critical to a practicing engineer attempting the design of a mitigation scheme for laboratories. Here we attempt to raise research questions that emerge in the development of performance-based earthquake engineering assessment methodology as developed by PEER.

In general, the testbed demonstrated a successful trial of the methodology, but it also demonstrated the high level of complexity required for performance assessment, and the large amount of calibration data needed to predict quantitative damage measures in dollars, casualties, and duration of downtime.

Each component of the PEER methodology, the hazard analysis, the structural analysis, the development of damage measures, loss estimates and decision variables, relies on sophisticated analytic procedures. However, to provide input data from one stage to the next, many simplifications and assumptions were needed to complete the process. For example, the estimate of operational failure of laboratory equipment relied on fragility curves derived from shake table tests of a relatively small number of equipment samples, where the true scale of input motions could not be simulated because of shake table limitations. Further, the estimate of operational and life-safety failure was based primarily on sliding. The results did not take into account the presence of a shelf lip, overturning, and a number of other more subtle damage conditions that were not tested for in our laboratory experiments. Nor did the results consider the likelihood of injury to occupants, given a failure. Unfortunately, an enormous amount of detailed data on how each piece of equipment responds to the shaking at the floor or bench level would

be necessary to translate the engineering demand parameters, such as peak floor acceleration, or interstory drift, into accurate measures of damage and its influence on downtime.

The testbed research raises several questions regarding the direction of performance modeling in general, and the development of the PEER methodology, specifically. *First, what is the real goal of a performance measure?* The PEER method argues that comparing losses (the probability of exceeding losses such as casualties, repairs costs, or downtime) provides a rationale for performance design trade-offs. However, researchers who work on loss modeling are typically wary of estimates of losses based on a single building or structure. With the best analytic procedures, it may be possible to accurately represent damage, and estimate construction costs for repairs, but casualties¹³ and downtime are difficult to model, as methods and data are scarce. Still, an important outcome from the PEER performance engineering methodology will be to develop a basis for consistent assessment of performance between systems (concrete, steel, wood, etc.). These could be used in the prescriptive code provisions and to allow alternative analysis and design methods that will give equivalent or measurably better performance than the prescriptive code. As a broad goal, this is achievable and PEER's benchmarking studies of existing code buildings will contribute to that goal.

There have been significant breakthroughs in the field of structural engineering in the last decade, in part based on the wealth of measured ground motions and building and infrastructure behavior in recent earthquakes. At the same time, it was the enormity of the financial losses that

¹³ A great deal of work needs to be done to associate physical damage to facility components with probability of deaths, injuries, and related *DVs*. One can see evidence of this need in the present study. For example, we associate only class-D life-safety hazards (see Table 7-1) with a significant threat to life safety by blunt-force trauma. This is an engineer's assumption, not yet validated by empirical evidence or review by public-health experts. Furthermore, the assertion that overturning of class-D objects is a significant life-safety threat does not address important *DVs*: the probability of a person being struck by the overturning object; the severity of the consequent injury; victim morbidity, mortality, demand for healthcare services, or duration and cost of disability. To perform defensible cost-benefit analysis of contents mitigation including potentially substantial savings in healthcare costs will require such gaps to be filled. In the future, it would be valuable to be able to identify equipment capable of threatening life safety by establishing a defensible relationship between the characteristics of the object (e.g., dimensions, weight, and height relative to occupants), their *DMs*, and these *DVs*.

prompted the engineering community to look for ways to give clients a voice in the “performance expectations.” However, the post-event research on losses has demonstrated that costs are largely resulting from damage to nonstructural systems and contents, which leads to the second key question on performance-based design. *How well can structural engineers model the impacts to nonstructural systems and contents?*

There is little fundamental research on the behavior of nonstructural systems, equipment and contents, compared with what has been done for structural systems. Although work is progressing (see ATC 29-2, 2003), it is not clear that we can expect to understand with precision how these building subsystems will be damaged (again the absence of models and data). As such, the link between coarse estimates of damage and actual losses is tenuous. At first glance, it may appear to be easier to simply estimate whether structural systems will have greater or lesser impacts on damage to nonstructural systems, and focus the performance attention (and the design trade-offs) on the structural system. However, nonstructural performance cannot be predicted solely on structural behavior, as it is dependent on (1) drift, (2) floor accelerations (that trend opposite from drift), and (3) the design of and interaction between the nonstructural systems themselves.

Despite the difficulties in modeling, it is critically important for PEER to continue to include all building components in the performance assessment methodology, in order to represent the relationship between the earthquake hazard, the performance of all systems and contents, damage, and the consequences associated with specific design decisions or standards. This testbed pushed the limits of performance modeling by attempting to quantify the potential losses to laboratory contents using the PEER methodology. We have shown the difficulty of taking the process down to individual components, or worse, to inter-related groups of components. At the same time, we learned that perhaps we can simplify the procedure by devising fragilities for spatial components—such as an individual laboratory—to make the analysis more manageable.

The third and final question that is raised by the UC Science testbed experience is *Can the methodology be simplified?* This question has a larger philosophical component as well as a more direct pragmatic component. More broadly, it asks whether or not performance design trade-offs are best understood in terms of probable losses (in terms of deaths, dollars, and downtime), given the uncertainties in translating intensity measures into engineering demand

parameters, into damage measures, and finally into losses. Today, professionals tend to separate damage estimates (and probable repair costs) from estimates of casualties or downtime. Within the PEER methodology, these are integrated to include a range of alternative and interdependent consequences. At a practical level, however, each of the PEER analytic components (hazard, structure, damage, and loss models) currently employs sophisticated and time-consuming methods. It would be practical to develop simplified approaches to each component so that an engineer could choose which component to explore in detail, or in combination with shorthand inputs from simplified methods.

For example, it was shown in Chapter 8 that one can create a fragility function for a laboratory without analyzing every piece of equipment, as long as certain conditions are met: (1) the equipment is similar to the equipment in the sample laboratories, (2) is similarly close to the edge of surfaces, (3) the failure of any critical component causes failure of the operational unit, and (4) there are fewer than about 15 pieces of critical equipment in the laboratory (which was the maximum number examined here). This is a promising simplification, and warrants additional investigation to reduce the restrictions.

In summary, the PEER methodology for performance-based design offers a conceptual approach to quantifying design trade-offs. It lays out the relationships between ground motions, structural behavior, damage, and losses and suggests that the analytic techniques used by different engineering professionals and decision makers can find common ground through the use of a common language. The PEER testbeds demonstrated applications of this approach in buildings and bridges. The results from that experience have demonstrated the strengths and weaknesses in the methodology and point to a variety of ways to improve and simplify performance-engineering design. Other research is needed to fully investigate how changes in design methods will be adopted into current regulatory systems and decision processes.

11.1 REFERENCES

Applied Technology Council (2003) *Proceedings: Seminar on Seismic Design, Performance, and Retrofit of Nonstructural Components*. Applied Technology Council Publication # ATC-29-2, Redwood City, CA.

PEER REPORTS

PEER reports are available from the National Information Service for Earthquake Engineering (NISEE). To order PEER reports, please contact the Pacific Earthquake Engineering Research Center, 1301 South 46th Street, Richmond, California 94804-4698. Tel.: (510) 231-9468; Fax: (510) 231-9 461.

- PEER 2005/12** *PEER Testbed Study on a Laboratory Building: Exercising Seismic Performance Assessment.* Mary C. Comerio, editor. November 2005.
- PEER 2005/11** *Van Nuys Hotel Building Testbed Report: Exercising Seismic Performance Assessment.* Helmut Krawinkler, editor. October 2005.
- PEER 2005/10** *First NEES/E-Defense Workshop on Collapse Simulation of Reinforced Concrete Building Structures.* September 2005.
- PEER 2005/06** *Global Collapse of Frame Structures under Seismic Excitations.* Luis F. Ibarra and Helmut Krawinkler. September 2005.
- PEER 2005/01** *Empirical Characterization of Site Conditions on Strong Ground Motion.* Jonathan P. Stewart, Yoojoong Choi, and Robert W. Graves. June 2005.
- PEER 2004/09** *Electrical Substation Equipment Interaction: Experimental Rigid Conductor Studies.* Christopher Stearns and André Filiatrault. February 2005.
- PEER 2004/08** *Seismic Qualification and Fragility Testing of Line Break 550-kV Disconnect Switches.* Shakhzod M. Takhirov, Gregory L. Fenves, and Eric Fujisaki. January 2005.
- PEER 2004/07** *Ground Motions for Earthquake Simulator Qualification of Electrical Substation Equipment.* Shakhzod M. Takhirov, Gregory L. Fenves, Eric Fujisaki, and Don Clyde. January 2005.
- PEER 2004/06** *Performance-Based Regulation and Regulatory Regimes.* Peter J. May and Chris Koski. September 2004.
- PEER 2004/05** *Performance-Based Seismic Design Concepts and Implementation: Proceedings of an International Workshop.* Peter Fajfar and Helmut Krawinkler, editors. September 2004.
- PEER 2004/04** *Seismic Performance of an Instrumented Tilt-up Wall Building.* James C. Anderson and Vitelmo V. Bertero. July 2004.
- PEER 2004/03** *Evaluation and Application of Concrete Tilt-up Assessment Methodologies.* Timothy Graf and James O. Malley. October 2004.
- PEER 2004/02** *Analytical Investigations of New Methods for Reducing Residual Displacements of Reinforced Concrete Bridge Columns.* Junichi Sakai and Stephen A. Mahin. August 2004.
- PEER 2004/01** *Seismic Performance of Masonry Buildings and Design Implications.* Kerri Anne Taeko Tokoro, James C. Anderson, and Vitelmo V. Bertero. February 2004.
- PEER 2003/18** *Performance Models for Flexural Damage in Reinforced Concrete Columns.* Michael Berry and Marc Eberhard. August 2003.
- PEER 2003/17** *Predicting Earthquake Damage in Older Reinforced Concrete Beam-Column Joints.* Catherine Pagni and Laura Lowes. October 2004.
- PEER 2003/16** *Seismic Demands for Performance-Based Design of Bridges.* Kevin Mackie and Božidar Stojadinovi . August 2003.
- PEER 2003/15** *Seismic Demands for Nondeteriorating Frame Structures and Their Dependence on Ground Motions.* Ricardo Antonio Medina and Helmut Krawinkler. May 2004.
- PEER 2003/14** *Finite Element Reliability and Sensitivity Methods for Performance-Based Earthquake Engineering.* Terje Haukaas and Armen Der Kiureghian. April 2004.
- PEER 2003/13** *Effects of Connection Hysteretic Degradation on the Seismic Behavior of Steel Moment-Resisting Frames.* Janise E. Rodgers and Stephen A. Mahin. March 2004.
- PEER 2003/12** *Implementation Manual for the Seismic Protection of Laboratory Contents: Format and Case Studies.* William T. Holmes and Mary C. Comerio. October 2003.

- PEER 2003/11** *Fifth U.S.-Japan Workshop on Performance-Based Earthquake Engineering Methodology for Reinforced Concrete Building Structures.* February 2004.
- PEER 2003/10** *A Beam-Column Joint Model for Simulating the Earthquake Response of Reinforced Concrete Frames.* Laura N. Lowes, Nilanjan Mitra, and Arash Altoontash. February 2004.
- PEER 2003/09** *Sequencing Repairs after an Earthquake: An Economic Approach.* Marco Casari and Simon J. Wilkie. April 2004.
- PEER 2003/08** *A Technical Framework for Probability-Based Demand and Capacity Factor Design (DCFD) Seismic Formats.* Fatemeh Jalayer and C. Allin Cornell. November 2003.
- PEER 2003/07** *Uncertainty Specification and Propagation for Loss Estimation Using FOSM Methods.* Jack W. Baker and C. Allin Cornell. September 2003.
- PEER 2003/06** *Performance of Circular Reinforced Concrete Bridge Columns under Bidirectional Earthquake Loading.* Mahmoud M. Hachem, Stephen A. Mahin, and Jack P. Moehle. February 2003.
- PEER 2003/05** *Response Assessment for Building-Specific Loss Estimation.* Eduardo Miranda and Shahram Taghavi. September 2003.
- PEER 2003/04** *Experimental Assessment of Columns with Short Lap Splices Subjected to Cyclic Loads.* Murat Melek, John W. Wallace, and Joel Conte. April 2003.
- PEER 2003/03** *Probabilistic Response Assessment for Building-Specific Loss Estimation.* Eduardo Miranda and Hesameddin Aslani. September 2003.
- PEER 2003/02** *Software Framework for Collaborative Development of Nonlinear Dynamic Analysis Program.* Jun Peng and Kincho H. Law. September 2003.
- PEER 2003/01** *Shake Table Tests and Analytical Studies on the Gravity Load Collapse of Reinforced Concrete Frames.* Kenneth John Elwood and Jack P. Moehle. November 2003.
- PEER 2002/24** *Performance of Beam to Column Bridge Joints Subjected to a Large Velocity Pulse.* Natalie Gibson, André Filiatrault, and Scott A. Ashford. April 2002.
- PEER 2002/23** *Effects of Large Velocity Pulses on Reinforced Concrete Bridge Columns.* Greg L. Orozco and Scott A. Ashford. April 2002.
- PEER 2002/22** *Characterization of Large Velocity Pulses for Laboratory Testing.* Kenneth E. Cox and Scott A. Ashford. April 2002.
- PEER 2002/21** *Fourth U.S.-Japan Workshop on Performance-Based Earthquake Engineering Methodology for Reinforced Concrete Building Structures.* December 2002.
- PEER 2002/20** *Barriers to Adoption and Implementation of PBEE Innovations.* Peter J. May. August 2002.
- PEER 2002/19** *Economic-Engineered Integrated Models for Earthquakes: Socioeconomic Impacts.* Peter Gordon, James E. Moore II, and Harry W. Richardson. July 2002.
- PEER 2002/18** *Assessment of Reinforced Concrete Building Exterior Joints with Substandard Details.* Chris P. Pantelides, Jon Hansen, Justin Nadauld, and Lawrence D. Reaveley. May 2002.
- PEER 2002/17** *Structural Characterization and Seismic Response Analysis of a Highway Overcrossing Equipped with Elastomeric Bearings and Fluid Dampers: A Case Study.* Nicos Makris and Jian Zhang. November 2002.
- PEER 2002/16** *Estimation of Uncertainty in Geotechnical Properties for Performance-Based Earthquake Engineering.* Allen L. Jones, Steven L. Kramer, and Pedro Arduino. December 2002.
- PEER 2002/15** *Seismic Behavior of Bridge Columns Subjected to Various Loading Patterns.* Asadollah Esmaeily-Gh. and Yan Xiao. December 2002.
- PEER 2002/14** *Inelastic Seismic Response of Extended Pile Shaft Supported Bridge Structures.* T.C. Hutchinson, R.W. Boulanger, Y.H. Chai, and I.M. Idriss. December 2002.
- PEER 2002/13** *Probabilistic Models and Fragility Estimates for Bridge Components and Systems.* Paolo Gardoni, Armen Der Kiureghian, and Khalid M. Mosalam. June 2002.
- PEER 2002/12** *Effects of Fault Dip and Slip Rake on Near-Source Ground Motions: Why Chi-Chi Was a Relatively Mild M7.6 Earthquake.* Brad T. Aagaard, John F. Hall, and Thomas H. Heaton. December 2002.

- PEER 2002/11** *Analytical and Experimental Study of Fiber-Reinforced Strip Isolators.* James M. Kelly and Shakhzod M. Takhirov. September 2002.
- PEER 2002/10** *Centrifuge Modeling of Settlement and Lateral Spreading with Comparisons to Numerical Analyses.* Sivapalan Gajan and Bruce L. Kutter. January 2003.
- PEER 2002/09** *Documentation and Analysis of Field Case Histories of Seismic Compression during the 1994 Northridge, California, Earthquake.* Jonathan P. Stewart, Patrick M. Smith, Daniel H. Whang, and Jonathan D. Bray. October 2002.
- PEER 2002/08** *Component Testing, Stability Analysis and Characterization of Buckling-Restrained Unbonded Braces™.* Cameron Black, Nicos Makris, and Ian Aiken. September 2002.
- PEER 2002/07** *Seismic Performance of Pile-Wharf Connections.* Charles W. Roeder, Robert Graff, Jennifer Soderstrom, and Jun Han Yoo. December 2001.
- PEER 2002/06** *The Use of Benefit-Cost Analysis for Evaluation of Performance-Based Earthquake Engineering Decisions.* Richard O. Zerbe and Anthony Falit-Baiamonte. September 2001.
- PEER 2002/05** *Guidelines, Specifications, and Seismic Performance Characterization of Nonstructural Building Components and Equipment.* André Filiatrault, Constantin Christopoulos, and Christopher Stearns. September 2001.
- PEER 2002/04** *Consortium of Organizations for Strong-Motion Observation Systems and the Pacific Earthquake Engineering Research Center Lifelines Program: Invited Workshop on Archiving and Web Dissemination of Geotechnical Data, 4–5 October 2001.* September 2002.
- PEER 2002/03** *Investigation of Sensitivity of Building Loss Estimates to Major Uncertain Variables for the Van Nuys Testbed.* Keith A. Porter, James L. Beck, and Rustem V. Shaikhutdinov. August 2002.
- PEER 2002/02** *The Third U.S.-Japan Workshop on Performance-Based Earthquake Engineering Methodology for Reinforced Concrete Building Structures.* July 2002.
- PEER 2002/01** *Nonstructural Loss Estimation: The UC Berkeley Case Study.* Mary C. Comerio and John C. Stallmeyer. December 2001.
- PEER 2001/16** *Statistics of SDF-System Estimate of Roof Displacement for Pushover Analysis of Buildings.* Anil K. Chopra, Rakesh K. Goel, and Chatpan Chintanapakdee. December 2001.
- PEER 2001/15** *Damage to Bridges during the 2001 Nisqually Earthquake.* R. Tyler Ranf, Marc O. Eberhard, and Michael P. Berry. November 2001.
- PEER 2001/14** *Rocking Response of Equipment Anchored to a Base Foundation.* Nicos Makris and Cameron J. Black. September 2001.
- PEER 2001/13** *Modeling Soil Liquefaction Hazards for Performance-Based Earthquake Engineering.* Steven L. Kramer and Ahmed-W. Elgamal. February 2001.
- PEER 2001/12** *Development of Geotechnical Capabilities in OpenSees.* Boris Jeremi . September 2001.
- PEER 2001/11** *Analytical and Experimental Study of Fiber-Reinforced Elastomeric Isolators.* James M. Kelly and Shakhzod M. Takhirov. September 2001.
- PEER 2001/10** *Amplification Factors for Spectral Acceleration in Active Regions.* Jonathan P. Stewart, Andrew H. Liu, Yoojoong Choi, and Mehmet B. Baturay. December 2001.
- PEER 2001/09** *Ground Motion Evaluation Procedures for Performance-Based Design.* Jonathan P. Stewart, Shyh-Jeng Chiou, Jonathan D. Bray, Robert W. Graves, Paul G. Somerville, and Norman A. Abrahamson. September 2001.
- PEER 2001/08** *Experimental and Computational Evaluation of Reinforced Concrete Bridge Beam-Column Connections for Seismic Performance.* Clay J. Naito, Jack P. Moehle, and Khalid M. Mosalam. November 2001.
- PEER 2001/07** *The Rocking Spectrum and the Shortcomings of Design Guidelines.* Nicos Makris and Dimitrios Konstantinidis. August 2001.
- PEER 2001/06** *Development of an Electrical Substation Equipment Performance Database for Evaluation of Equipment Fragilities.* Thalia Agnanos. April 1999.
- PEER 2001/05** *Stiffness Analysis of Fiber-Reinforced Elastomeric Isolators.* Hsiang-Chuan Tsai and James M. Kelly. May 2001.

- PEER 2001/04** *Organizational and Societal Considerations for Performance-Based Earthquake Engineering.* Peter J. May. April 2001.
- PEER 2001/03** *A Modal Pushover Analysis Procedure to Estimate Seismic Demands for Buildings: Theory and Preliminary Evaluation.* Anil K. Chopra and Rakesh K. Goel. January 2001.
- PEER 2001/02** *Seismic Response Analysis of Highway Overcrossings Including Soil-Structure Interaction.* Jian Zhang and Nicos Makris. March 2001.
- PEER 2001/01** *Experimental Study of Large Seismic Steel Beam-to-Column Connections.* Egor P. Popov and Shakhzod M. Takhirov. November 2000.
- PEER 2000/10** *The Second U.S.-Japan Workshop on Performance-Based Earthquake Engineering Methodology for Reinforced Concrete Building Structures.* March 2000.
- PEER 2000/09** *Structural Engineering Reconnaissance of the August 17, 1999 Earthquake: Kocaeli (Izmit), Turkey.* Halil Sezen, Kenneth J. Elwood, Andrew S. Whittaker, Khalid Mosalam, John J. Wallace, and John F. Stanton. December 2000.
- PEER 2000/08** *Behavior of Reinforced Concrete Bridge Columns Having Varying Aspect Ratios and Varying Lengths of Confinement.* Anthony J. Calderone, Dawn E. Lehman, and Jack P. Moehle. January 2001.
- PEER 2000/07** *Cover-Plate and Flange-Plate Reinforced Steel Moment-Resisting Connections.* Taejin Kim, Andrew S. Whittaker, Amir S. Gilani, Vitelmo V. Bertero, and Shakhzod M. Takhirov. September 2000.
- PEER 2000/06** *Seismic Evaluation and Analysis of 230-kV Disconnect Switches.* Amir S. J. Gilani, Andrew S. Whittaker, Gregory L. Fenves, Chun-Hao Chen, Henry Ho, and Eric Fujisaki. July 2000.
- PEER 2000/05** *Performance-Based Evaluation of Exterior Reinforced Concrete Building Joints for Seismic Excitation.* Chandra Clyde, Chris P. Pantelides, and Lawrence D. Reaveley. July 2000.
- PEER 2000/04** *An Evaluation of Seismic Energy Demand: An Attenuation Approach.* Chung-Che Chou and Chia-Ming Uang. July 1999.
- PEER 2000/03** *Framing Earthquake Retrofitting Decisions: The Case of Hillside Homes in Los Angeles.* Detlof von Winterfeldt, Nels Roselund, and Alicia Kitsuse. March 2000.
- PEER 2000/02** *U.S.-Japan Workshop on the Effects of Near-Field Earthquake Shaking.* Andrew Whittaker, ed. July 2000.
- PEER 2000/01** *Further Studies on Seismic Interaction in Interconnected Electrical Substation Equipment.* Armen Der Kiureghian, Kee-Jeung Hong, and Jerome L. Sackman. November 1999.
- PEER 1999/14** *Seismic Evaluation and Retrofit of 230-kV Porcelain Transformer Bushings.* Amir S. Gilani, Andrew S. Whittaker, Gregory L. Fenves, and Eric Fujisaki. December 1999.
- PEER 1999/13** *Building Vulnerability Studies: Modeling and Evaluation of Tilt-up and Steel Reinforced Concrete Buildings.* John W. Wallace, Jonathan P. Stewart, and Andrew S. Whittaker, editors. December 1999.
- PEER 1999/12** *Rehabilitation of Nonductile RC Frame Building Using Encasement Plates and Energy-Dissipating Devices.* Mehrdad Sasani, Vitelmo V. Bertero, James C. Anderson. December 1999.
- PEER 1999/11** *Performance Evaluation Database for Concrete Bridge Components and Systems under Simulated Seismic Loads.* Yael D. Hose and Frieder Seible. November 1999.
- PEER 1999/10** *U.S.-Japan Workshop on Performance-Based Earthquake Engineering Methodology for Reinforced Concrete Building Structures.* December 1999.
- PEER 1999/09** *Performance Improvement of Long Period Building Structures Subjected to Severe Pulse-Type Ground Motions.* James C. Anderson, Vitelmo V. Bertero, and Raul Bertero. October 1999.
- PEER 1999/08** *Envelopes for Seismic Response Vectors.* Charles Menun and Armen Der Kiureghian. July 1999.
- PEER 1999/07** *Documentation of Strengths and Weaknesses of Current Computer Analysis Methods for Seismic Performance of Reinforced Concrete Members.* William F. Cofer. November 1999.
- PEER 1999/06** *Rocking Response and Overturning of Anchored Equipment under Seismic Excitations.* Nicos Makris and Jian Zhang. November 1999.
- PEER 1999/05** *Seismic Evaluation of 550 kV Porcelain Transformer Bushings.* Amir S. Gilani, Andrew S. Whittaker, Gregory L. Fenves, and Eric Fujisaki. October 1999.

- PEER 1999/04** *Adoption and Enforcement of Earthquake Risk-Reduction Measures.* Peter J. May, Raymond J. Burby, T. Jens Feeley, and Robert Wood.
- PEER 1999/03** *Task 3 Characterization of Site Response General Site Categories.* Adrian Rodriguez-Marek, Jonathan D. Bray, and Norman Abrahamson. February 1999.
- PEER 1999/02** *Capacity-Demand-Diagram Methods for Estimating Seismic Deformation of Inelastic Structures: SDF Systems.* Anil K. Chopra and Rakesh Goel. April 1999.
- PEER 1999/01** *Interaction in Interconnected Electrical Substation Equipment Subjected to Earthquake Ground Motions.* Armen Der Kiureghian, Jerome L. Sackman, and Kee-Jeung Hong. February 1999.
- PEER 1998/08** *Behavior and Failure Analysis of a Multiple-Frame Highway Bridge in the 1994 Northridge Earthquake.* Gregory L. Fenves and Michael Ellery. December 1998.
- PEER 1998/07** *Empirical Evaluation of Inertial Soil-Structure Interaction Effects.* Jonathan P. Stewart, Raymond B. Seed, and Gregory L. Fenves. November 1998.
- PEER 1998/06** *Effect of Damping Mechanisms on the Response of Seismic Isolated Structures.* Nicos Makris and Shih-Po Chang. November 1998.
- PEER 1998/05** *Rocking Response and Overturning of Equipment under Horizontal Pulse-Type Motions.* Nicos Makris and Yiannis Roussos. October 1998.
- PEER 1998/04** *Pacific Earthquake Engineering Research Invitational Workshop Proceedings, May 14–15, 1998: Defining the Links between Planning, Policy Analysis, Economics and Earthquake Engineering.* Mary Comerio and Peter Gordon. September 1998.
- PEER 1998/03** *Repair/Upgrade Procedures for Welded Beam to Column Connections.* James C. Anderson and Xiaojing Duan. May 1998.
- PEER 1998/02** *Seismic Evaluation of 196 kV Porcelain Transformer Bushings.* Amir S. Gilani, Juan W. Chavez, Gregory L. Fenves, and Andrew S. Whittaker. May 1998.
- PEER 1998/01** *Seismic Performance of Well-Confined Concrete Bridge Columns.* Dawn E. Lehman and Jack P. Moehle. December 2000.